

STUDY OF SOLAR POTENTIAL THROUGH THE APPLICATION OF THE gSolarRoof MODEL IN THE INDUSTRIAL ESTATES OF DON BENITO AND PLASENCIA (SPAIN)

Martín Ávila, A.M.
Domínguez Bravo, J.
Ferrer Tebar, J.A.
Díaz Herrero, G.



GOBIERNO
DE ESPAÑA

MINISTERIO
DE CIENCIA
E INNOVACIÓN

Ciemat

Centro de Investigaciones
Energéticas, Medioambientales
y Tecnológicas

**STUDY OF SOLAR
POTENTIAL THROUGH
THE APPLICATION OF
THE gSolarRoof MODEL
IN THE INDUSTRIAL
ESTATES OF DON
BENITO AND
PLASENCIA (SPAIN)**

Martín Ávila, A.M.
Domínguez Bravo, J.
Ferrer Tebar, J.A.
Díaz Herrero, G.

Departamento de Energía

Publication available in [catalog of official publications](#)

© CIEMAT, 2021

ISSN: 2695-8864

NIPO: 832-21-018-8

Edition and Publication:

Editorial CIEMAT

Avda. Complutense, 40 28040-MADRID

e-mail: editorial@ciemat.es

[Editorial news](#)

CIEMAT do not share necessarily the opinions expressed in this published work, whose responsibility corresponds to its author(s).

All rights reserved. No part of this published work may be reproduced, stored in a retrieval system, or transmitted in any form or by any existing or future means, electronic, mechanical, photocopying, recording, or otherwise, without written permission from the publisher.

ESTUDIO DEL POTENCIAL SOLAR MEDIANTE LA APLICACIÓN DE LA METODOLOGÍA gSolarRoof EN LOS POLÍGONOS INDUSTRIALES DE DON BENITO Y PLASENCIA

Martín Ávila, A.M.; Domínguez Bravo, J.; Ferrer Tebar, J.A.; Díaz Herrero, G.

84 pp., 83 Fig., 7 tbls, 19 ref.

Resumen:

El modelo gSolarRoof, desarrollado en el CIEMAT por el grupo de Tecnologías de la Información Geográfica y Energías Renovables (gTIGER), es capaz de evaluar con gran precisión la superficie potencial para el aprovechamiento solar en distintos tipos de edificios. A partir de la valoración de la superficie, el modelo calcula también la potencia que se podría instalar, así como la energía que se produciría en un año y las emisiones de CO₂ que se podrían evitar.

gSolarRoof ha sido aplicado en el proyecto IDERCEXA en dos polígonos industriales de Extremadura (España). Una de las principales novedades ha sido la adquisición de datos de alta resolución con un dron. La gran resolución y enorme cantidad de datos han supuesto un enorme reto para el análisis y tratamiento de la información. Esto ha supuesto un hito relevante tanto en IDERCEXA como para la evolución del modelo gSolarRoof. Además, el proyecto incorpora novedades en la evaluación del potencial solar para el calentamiento de agua y su aprovechamiento industrial. También se ha desarrollado [geoportal](#) para consultar los resultados del proyecto.

STUDY OF SOLAR POTENTIAL THROUGH THE APPLICATION OF THE gSolarRoof METHODOLOGY IN THE DON BENITO AND PLASENCIA INDUSTRIAL ESTATES

Martín Ávila, A.M.; Domínguez Bravo, J.; Ferrer Tebar, J.A.; Díaz Herrero, G.

84 pp., 83 Fig., 7 tbls, 19 ref.

Abstract:

The gSolarRoof model, developed at CIEMAT by the Geographic Information Technologies and Renewable Energies (gTIGER) group, is capable of assessing with great precision the potential surface area for solar use in different types of buildings. Based on the assessment of the surface area, the model also calculates the power that could be installed, as well as the energy that would be produced in a year and the CO₂ emissions that could be avoided.

gSolarRoof has been applied in the IDERCEXA project in two industrial estates in Extremadura (Spain). One of the main innovations has been the acquisition of high-resolution data with a drone. The high resolution and huge amount of data have posed a huge challenge for the analysis and processing of the information. This has been an important milestone both for IDERCEXA and for the evolution of the gSolarRoof model. In addition, the project incorporates new developments in the evaluation of solar potential for water heating and its industrial use. A [web site](#) has also been developed to consult the results of the project.

ACKNOWLEDGEMENTS

The authors are grateful to the INTERREG V Spain-Portugal cooperation programme (POCTEP) 2014-2020, for funding the IDERCEXA project, "Research, Development and Renewable Energies for new business models in Centro, Extremadura and Alentejo", 0330_IDERCEXA_4_E, coordinated by AGENEX, of which this report is a part.



TABLE OF CONTENTS

1	INTRODUCTION	10
2	CHARACTERISATION OF THE STUDY AREA	11
	2.1 DON BENITO INDUSTRIAL ESTATE.....	11
	2.2 PLASENCIA INDUSTRIAL ESTATE.....	12
3	INPUT DATA	14
4	METHODOLOGY	16
	4.1 PHOTOGRAMMETRIC FLIGHT	16
	4.2 INFORMATION PROCESSING.....	17
	4.3 GEOGRAPHICAL MODEL FOR THE ANALYSIS OF SOLAR POTENTIAL.....	19
5	GLOBAL RESULTS FOR THE INDUSTRIAL ESTATES.....	23
6	GEOWEB FOR SESTTING OUT THE RESULTS	26
7	BIBLIOGRAPHY	28
	APPENDIX I. CONTROL POINTS	31
	APPENDIX II. QUALITY REPORT OF DON BENITO.....	32
	APPENDIX III. QUALITY REPORT OF PLASENCIA	36
	APPENDIX IV. GEOWEB GSOLARROOF USER MANUAL.....	42
	APPENDIX V. THEMATIC MAPS OF DON BENITO INDUSTRIAL ESTATE.....	51
	APPENDIX VI. THEMATIC MAPS OF PLASENCIA INDUSTRIAL ESTATE	73

LIST OF FIGURES

Figure 1.	Location of Don Benito industrial estate.	11
Figure 2	Companies and workers by sector of economic activity (September 2020) of Don Benito (IEEX, 2020).	12
Figure 3.	Location of Plasencia industrial estate.	13
Figure 4.	Companies and workers by sector of economic activity (September 2020) of Plasencia (IEEX, 2020).	13
Figure 5.	General methodology workflow.	16
Figure 6.	Point clouds from the photogrammetric flight. Don Benito industrial estate.	18
Figure 7.	Orthophoto from the photogrammetric flight. Don Benito industrial estate.	18
Figure 8.	Point clouds from the photogrammetric flight. Plasencia industrial estate.	18
Figure 9.	Orthophoto from the photogrammetric flight. Plasencia industrial estate.	18
Figure 10	Rooftop orientation. Don Benito industrial estate.	21
Figure 11.	Shaded areas. Don Benito industrial estate.	21
Figure 12.	Annual global solar irradiation. Don Benito industrial estate.	21
Figure 13.	Rooftop orientation. Plasencia industrial estate.	22
Figure 14.	Shaded areas. Plasencia industrial estate.	22
Figure 15.	Annual global solar irradiation. Plasencia industrial estate.	22
Figure 16.	Distribution of buildings depending on to the rooftop area available for Don Benito industrial estate.	23
Figure 17.	Distribution of buildings depending on the rooftop area available for Plasencia industrial estate.	23
Figure 18.	Geoweb gSolarRoof for industrial estates (CIEMAT, 2020).	26
Figure A 1.	Distribution of the control points in Don Benito industrial estate.	31
Figure A 2	Distribution of the control points in Plasencia industrial estate.	31
Figure A 3	Pop-ups of buildings.	42
Figure A 4	Widget 'Address search'.	43
Figure A 5.	Result widget 'Address search'.	43
Figure A 6.	Widget 'Zoom slider'.	43
Figure A 7	Widget 'Home button'.	44
Figure A 8.	Widget 'My location'.	44
Figure A 9	Widget 'Full screen'.	45
Figure A 10	Widget 'Extent navigate'.	45
Figure A 11	Widget 'Overview map'.	45
Figure A 12	Widget 'Bookmark industrial estate'.	46
Figure A 13	Widget 'Basemap gallery'.	46
Figure A 14	Widget 'Measurement'.	47

Figure A 15	Widget 'Swipe'.....	47
Figure A 16	Widget 'Print'.	48
Figure A 17.	Widget 'Legend'.....	48
Figure A 18.	Widget 'Layer list'.....	49
Figure A 19.	Drop-down of widget 'Layer list'.	49
Figure A 20.	Drop-down options of a layer.	49
Figure A 21.	Widget 'Help'.	50
Figure A 22.	Photovoltaic: Available surface of rooftop. Don Benito.	51
Figure A 23.	Photovoltaic: Potential power (Monocrystalline silicon module). Don Benito.	52
Figure A 24.	Photovoltaic: Potential power (Multicrystalline silicon module). Don Benito.	53
Figure A 25.	Photovoltaic: Annual energy generated (Monocrystalline silicon module). Don Benito.	54
Figure A 26.	Photovoltaic: Annual energy generated (Multicrystalline silicon module). Don Benito.	55
Figure A 27.	Photovoltaic: Annual CO ₂ emissions saved (Monocrystalline silicon module). Don Benito.....	56
Figure A 28.	Photovoltaic: Annual CO ₂ emissions saved (Multicrystalline silicon module). Don Benito.....	57
Figure A 29.	Thermal: Available surface of rooftop. Don Benito.	58
Figure A 30.	Thermal: Annual energy generated (Vacuum tube collector) at the temperature of 40 °C. Don Benito.	59
Figure A 31.	Thermal: Annual energy generated (Vacuum tube collector) at the temperature of 70 °C. Don Benito.	60
Figure A 32.	Thermal: Annual energy generated (Vacuum tube collector) at the temperature of 90 °C. Don Benito.	61
Figure A 33.	Thermal: Annual energy generated (Selective flat plate collector) at the temperature of 40 °C. Don Benito.	62
Figure A 34.	Thermal: Annual energy generated (Selective flat plate collector) at the temperature of 70 °C. Don Benito.	63
Figure A 35.	Thermal: Annual energy generated (Selective flat plate collector) at the temperature of 90 °C. Don Benito.	64
Figure A 36.	Thermal: Annual energy generated (Nonselective flat plate collector) at the temperature of 40 °C. Don Benito.	65
Figure A 37.	Thermal: Annual CO ₂ emissions saved (Vacuum tube collector) at the temperature of 40 °C. Don Benito.	66
Figure A 38.	Thermal: Annual CO ₂ emissions saved (Vacuum tube collector) at the temperature of 70 °C. Don Benito.	67
Figure A 39.	Thermal: Annual CO ₂ emissions saved (Vacuum tube collector) at the temperature of 90 °C. Don Benito.	68

Figure A 40.	Thermal: Annual CO ₂ emissions saved (Selective flat plate collector) at the temperature of 40 °C. Don Benito.	69
Figure A 41.	Thermal: Annual CO ₂ emissions saved (Selective flat plate collector) at the temperature of 70 °C. Don Benito.	70
Figure A 42.	Thermal: Annual CO ₂ emissions saved (Selective flat plate collector) at the temperature of 90 °C. Don Benito.	71
Figure A 43.	Thermal: Annual CO ₂ emissions saved (Nonselective flat plate collector) at the temperature of 40 °C. Don Benito.	72
Figure A 44.	Photovoltaic: Available surface of rooftop. Plasencia.	73
Figure A 45.	Photovoltaic: Potential power (Monocrystalline silicon module). Plasencia.	74
Figure A 46.	Photovoltaic: Potential power (Multicrystalline silicon module). Plasencia.....	75
Figure A 47.	Photovoltaic: Annual energy generated (Monocrystalline silicon module). Plasencia.....	76
Figure A 48.	Photovoltaic: Annual energy generated (Multicrystalline silicon module). Plasencia.....	77
Figure A 49.	Photovoltaic: Annual CO ₂ emissions saved (Monocrystalline silicon module). Plasencia.....	78
Figure A 50.	Photovoltaic: Annual CO ₂ emissions saved (Multicrystalline silicon module). Plasencia.....	79
Figure A 51.	Thermal: Available surface of rooftop. Plasencia.	80
Figure A 52.	Thermal: Annual energy generated (Vacuum tube collector) at the temperature of 40 °C. Plasencia.....	81
Figure A 53.	Thermal: Annual energy generated (Vacuum tube collector) at the temperature of 70 °C. Plasencia.....	82
Figure A 54.	Thermal: Annual energy generated (Vacuum tube collector) at the temperature of 90 °C. Plasencia.....	83
Figure A 55.	Thermal: Annual energy generated (Selective flat plate collector) at the temperature of 40 °C. Plasencia.....	84
Figure A 56.	Thermal: Annual energy generated (Selective flat plate collector) at the temperature of 70 °C. Plasencia.....	85
Figure A 57.	Thermal: Annual energy generated (Selective flat plate collector) at the temperature of 90 °C. Plasencia.....	86
Figure A 58.	Thermal: Annual energy generated (Nonselective flat plate collector) at the temperature of 40 °C. Plasencia.....	87
Figure A 59.	Thermal: Annual CO ₂ emissions saved (Vacuum tube collector) at the temperature of 40 °C. Plasencia.....	88
Figure A 60.	Thermal: Annual CO ₂ emissions saved (Vacuum tube collector) at the temperature of 70 °C. Plasencia.....	89
Figure A 61.	Thermal: Annual CO ₂ emissions saved (Vacuum tube collector) at the temperature of 90 °C. Plasencia.....	90

Figure A 62.	Thermal: Annual CO ₂ emissions saved (Selective flat plate collector) at the temperature of 40 °C. Plasencia.....	91
Figure A 63.	Thermal: Annual CO ₂ emissions saved (Selective flat plate collector) at the temperature of 70 °C. Plasencia.....	92
Figure A 64.	Thermal: Annual CO ₂ emissions saved (Selective flat plate collector) at the temperature of 90 °C. Plasencia.....	93
Figure A 65.	Thermal: Annual CO ₂ emissions saved (Nonselective flat plate collector) at the temperature of 40 °C. Plasencia.....	94

LIST OF TABLES

Table 1.	LIDAR data (IGN, 2020).	14
Table 2.	Classification of unique buildings.....	19
Table 3.	Time-slot to calculate shading.	20
Table 4.	Photovoltaic: Summary of total results of Don Benito industrial estate.....	24
Table 5.	Thermal: Summary of total results of Don Benito industrial estate.....	24
Table 6.	Photovoltaic: Summary of total results of Plasencia industrial estate.....	24
Table 7.	Thermal: Summary of total results of Plasencia industrial estate.....	24

1 INTRODUCTION

The [IDERCEXA](#) project has the purpose to help the development and innovation of the EUROACE region (Alentejo and Centre in Portugal and Extremadura in Spain) through the implementation and dissemination of renewable technologies that, with prototypes, expect to promote a technological fabric that promotes the regional industry growth.

CIEMAT, as a partner of this consortium, has contributed its technological capabilities both supporting regional companies and the development of these prototypes. In this sense, below we present the work developed by the Geographic Information Technologies and Renewable Energies Group (gTIGER) of CIEMAT within the activities of this organization in the framework of the IDERCEXA project.

If we observe the zoning of any urban area, we can see that the areas with the greatest potential for exploiting their roofs to use solar energy are shopping centres, industrial estates, and service and equipment areas (schools, hospitals, etc.). The object of this study is to evaluate the solar photovoltaic and thermal potential of two industrial estates by the application of gSolarRoof geographic model developed by CIEMAT. For this analysis have been selected the industrial estates of Don Benito (Badajoz) and Plasencia (Cáceres) in the autonomous community of Extremadura.

This study is included in the gSolarRoof project aimed at the implementation of geographic models to evaluate the capacity of urban areas to incorporate renewable energies and specifically the use of solar energy, as part of urban planning. Therefore, the project relies on both, the analytical capacity that geographic information technologies have shown and high-resolution data to define surfaces through the use of UAS (Unmanned Aerial System) commonly known as drones.

In addition to the images taken with UAS, the information necessary for the project has been obtained from geographic databases available in different national and regional official services. The study is based on generating a three-dimensional model of the industrial estates from which the analysis of the solar potential is carried out by applying the gSolarRoof model, developed with the ArcGIS software. The model assesses the surfaces available for solar installations on each roof, the incident radiation, the power potential that could be installed and the energy that would be obtained throughout the year.

For the dissemination of the project results, a [web map](#) is used as support where a series of maps with the results can be displayed, facilitating the access to data and detailed information on the industrial buildings.

2 CHARACTERISATION OF THE STUDY AREA

2.1 DON BENITO INDUSTRIAL ESTATE

Don Benito is a town placed in the north of the Badajoz province and is part of the Las Vegas Altas community, 96 km from the capital of the province. The industrial estate, with an area of 343 ha, is located at latitude 38° 57' 56.44" North and longitude 5° 21' 7.06" West. It is located in a primarily flat area near the Guadiana river, that flows from north to west of the urban centre. The town has access to the EX-A2 highway that connects Don Benito with the south-west highway A-5 (see figure 1).

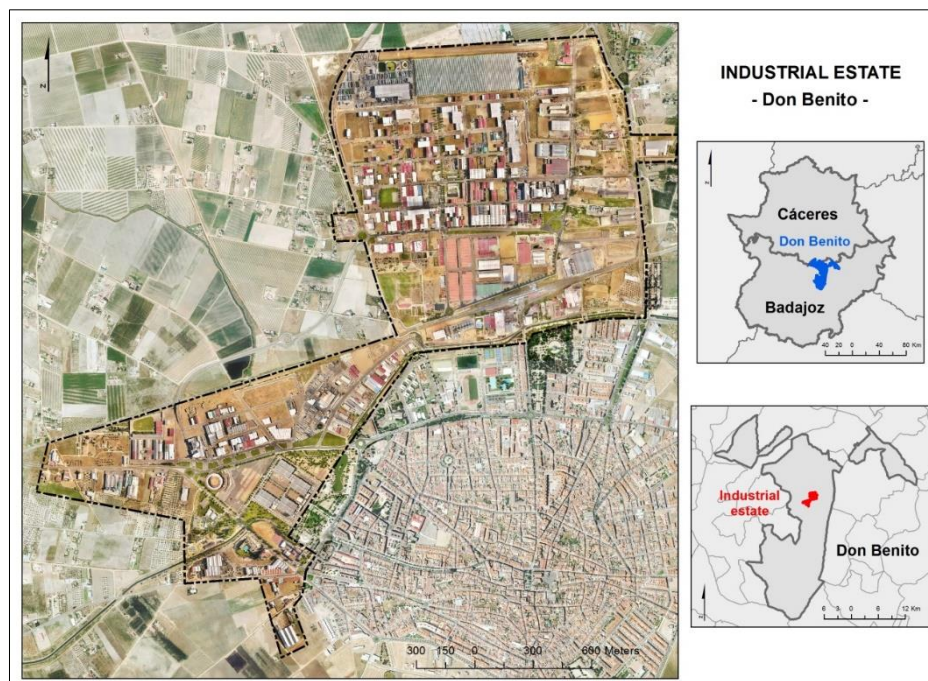


Figure 1. Location of Don Benito industrial estate.

Don Benito presents the typical characteristics of regions with a Mediterranean climate. The average annual temperature is 16.4 °C and the annual precipitation is 477 mm. During the summer the temperatures are high, being in these warmer months the maximum average temperature of 34 °C and sometimes can exceed 40 °C. In the winter months, with average minimum of 3 - 4 °C, temperatures tend to drop below 0 °C around 25 days per year (AEMET, 2020). At ground level, the average annual radiation exceeds the 1,800 kWh/m².

The municipality has a population of 37,151 (INE, 2019). Economic activity, favoured by its position as the main town in the region, is dominated by the service sector with a fairly developed retail and wholesale dedicated to food and beverages, agricultural raw materials, textiles or building. Besides, it has facilities for the commercial and business promotion such as the FEVAL-Extremadura Fair Institution where organize congresses, fairs and exhibitions.

The agricultural sector is important in the municipality. Due to it is close to the Guadiana and Ortiga rivers, irrigated agricultural exploitation has been promoted in the area, although other areas of the municipality are also dedicated to extensive non-irrigated crops and livestock in the pasture. However, related to agriculture is the industrial sector such as, the fruit concentrate industry, rice factories, the transformation of cereal into feed or cooperatives that select fruit for distribution. The agricultural sector has been the base of the industrial development of the municipality that has been expanding with new companies settled in the area (see Figure2).

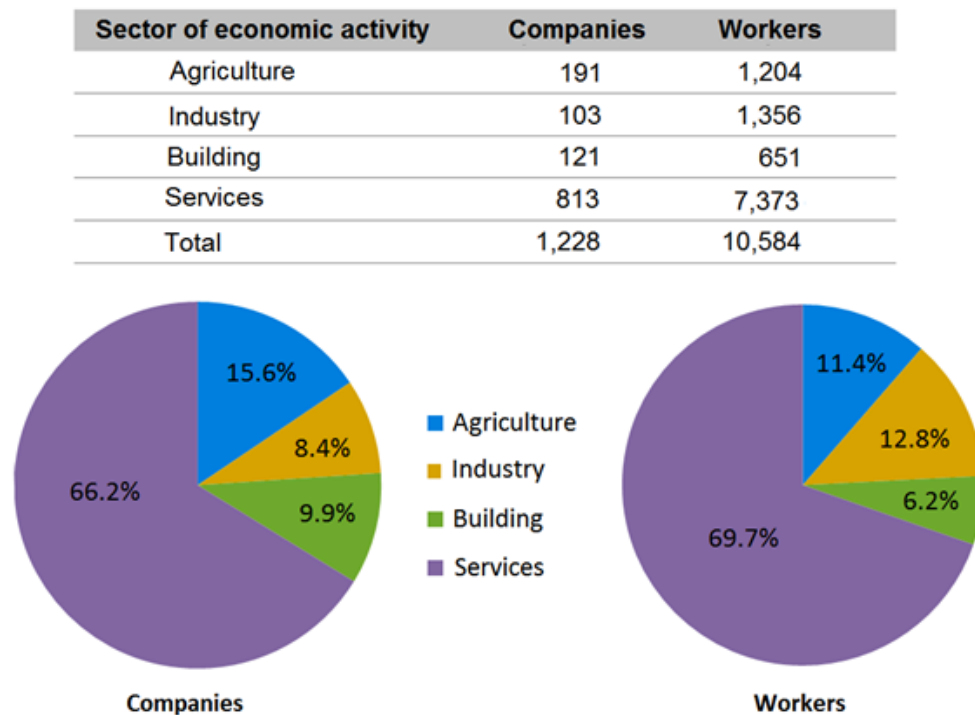


Figure 2 Companies and workers by sector of economic activity (September 2020) of Don Benito (IEEX, 2020).

2.2 PLASENCIA INDUSTRIAL ESTATE

Plasencia is a city in the north of Cáceres province placed at the entrance to the Jerte Valley, 68 km from the capital of the province. The industrial estate, with an area of 257 ha, is located at latitude 40° 0' 22.20" North and longitude 6° 6' 44.78" West. It is located in an area in the southwest of the urban centre and with access to the North de Extremadura (EX-A1) and Ruta de la Plata (A-66) motorways (see Figure 3).

Plasencia presents the characteristics of Mediterranean and continental climates. The average annual temperature is 15.9 °C and the precipitation is 711 mm. During the summer the average maximum temperature is 34 °C in the hottest month, although they can exceed 40 °C. However, in the winter months, the temperatures with average minimums of 3 - 4 °C also fall below 0 °C around 23 days per year (AEMET, 2020). Just as the Don Benito industrial estate, it has good annual radiation that can exceed on average 1,800 kWh/m².

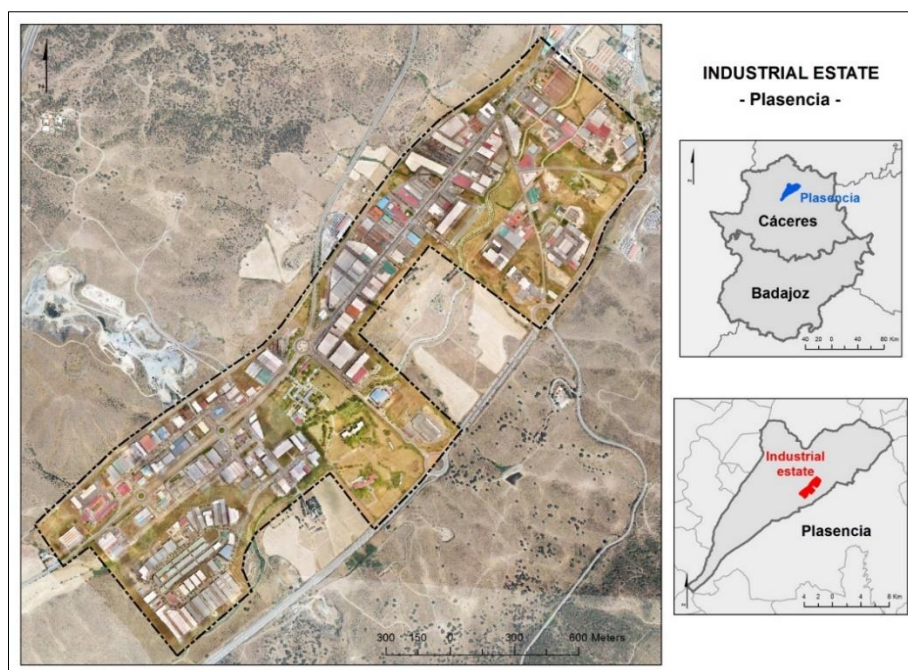


Figure 3. Location of Plasencia industrial estate.

The municipality has a population of 39,913 (INE, 2019). The main economic activity is related to the service sector with a commercial and tourist activity strengthened by being the largest city in the north of Extremadura and being surrounded by several communities. The city has a campus with several faculties of the Extremadura University and the Department for Ecological and Mountain Agriculture (CAEM) is located there. In the industrial sector, stand out the food industry, manufacture of metal for construction, wood industry and manufacture of furniture (see Figure 4).

Sector of economic activity	Companies	Workers
Agriculture	64	178
Industry	85	939
Building	155	1,038
Services	967	7,590
Total	1,271	9,745

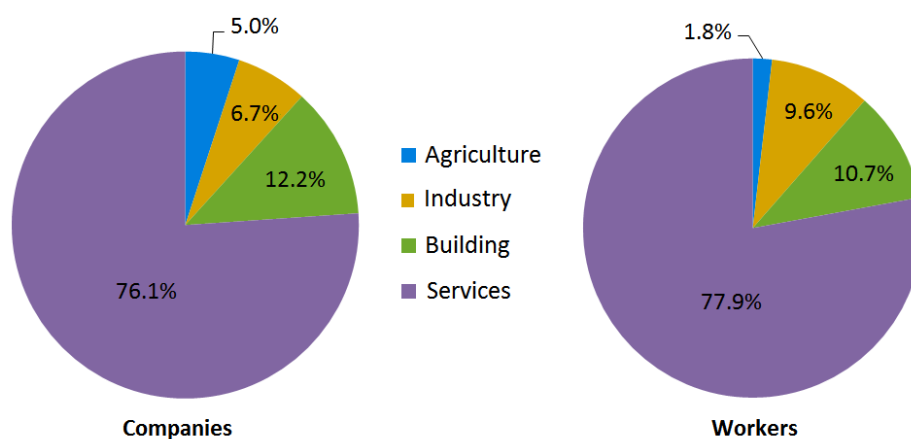


Figure 4. Companies and workers by sector of economic activity (September 2020) of Plasencia (IEEX, 2020).

3 INPUT DATA

In the development of the study, it was necessary to have information from two main sources, the geographic databases of official organizations with free access and the information provided by the photogrammetric flights carried out for this project of the industrial estates by UAS.

From the different data sources review, the following layers of information have been obtained:

- Point clouds: These files are basic to perform the analysis of the solar potential of buildings and form the three-dimensional model of industrial estates. Two types of point clouds have been used in this work:
 - LIDAR (Light Detection and Ranging): They correspond to the LIDAR project of the National Plan for Aerial Orthophotography (PNOA) provided by the Spanish National Geographic Institute (IGN). The LIDAR files are in LAZ format (LAS files version 1.2 compressed) and have been classified in buildings, vegetation (high, medium and low) and terrain. Furthermore, point clouds also include colour (RGB) or infrared (IRC) (see Table 1).

LIDAR DATA	FIRST COVERAGE	SECOND COVERAGE
Coordinate System	ETRS 1989 UTM Zone 29N	ETRS 1989 UTM Zone 30N
Year	2010	2018
Point density	0,5 points/m ²	1 point/m ²
Area	2 x 2 km	2 x 2 km
Files	Plasencia. Flight zone of Extremadura (Lote8_EXT) Don Benito. Flight zone of Extremadura (Lote9_EXT)	Don Benito → Flight zone of Extremadura - South (EXT-S)

Table 1. LIDAR data (IGN, 2020).

- Photogrammetry: UAS flight carried out by AZIMUT S.L. for this project in 2020. The point clouds have been generated with Pix4D, a photogrammetry software for drone mapping. The files obtained are in LAS format (version 1.2) with a resolution of 1 point/4 cm, the coordinate system is WGS 1984 UTM (Don Benito - zone 30 and Plasencia - zone 29) and they also include colour (RGB).
- Orthophotos: In order to have an aerial perspective of the industrial estates of both municipalities, we have used the series of orthophotos of the PNOA corresponding to the years 2010 to 2019 (IGN, 2020) with a resolution between 25 and 50 cm. Furthermore, from the images obtained with the UAS flight, orthophotos of the polygons have been calculated at the maximum resolution of 4 cm. The images have been used as a guide to delineate the study area, examine the buildings, and carry out a detailed review of the rooftops for data preparation.

- Sun position data: [The Solar Energy Services for Professionals \(SoDa\)](#) web service (MINES Paris Tech and Transvalor, 2020) offers a catalogue of links and map services related to solar radiation and meteorological information. One of the services available in the astronomy section is Solar Geometry 2 (SG-2) for calculating the position of the sun, necessary to establish which the shaded areas of the rooftops are. In this website, selecting a location the solar position is obtained. For each industrial estate the data corresponding to 2020 and have a time interval of 30 minutes.
- Monthly solar radiation data: The [ADRASE web](#) (CIEMAT, 2020) allows you to consult and download data for the whole of Spain of the monthly averages of horizontal global solar radiation with a resolution of 5 km. This information is necessary to calculate the atmospheric parameters for the determination of solar radiation with a better adjust to its monthly variations throughout the year.
- Distribution of buildings: One of the layers of information used is the location and boundary of buildings. The [General Management of Cadastre](#) (2020) has a service for downloading cartography in vector format of the cadastre. It can be obtained data on the distribution of the parcel, cadastre references, boundary of buildings, construction elements located in each parcel and public data associated with the cadastre plots such as the uses of the buildings. As a complement to this information we have also used the cartography of the [Extremadura Spatial Data Infrastructure](#) (Junta de Extremadura, 2020).
- Protected buildings or monuments: Situation of buildings with some category of patrimonial protection that could be included in the area of industrial estates (Ayuntamiento Benito, 2020; Ayuntamiento Plasencia, 2020).
- Monthly temperature data: The [State Meteorological Agency](#) (AEMET, 2020) provides data series and general climatological information from its meteorological stations. This type of data can also be accessed through the [‘Climate Atlas Viewer’](#) which includes temperature and precipitation data. This viewer generates a report with the data selected for an autonomous community, provinces, municipalities or other territorial unit, setting a location on the map.

4 METHODOLOGY

The study of the solar potential of the industrial estates has been developed in three main phases that include a photogrammetric flight of the industrial estates, the previous treatment of all the information and the geographic analysis by applying the gSolarRoof model for the analysis of the solar potential of buildings (see Figure 5).

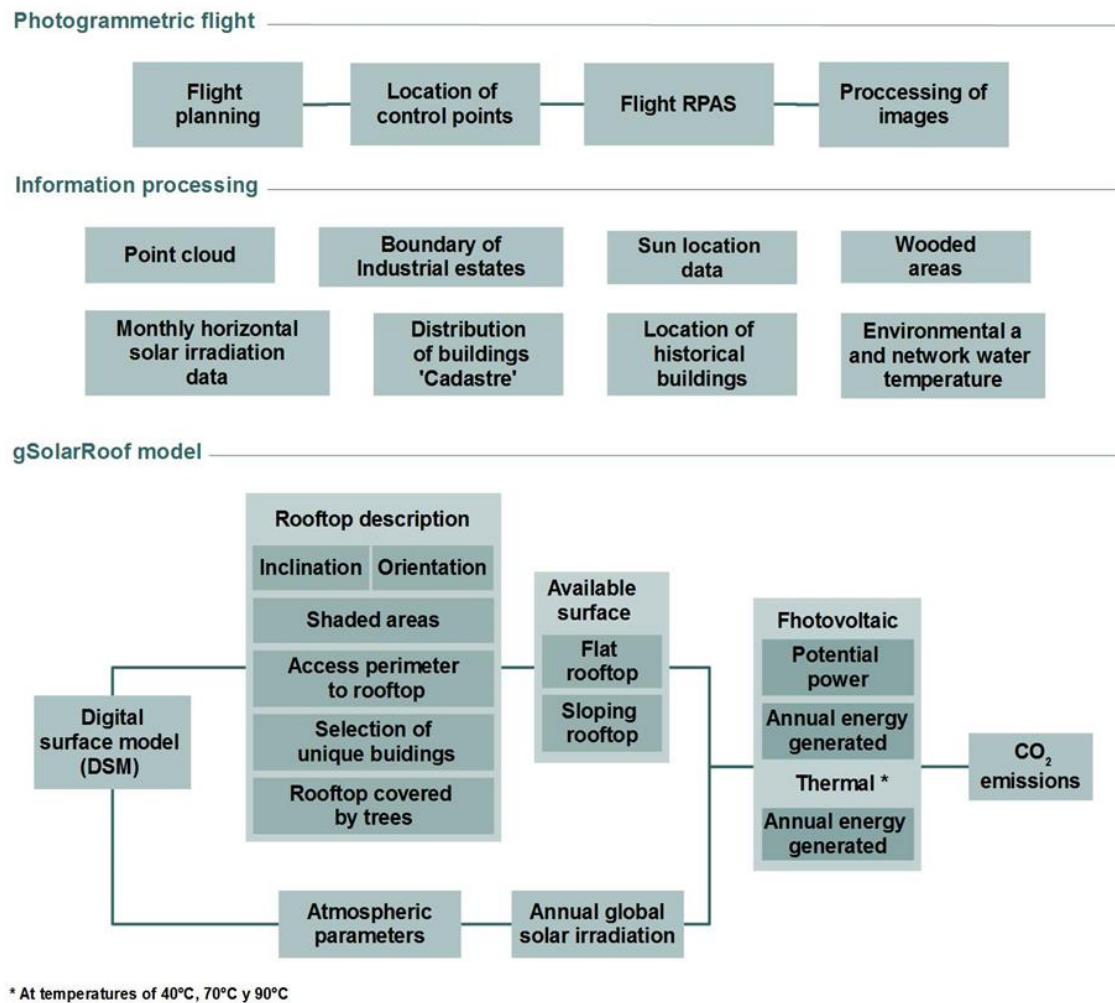


Figure 5. General methodology workflow.

4.1 PHOTOGRAMMETRIC FLIGHT

The photogrammetric flights of both industrial estates have been carried out with UAS by the company [AZIMUT Topografía y drones S.L.](#) who has carried out the following tasks:

- Flight planning for each industrial estate detailing the number of missions (17 in Don Benito and 16 in Plasencia) and the covered area, their duration, flight parameters, number of photos and precision, overlap and camera settings.

- Location of the support and control points taken in field with a precision GPS necessary to adequately georeference the drones flights and collate the results obtained in the data layers generated from the photographs. They have placed the topographic position of 66 points in Don Benito and 49 points in Plasencia (Appendix I).
- UAS flight following the routes planned for each mission to obtain photographs (2,117 in Don Benito and 2,319 in Plasencia).
- Image processing to generate the data files required by the model: point clouds, orthophotos and digital surface model (DSM) with a resolution of 4 cm (APPENDIX II and APPENDIX III). The processing data has been prepared using Pix4d software (see Figure 6 to Figure 9).

4.2 INFORMATION PROCESSING

- Before the analysis of the geographic model, it is important to prepare the point clouds, create the data layers, and provide them with the appropriate format according to the data structure established for input to the gSolarRoof model. The information processing method includes the following basic steps: Prepare the data layers and tables (limits of industrial estates, distribution of buildings, data of the sun position, temperatures, etc.). From the set of information collected, only the data used in the analysis are selected and the structure, georeference and format necessary to run the model are assigned.
- Review the point clouds and identify and correct any errors that may present, always preserving the form of the elements surfaces defined by the points. In the process of editing these files, duplicate or redundant points are removed to reduce the size of the files by suppressing unnecessary points. The noise generated by erroneous points whose position does not conform to those of their environment is eliminated too. It is also checked whether the definition of the relevant elements such as buildings, vegetation and land surface are adjusted to the resolution of the point clouds.
- Create a database where all the information previously treated is ordered following the specific data model of gSolarRoof. The design of the database will allow connect spatial data of various formats, providing a global view of the area. The design of the database will allow later in the analysis to relate spatial data of various formats, providing a joint vision of the area.



Figure 6. Point clouds from the photogrammetric flight. Don Benito industrial estate.



Figure 8. Point clouds from the photogrammetric flight. Plasencia industrial estate.



Figure 7. Orthophoto from the photogrammetric flight. Don Benito industrial estate.



Figure 9. Orthophoto from the photogrammetric flight. Plasencia industrial estate.

4.3 GEOGRAPHICAL MODEL FOR THE ANALYSIS OF SOLAR POTENTIAL

In CIEMAT's gSolarRoof geographic model (Martín et al., 2016) the variables that will determine the solar potential of industrial estates are defined, analysing which are the appropriate locations for solar modules and energy generation, according to solar radiation in the zone. It has been designed with ModelBuider application of ArcGIS software to create and manage these types of models. The workflows implemented in gSolarRoof have required to be updated and modified for the case of the industrial estates. The main functions included in this project are the following:

- Generate a DSMS of the industrial estates from the point clouds files to have a three-dimensional representation of the urban areas. The DSM characterize the dimensions of the buildings, the shape of the rooftops and the distribution of the elements located in the urban environment. Depending on the point clouds density, several tests have been performed with the precisions of 1 m, 50 cm and 20 cm.
- Analysis of the orientation and inclination of the rooftops. In photovoltaics, a maximum inclination of 60° is considered with energy losses of 40 % for the solar radiation use compared to the optimal position of the rooftops (south). In thermal, a maximum inclination of 90° and an orientation according to the east - south - west position has been defined.
- Delimit a perimeter access zone around the rooftops of the contour of the roofs, including the delimitation of the different sections that make up the buildings. The area of each building unit defines the width of the assigned strip (between 0.5 m and 1 m).
- Identify buildings with unique characteristics that partly or totally exclude them from the installation of solar modules, such as protected buildings for their heritage value, state of ruin, in process of construction, without information, etc. (see table 2).

BUILDING	BUILDING SECTION
Protected building	Modified section
Building under construction	State of ruin section
State of ruin	Section without information
Modified building	Glazed rooftop
Not buidt	Solar modules installed
Building without information	Unbuilt section
Demolished building	Demolished section

Table 2. *Classification of unique buildings.*

- Review of wooded areas close to buildings and rule out those sections of the rooftops that are covered by trees.
- Analysis of the rooftops shading to take advantage of the central hours of the day with greatest solar radiation. ArcGIS software has a tool for calculating the shading for a

position of the sun at any given time of day and year. The analysis is carried out for the whole year, taking into account the distribution of the buildings in the industrial estate, the trees or any other shading element of the urban area. Shadow maps are calculated for each day of the year in a central time-slot of the day (see table 3).

MONTH	HOURS
February - March - April	10:30 / 11:00 / 12:00 / 13:00 / 13:30
May - June - July	10:00 / 11:00 / 12:00 / 13:00 / 14:00
August - September - October	10:30 / 11:00 / 12:00 / 13:00 / 13:30
November - December - January	11:00 / 12:00 / 13:00

Table 3. Time-slot to calculate shading.

- Determine the useful rooftops area of the buildings for solar installations by selecting the areas that due to their position (inclination and orientation) would have a better use of solar radiation, avoiding shadows at certain times of the day, are not covered by trees and have access to facilities. In the available area, a differentiation has also been made between flat and sloping rooftops.
- Calculate the solar radiation that annually affects the rooftops using the tool 'Solar radiation of areas' of the ArcGIS software. This tool needs a DSM to include the diversity of shapes rooftops of the industrial buildings and the configuration of the atmospheric parameters that influence in the variation of radiation throughout the year (Martín and Domínguez, 2019).
- Evaluate the power potential and annual electrical energy production (Defaix et al., 2012) with photovoltaic modules of the types 'Monocrystalline Silicon' (Viessmann, 2016) and 'Multicrystalline Silicon' (Canadian Solar, 2017).
- Calculate the annual energy production taking as reference several use temperatures (40 °C, 70 °C and 90 °C) with thermal solar collectors of the types 'Vacuum tube' , 'Selective plane' and 'Non-selective plane' (IDAE and ASIT, 2020).
- Determine the annual CO₂ emissions in atmosphere saved with the generated solar energy generated in relation to conventional electricity for photovoltaics and the used fuel (natural gas) to generate thermal solar energy (IDAE, 2014).
- Joint each building with the results obtained of all the parameters calculated in the model for photovoltaic and thermal solar energy, following the distribution of buildings defined by the cadastre parcel (see figures 10-15).



Figure 10 Rooftop orientation. Don Benito industrial estate.

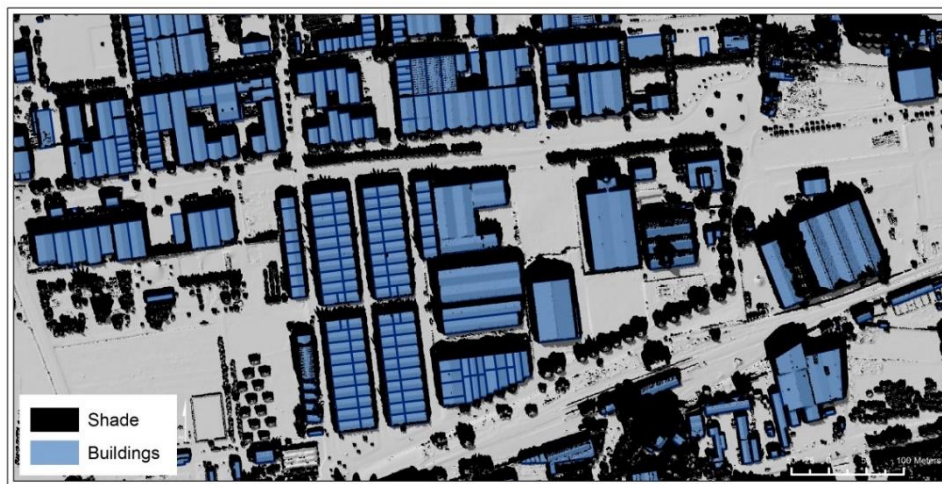


Figure 11. Shaded areas. Don Benito industrial estate.

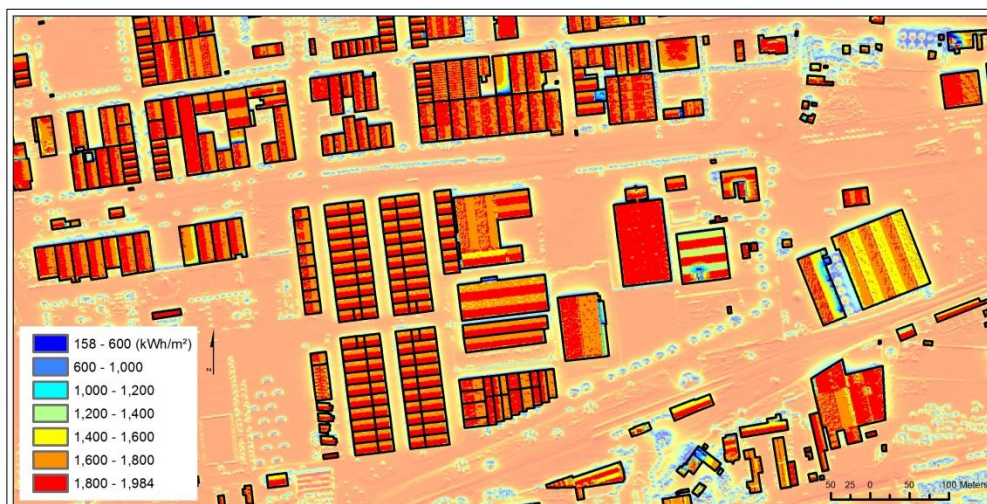


Figure 12. Annual global solar irradiation. Don Benito industrial estate.



Figure 13. Rooftop orientation. Plasencia industrial estate.

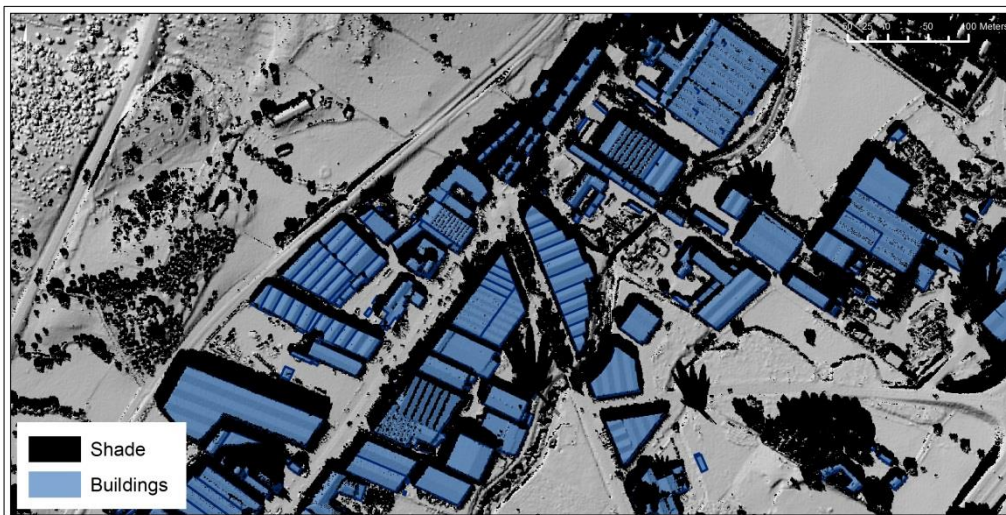


Figure 14. Shaded areas. Plasencia industrial estate.

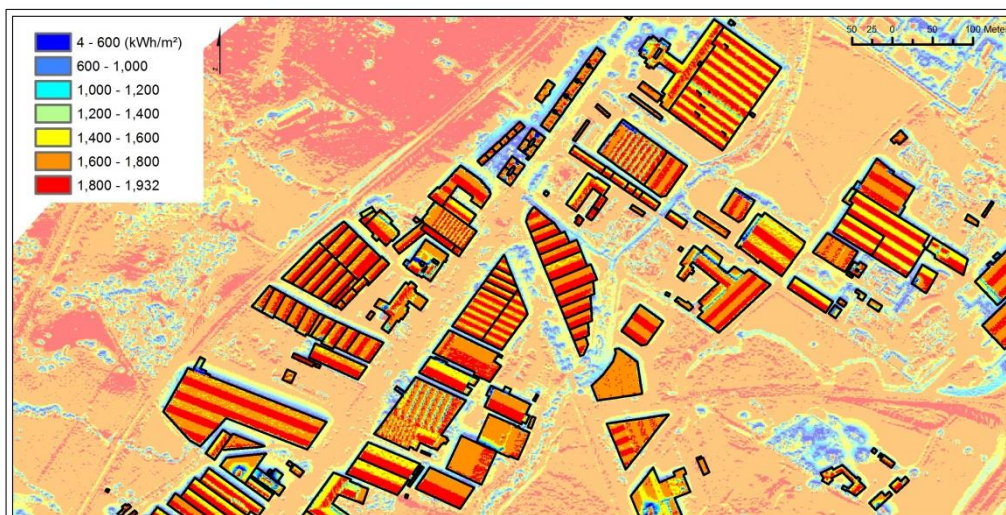


Figure 15. Annual global solar irradiation. Plasencia industrial estate.

5 GLOBAL RESULTS FOR THE INDUSTRIAL ESTATES

As results of the study of the solar potential with the gSolarRoof model, data of 720 cadastre plots have been obtained from Don Benito municipality. The total built area is 616,585 m² that representing the 18 % urbanized of the industrial estate surface. The 3 % of the total studied buildings do not adjust to the criteria established to be classified a useful surface for the installation of photovoltaic modules. Also the 4 % of the buildings do not have an available surface where to place thermal collectors. The percentage of capture potential surface respect to the building surface reaches 58.79 % for photovoltaic and 33.36 % for thermal (see Figure 16).

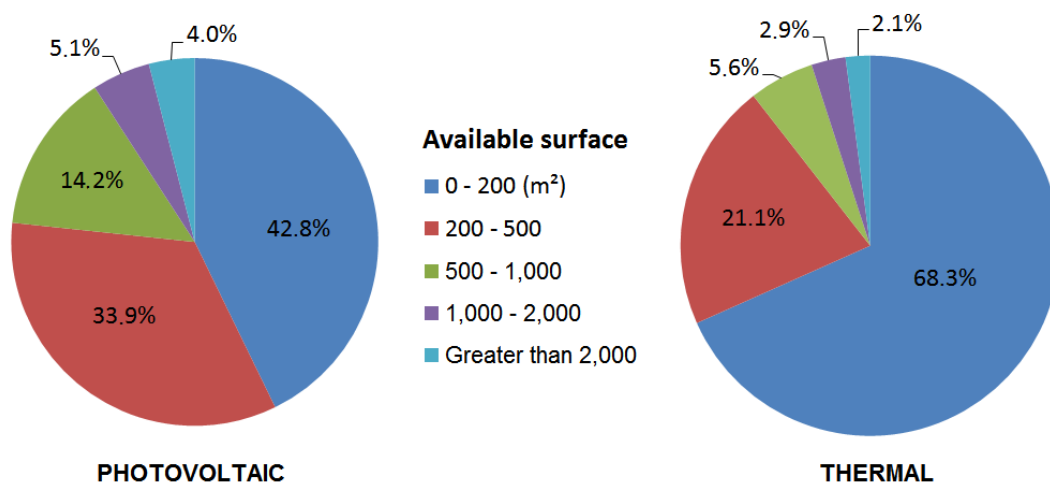


Figure 16. Distribution of buildings depending on to the rooftop area available for Don Benito industrial estate.

In relation to Plasencia industrial estate, data of 716 cadastre plots have been obtained with a total built area of 611,979 m² that representing the 24% urbanized of the industrial estate. The 1% of the total analysed buildings do not adjust to the criteria for the installation of photovoltaic modules and thermal collectors. The percentage of capture potential surface respect to the building surface reaches 65.55 % for photovoltaic and 36.89% for thermal (see Figure 17).

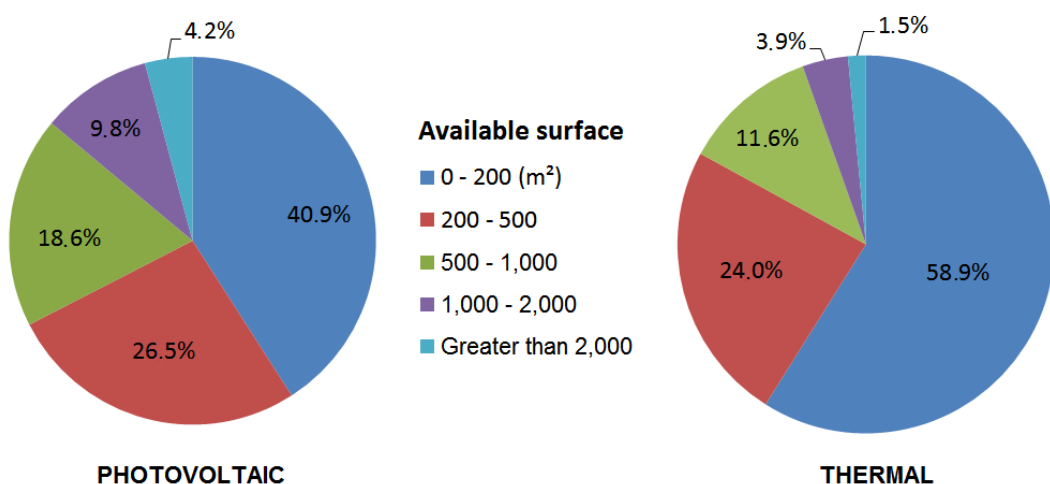


Figure 17. Distribution of buildings depending on the rooftop area available for Plasencia industrial estate.

The global results of the industrial estates for the different technologies of photovoltaic modules and thermal collectors are summarized in the tables 4 to 7.

PHOTOVOLTAIC MODULES	POTENTIAL POWER (MWp)	ANNUAL ENERGY	ANNUAL CO ₂ EMISSIONS SAVED
Monocrystalline silicon	45.01	60.63	20.07
Multicrystalline silicon	41.78	56.27	18.63

Table 4. Photovoltaic: Summary of total results of Don Benito industrial estate.

THERMAL SOLAR COLLECTORS	TEMPERATURE	ANNUAL ENERGY GENERATED (GWh)	ANNUAL CO ₂ EMISSIONS SAVED (T)
Vacuum tube	90 °C	58.58	14.76
Vacuum tube	70 °C	103.28	26.03
Vacuum tube	40 °C	165.09	41.60
Selective flat plate	90 °C	12.20	3.08
Selective flat plate	70 °C	58.79	14.82
Selective flat plate	40 °C	150.20	37.85
Nonselective flat plate	90 °C	0.00	0.00
Nonselective flat plate	70 °C	0.09	24.00
Nonselective flat plate	40 °C	97.88	24.67

Table 5. Thermal: Summary of total results of Don Benito industrial estate.

PHOTOVOLTAIC MODULES	POTENTIAL POWER (MWp)	ANNUAL ENERGY	ANNUAL CO ₂ EMISSIONS SAVED
Monocrystalline silicon	46.47	57.00	18.87
Multicrystalline silicon	43.13	52.91	17.51

Table 6. Photovoltaic: Summary of total results of Plasencia industrial estate.

THERMAL SOLAR COLLECTORS	TEMPERATURE	ANNUAL ENERGY GENERATED (GWh)	ANNUAL CO ₂ EMISSIONS SAVED (T)
Vacuum tube	90 °C	52.44	13.22
Vacuum tube	70 °C	95.29	24.01
Vacuum tube	40 °C	154.89	39.03
Selective flat plate	90 °C	10.32	2.60
Selective flat plate	70 °C	52.27	13.17
Selective flat plate	40 °C	139.11	35.06
Nonselective flat plate	90 °C	0.00	0.00
Nonselective flat plate	70 °C	0.00	0.00
Nonselective flat plate	40 °C	89.82	22.64

Table 7. Thermal: Summary of total results of Plasencia industrial estate.

As these are industrial estates, the buildings with high energy generation rates are considerable due to the characteristic large dimensions of these rooftops. The generally homogeneous surfaces and without too many elements such as antennas, chimneys or skylights, makes them suitable for solar installations. The morphology and location of the roofs influences the energy that may be

generated. However, although the industrial buildings had enough rooftops surface to consider the use, it is always necessary to take into account that the rooftop structure is adequate to support the installation of these systems. This work has not had access to detailed information of the buildings and the special feature of structure and materials, so that some areas may not be suitable for this type of facility.

6 GEOWEB FOR SESTTING OUT THE RESULTS

For the display of the information, a [web map viewer](#) has been created to host the maps with the results of the project. In the geoweb, users can make queries, view buildings data and share information in a simple way.

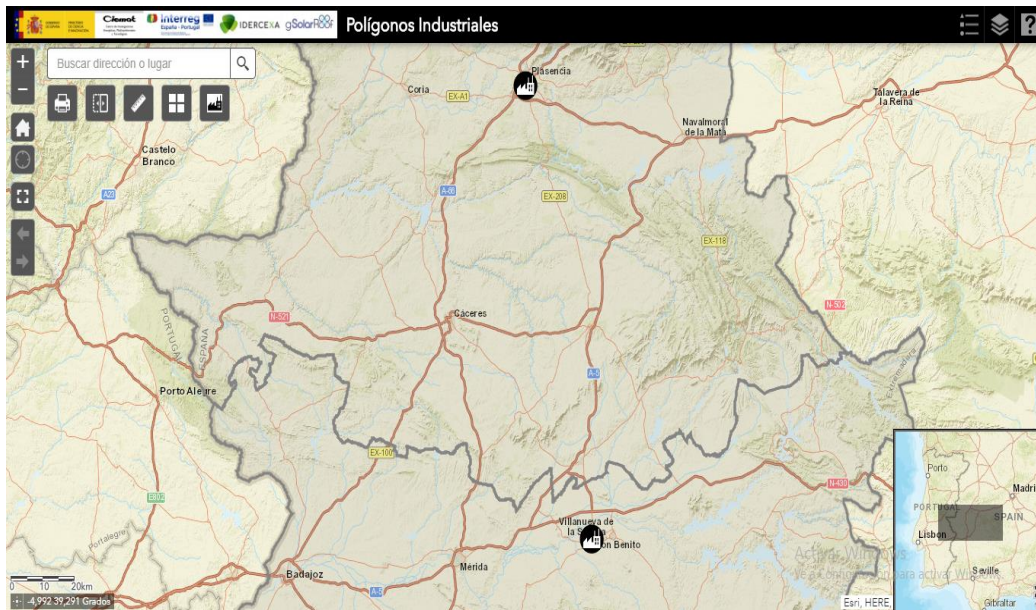


Figure 18. Geoweb gSolarRoof for industrial estates (CIEMAT, 2020).

Although there are different websites to upload geographic data on internet, we have selected the application ArcGIS Online (related to the software used with the model) to publish the results in the gSolarRoof 'Industrial Estates' geoweb.

This application allows us to generate online maps by uploading the data layers and assigning them the appropriate format for viewing. In addition, it facilitates customizing the layout of the viewer by configuring the tools, pop-up, drop-down menus and query buttons to access the information, move around the map and perform searches (for more information about how it works, see Appendix IV).

Among the data generated by the model, the information layers included in the web map are the following:

- Provincial and municipal administrative limits.
- Limits of the industrial estates of Don Benito and Plasencia.
- Layout of buildings according to cadastre plots.
- Photovoltaic: Available surface (m^2).
- Photovoltaic: Potential power (kWp).

- Photovoltaic: Annual energy generated (MWh).
- Photovoltaic: Annual CO₂ emissions saved (T).
- Thermal: Available surface (m²).
- Thermal: Annual energy generated (MWh) for the temperatures of 40 °C, 70 °C and 90 °C.
- Thermal: Annual CO₂ emissions saved (T) for the temperatures of 40 °C, 70 °C and 90 °C.
- Annual global solar irradiation (kWh / m²).
- Updated orthoimages of the industrial estates.

Finally, to complete the information of the gSolarRoof geoweb, a compilation of all the results has been prepared in an Atlas (APPENDIX V and APPENDIX VI).

7 BIBLIOGRAPHY

- [1] Agencia Estatal de Meteorología (AEMET) (2020). *Visor del Atlas climático*. Available in: <http://agroclimap.aemet.es/#> [Accessed: 26 October 2021].
- [2] Ayuntamiento de Don Benito (2020). *Ayuntamiento de Don Benito*. Available in: <https://www.donbenito.es/> [Accessed: 26 October 2021].
- [3] Ayuntamiento de Plasencia (2020). *Ayuntamiento de Plasencia*. Available in: <https://www.plasencia.es/web/#> [Accessed: 26 October 2021].
- [4] Canadian Solar (2017). PV Module Product Datasheet V5.531EN. CS6K-260| 265| 270| 275P. Canadian Solar Inc.
- [5] Centro de Investigaciones Energéticas, Medioambientales y Tecnológicas (CIEMAT) (2020). *gSolarRoof: Polígonos Industriales*. Available in: <https://ciemat.maps.arcgis.com/apps/webappviewer/index.html?id=80d02c9736b9481aa7b4a361aa147f3a> [Accessed: 26 October 2021].
- [6] Centro de Investigaciones Energéticas, Medioambientales y Tecnológicas (CIEMAT) (2020). *ADRASE. Acceso a datos de radiación solar de España*. Available in: <http://www.adrase.com/> [Accessed: 26 October 2021].
- [7] Centro de Investigaciones Energéticas, Medioambientales y Tecnológicas (CIEMAT) (2021). *gSolarRoof Project Home*. Available in: <https://gsolarroof.eu/en/> [Accessed: 26 October 2021].
- [8] Defaix, P.R., Van Sark, W.G.J.H.M., Worrell, E. y De Visser, E. (2012). Technical potential for photovoltaics on buildings in the EU-27. *Solar Energy*, 86, 2644-2653.
- [9] Dirección General de Catastro (2020). *Sede Electrónica del Catastro. Dissemination of cadastre data*. Available in: <https://www.sedecatastro.gob.es/> [Accessed: 26 October 2021].
- [10] Instituto para la Diversificación y Ahorro de la Energía (IDAE) (2014). Factores de emisiones de CO₂ y coeficientes de paso a energía primaria de diferentes fuentes de energía final consumidas en el sector de edificios en España. Documento Reconocido del Reglamento de Instalaciones Térmicas en los Edificios (RITE). Madrid: IDAE.
- [11] Instituto para la Diversificación y Ahorro de la Energía (IDAE) y Asociación Solar de la Industria térmica (ASIT) (2020). *Guía IDEA 022: Guía técnica de energía solar térmica*. Madrid: IDAE.
- [12] Instituto de Estadística de Extremadura (IEEX) (2020). *Empresas dadas de alta en la Seguridad Social en Extremadura. Septiembre 2020*. Available in:

<https://ciudadano.gobex.es/web/ieex/publicaciones-tipo/-/publicacion-categoria/ficha/9893855> [Accessed: 26 October 2021].

- [13] Instituto Geográfico Nacional (IGN) (2020). *Centro de descargas*. Available in: <https://centrodedescargas.cnig.es/CentroDescargas/index.jsp> [Accessed: 26 October 2021].
- [14] Instituto Nacional de Estadística (INE) (2019). *INEbase*. Demografía y población. Available in: <https://www.ine.es/> [Accessed: 26 October 2021].
- [15] Junta de Extremadura (2020). *Infraestructura de Datos Espaciales de Extremadura. Centro de Descargas. Cartografía topográfica*. Available in: <http://www.ideextremadura.com/Geoportal/> [Accessed: 26 October 2021].
- [16] Martín Ávila, A.M., Domínguez Bravo, J. y Amador Guerra, J. (2016). Desarrollo de un modelo geográfico para la evaluación del potencial fotovoltaico en entornos urbanos. *GeoFocus. Revista Internacional de Ciencia y Tecnología de la Información Geográfica*, 18, 147-167.
- [17] Martín, A.M. and Domínguez J. (2019). Solar Radiation Interpolation. In Polo, J., Martín-Pomares, L., Sanfilippo, A. eds. *Solar Resources Mapping: Fundamentals and Applications*. Netherlands: Springer, pp. 221-243.
- [18] MINES Paris Tech / Transvalor (2020). *SoDa. Solar radiation data. Web Services. Astronomy. Solar Geometry 2*. Available in: <http://www.soda-pro.com/es/web-services/astronomy/solar-geometry-2> [Accessed: 26 October 2021].
- [19] Viessmann (2016). Technical data VITOVOLT 300. Modelo M290OA, M295OA, M300OA. Viessmann, S.L.

APPENDIXES

APPENDIX I. CONTROL POINTS

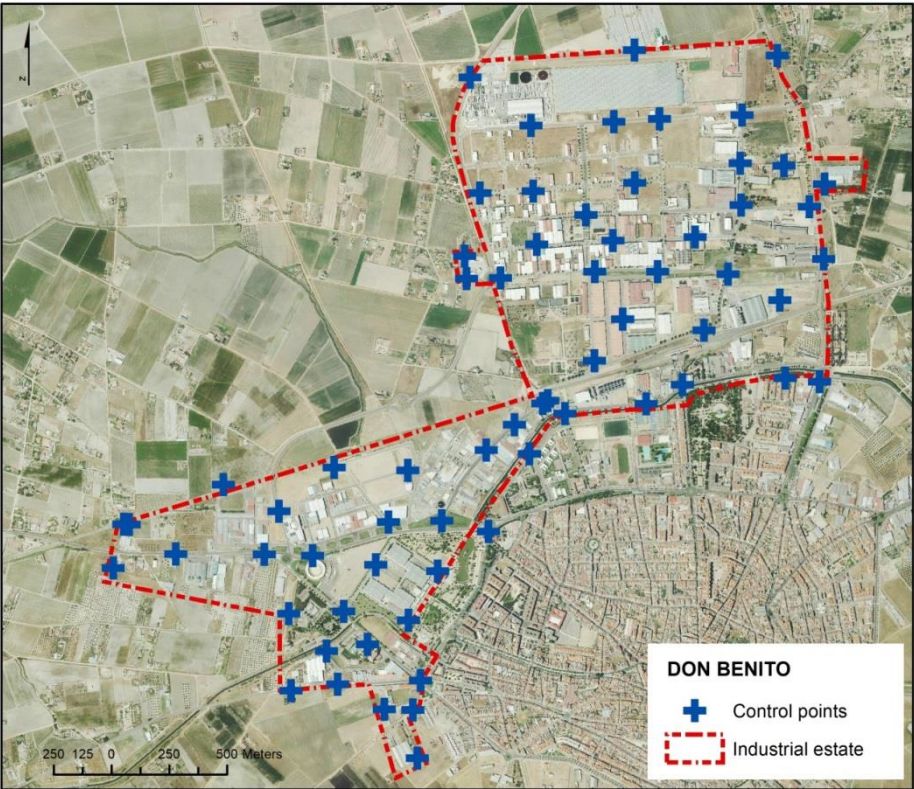


Figure A 1. Distribution of the control points in Don Benito industrial estate.

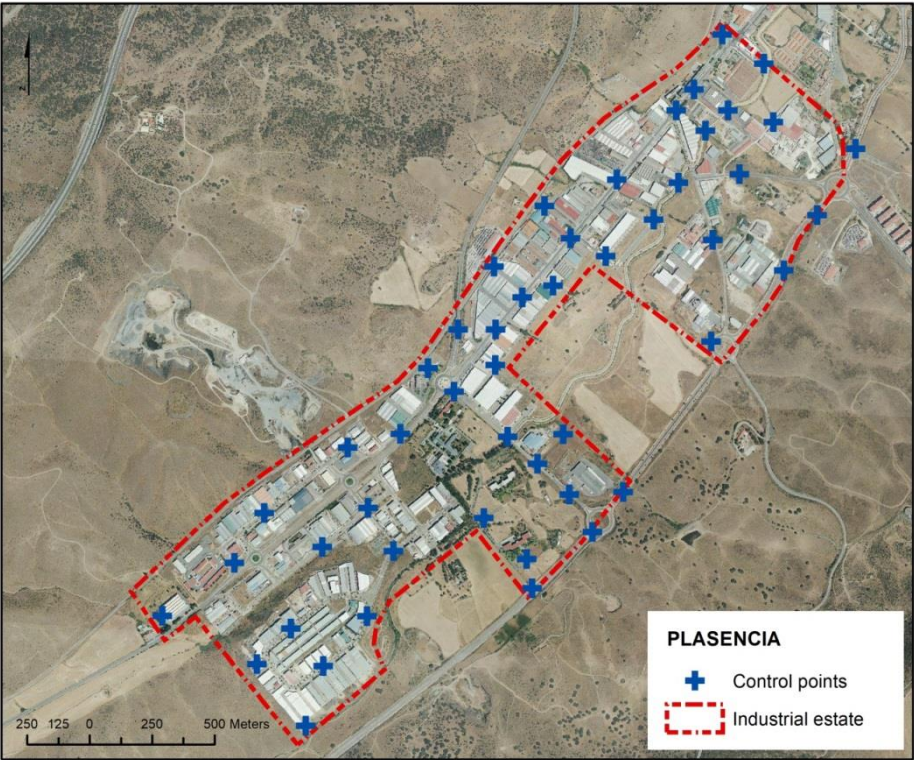
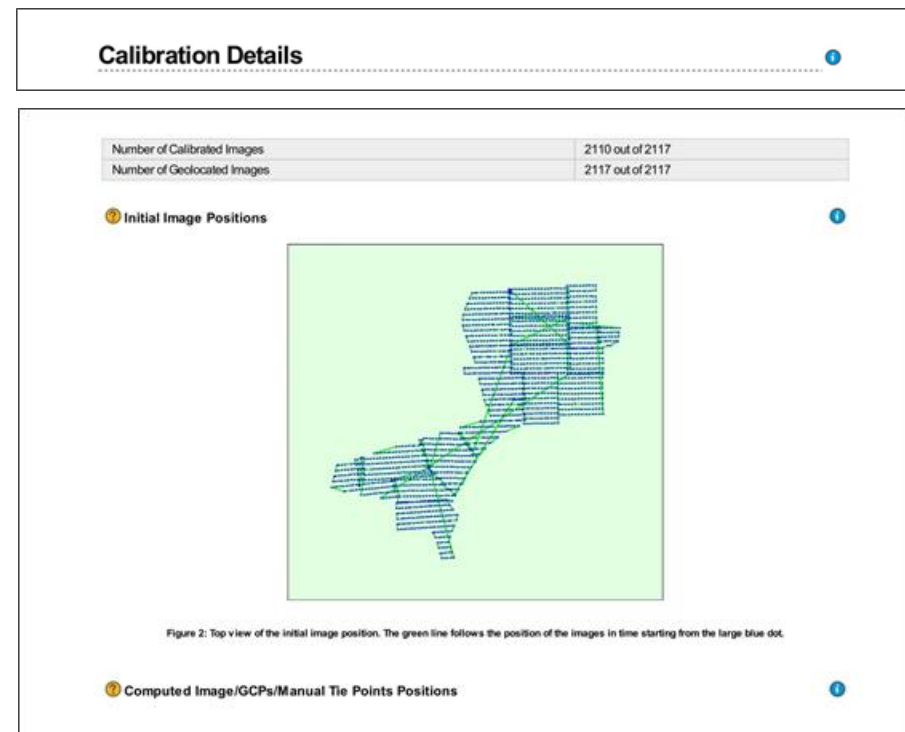
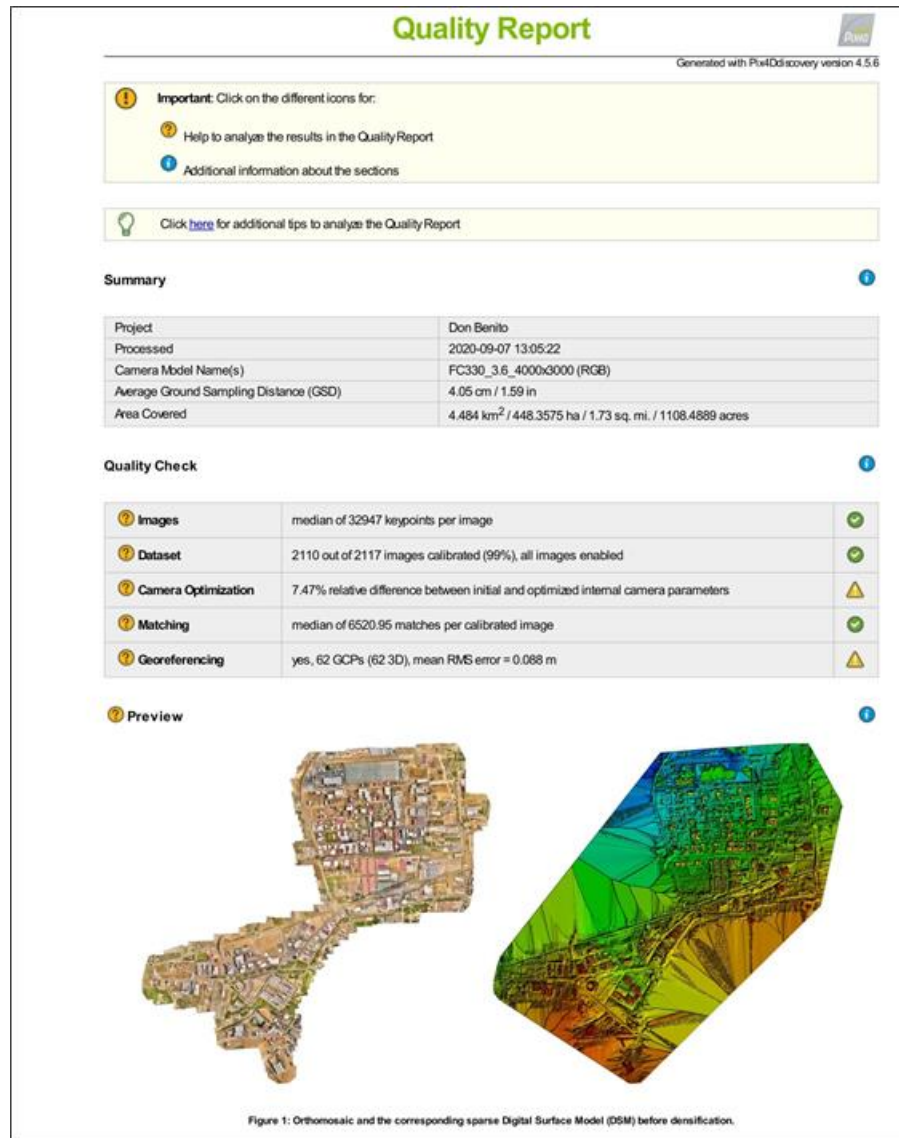


Figure A 2. Distribution of the control points in Plasencia industrial estate.

APPENDIX II. QUALITY REPORT OF DON BENITO





Uncertainty ellipses 500x magnified

Figure 3: Offset between initial (blue dots) and computed (green dots) image positions as well as the offset between the GCP's initial positions (blue crosses) and their computed positions (blue crosses) in the top-view (XY plane), front-view (XZ plane), and side-view (YZ plane). Red dots indicate disabled or uncalibrated images. Dark green ellipses indicate the absolute position uncertainty of the bundle block adjustment result.

2 Absolute camera position and orientation uncertainties

	X[m]	Y[m]	Z[m]	Omega [degree]	Phi [degree]	Kappa [degree]
Mean	0.030	0.025	0.100	0.012	0.015	0.005
Sigma	0.013	0.010	0.007	0.005	0.006	0.003

3 Overlap



Number of overlapping images: 1 2 3 4 5+

Figure 4: Number of overlapping images computed for each pixel of the orthomosaic. Red and yellow areas indicate low overlap for which poor results may be generated. Green areas indicate an overlap of over 5 images for every pixel. Good quality results will be generated as long as the number of keypoint matches is also sufficient for these areas (see Figure 5 for keypoint matches).

Bundle Block Adjustment Details

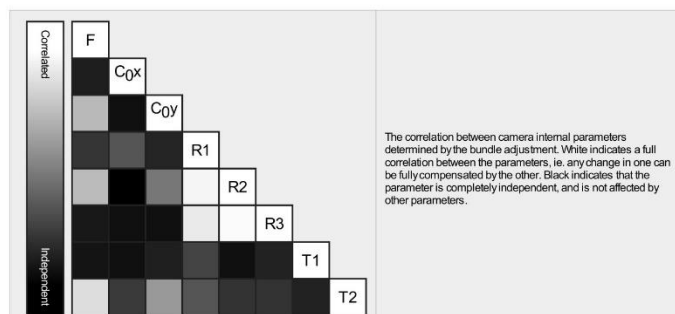
Number of 2D Keypoint Observations for Bundle Block Adjustment	15425490
Number of 3D Points for Bundle Block Adjustment	5044170
Mean Reprojection Error [pixels]	0.190

Internal Camera Parameters

FC330_3.6_4000x3000 (RGB). Sensor Dimensions: 6.317 [mm] x 4.738 [mm]

EXIF ID: FC330_3.6_4000x3000

	Focal Length	Principal Point x	Principal Point y	R1	R2	R3	T1	T2
Initial Values	2285.714 [pixel] 3.610 [mm]	2000.000 [pixel] 3.159 [mm]	1500.000 [pixel] 2.369 [mm]	0.000	0.000	0.000	0.000	0.000
Optimized Values	2456.584 [pixel] 3.880 [mm]	1991.729 [pixel] 3.146 [mm]	1506.135 [pixel] 2.379 [mm]	-0.007	0.001	-0.001	0.000	0.000
Uncertainties (Sigma)	2.423 [pixel] 0.004 [mm]	0.096 [pixel] 0.000 [mm]	0.113 [pixel] 0.000 [mm]	0.000	0.000	0.000	0.000	0.000



The number of Automatic Tie Points (ATPs) per pixel, averaged over all images of the camera model, is color coded between black and white. White indicates that, on average, more than 16 ATPs have been extracted at the pixel location. Black indicates that, on average, 0 ATPs have been extracted at the pixel location. Click on the image to see the average direction and magnitude of the re-projection error for each pixel. Note that the vectors are scaled for better visualization. The scale bar indicates the magnitude of 1 pixel error.

2D Keypoints Table

	Number of 2D Keypoints per Image	Number of Matched 2D Keypoints per Image
Median	32947	6521
Mn	12715	382
Max	74065	39241
Mban	33276	7311

3D Points from 2D Keypoint Matches

	Number of 3D Points Observed
In 2 Images	2900003
In 3 Images	980159
In 4 Images	435139
In 5 Images	246603
In 6 Images	169606
In 7 Images	110747
In 8 Images	72631
In 9 Images	50607
In 10 Images	33447
In 11 Images	21628
In 12 Images	12086
In 13 Images	5183
In 14 Images	2561
In 15 Images	1564
In 16 Images	953
In 17 Images	557
In 18 Images	292
In 19 Images	215
In 20 Images	107
In 21 Images	53
In 22 Images	21

In 23 Images

8

2D Keypoint Matches

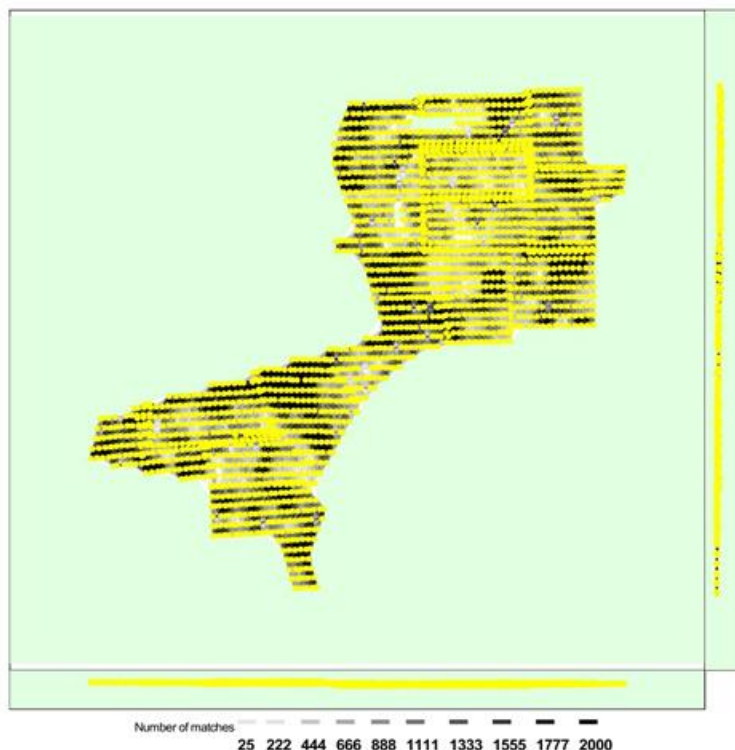


Figure 5: Computed image positions with links between matched images. The darkness of the links indicates the number of matched 2D keypoints between the images. Bright links indicate weak links and require manual tie points or more images.

Geolocation Details

Ground Control Points

GCP Name	Accuracy XYZ [m]	Error X [m]	Error Y [m]	Error Z [m]	Projection Error [pixel]	Verified/Marked
50 (3D)	0.020/ 0.020	0.066	-0.055	-0.006	1.229	16 / 16
7 (3D)	0.020/ 0.020	0.009	-0.028	0.002	0.355	9 / 9
8 (3D)	0.020/ 0.020	0.011	0.058	-0.022	0.738	6 / 6
59 (3D)	0.020/ 0.020	0.010	0.154	-0.075	0.693	7 / 7
49 (3D)	0.020/ 0.020	0.191	-0.017	-0.035	1.763	12 / 12

55 (3D)	0.020/0.020	0.031	0.206	-0.013	0.754	10/10
9 (3D)	0.020/0.020	0.037	0.230	0.001	1.955	12/12
46 (3D)	0.020/0.020	-0.032	0.270	0.050	0.759	9/9
47 (3D)	0.020/0.020	-0.034	0.067	0.008	0.836	11/11
48 (3D)	0.020/0.020	0.097	0.012	-0.011	0.693	11/11
4 (3D)	0.020/0.020	0.234	-0.045	-0.017	0.619	9/9
5 (3D)	0.020/0.020	0.034	-0.033	0.026	0.873	9/9
56 (3D)	0.020/0.020	-0.089	-0.042	0.012	0.666	10/10
6 (3D)	0.020/0.020	-0.237	-0.171	-0.004	2.519	11/11
54 (3D)	0.020/0.020	-0.244	-0.125	-0.003	1.038	10/10
52 (3D)	0.020/0.020	-0.025	-0.077	-0.028	0.706	10/10
53 (3D)	0.020/0.020	0.119	-0.016	0.005	0.454	9/9
51 (3D)	0.020/0.020	0.092	-0.177	-0.016	0.661	7/7
3 (3D)	0.020/0.020	0.084	0.002	-0.012	0.457	7/7
2 (3D)	0.020/0.020	-0.148	0.020	-0.022	2.183	9/9
58 (3D)	0.020/0.020	0.134	-0.090	0.023	0.621	6/6
57 (3D)	0.020/0.020	-0.055	-0.084	0.022	0.694	9/9
1 (3D)	0.020/0.020	-0.001	-0.005	-0.004	0.382	10/10
45 (3D)	0.020/0.020	-0.232	-0.029	-0.047	0.590	6/6
44 (3D)	0.020/0.020	-0.033	0.041	0.002	0.504	9/9
62 (3D)	0.020/0.020	0.071	0.119	-0.035	0.341	7/7
61 (3D)	0.020/0.020	0.119	0.086	0.010	0.535	9/9
63 (3D)	0.020/0.020	-0.055	-0.208	-0.015	0.379	6/6
10 (3D)	0.020/0.020	0.104	-0.002	-0.005	0.403	10/10
65 (3D)	0.020/0.020	-0.062	-0.126	0.003	0.420	6/6
11 (3D)	0.020/0.020	0.060	-0.234	0.011	0.596	7/7
37 (3D)	0.020/0.020	-0.148	-0.251	-0.000	0.850	9/9
38 (3D)	0.020/0.020	0.034	-0.204	-0.016	0.395	5/5
23 (3D)	0.020/0.020	-0.027	-0.038	-0.052	3.058	7/7
36 (3D)	0.020/0.020	-0.188	-0.185	0.025	0.631	9/9
39 (3D)	0.020/0.020	-0.060	-0.165	-0.019	1.007	15/15
41 (3D)	0.020/0.020	0.078	-0.068	-0.092	3.051	13/13
40 (3D)	0.020/0.020	0.107	0.005	-0.018	1.344	13/13
42 (3D)	0.020/0.020	0.108	-0.040	-0.018	1.065	18/18
12 (3D)	0.020/0.020	0.068	0.022	-0.005	0.846	12/12
35 (3D)	0.020/0.020	-0.045	-0.079	-0.002	0.810	15/15
22 (3D)	0.020/0.020	-0.255	-0.139	0.018	0.981	8/8
34 (3D)	0.020/0.020	-0.216	-0.025	-0.010	0.740	14/14
32 (3D)	0.020/0.020	0.011	0.060	0.002	1.119	21/21
33 (3D)	0.020/0.020	0.026	-0.010	-0.002	0.679	9/9
31 (3D)	0.020/0.020	0.009	-0.027	-0.007	0.554	10/10
29 (3D)	0.020/0.020	0.044	0.037	0.007	0.603	11/11
14 (3D)	0.020/0.020	0.030	-0.150	-0.038	0.624	7/7
15 (3D)	0.020/0.020	0.121	0.068	-0.090	0.532	5/5
16 (3D)	0.020/0.020	0.134	0.033	-0.006	0.660	10/10
60 (3D)	0.020/0.020	0.080	-0.005	-0.012	0.475	11/11
30 (3D)	0.020/0.020	0.157	-0.011	-0.001	0.546	19/19
17 (3D)	0.020/0.020	0.062	0.072	-0.024	0.540	9/9
26 (3D)	0.020/0.020	-0.006	0.279	-0.006	0.509	15/15
27 (3D)	0.020/0.020	0.048	0.252	-0.040	0.790	12/12
28 (3D)	0.020/0.020	0.112	0.261	0.040	0.708	7/7
25 (3D)	0.020/0.020	-0.061	0.233	0.021	1.022	16/16
102 (3D)	0.020/0.020	-0.080	0.091	-0.042	2.291	20/20
24 (3D)	0.020/0.020	-0.131	0.116	-0.003	2.837	14/14
43 (3D)	0.020/0.020	-0.195	0.176	0.014	0.692	13/13
20 (3D)	0.020/0.020	-0.022	0.043	0.003	0.377	10/10
18 (3D)	0.020/0.020	-0.061	-0.015	-0.055	2.369	7/7
Mean [m]		-0.000132	0.000624	-0.010041		
Sigma [m]		0.111384	0.127184	0.026763		

RMS Error [m]	0.111384	0.127186	0.028584	
---------------	----------	----------	----------	--

Localisation accuracy per GCP and mean errors in the three coordinate directions. The last column counts the number of calibrated images where the GCP has been automatically verified v.s. manually marked.

Absolute Geolocation Variance

Mn Error [m]	Max Error [m]	Geolocation Error X[%]	Geolocation Error Y[%]	Geolocation Error Z[%]
-	-15.00	0.00	0.00	26.45
-15.00	-12.00	0.00	0.00	0.00
-12.00	-9.00	0.09	0.00	0.00
-9.00	-6.00	9.19	0.00	0.00
-6.00	-3.00	11.66	1.37	0.00
-3.00	0.00	27.16	46.68	0.00
0.00	3.00	29.48	51.75	8.01
3.00	6.00	15.73	0.19	17.25
6.00	9.00	6.59	0.00	20.33
9.00	12.00	0.09	0.00	9.00
12.00	15.00	0.00	0.00	8.77
15.00	-	0.00	0.00	10.19
Mean [m]		0.292199	1.163731	-49.729671
Sigma [m]		3.897366	1.169674	15.024040
RMS Error [m]		3.908304	1.649972	51.949610

Min Error and Max Error represent geolocation error intervals between -1.5 and 1.5 times the maximum accuracy of all the images. Columns X, Y, Z show the percentage of images with geolocation errors within the predefined error intervals. The geolocation error is the difference between the initial and computed image positions. Note that the image geolocation errors do not correspond to the accuracy of the observed 3D points.

Geolocation Bias	X	Y	Z
Translation [m]	0.292199	1.163731	-49.729671

Bias between image initial and computed geolocation given in output coordinate system.

Relative Geolocation Variance

Relative Geolocation Error	Images X[%]	Images Y[%]	Images Z[%]
[-1.00, 1.00]	75.36	100.00	49.43
[-2.00, 2.00]	99.95	100.00	76.26
[-3.00, 3.00]	100.00	100.00	99.62
Mean of Geolocation Accuracy [m]	5.000000	5.000000	10.000000
Sigma of Geolocation Accuracy [m]	0.000000	0.000000	0.000000

Images X, Y, Z represent the percentage of images with a relative geolocation error in X, Y, Z.

Geolocation Orientational Variance	RMS [degree]
Omega	0.510
Phi	1.166
Kappa	4.377

Geolocation RMS error of the orientation angles given by the difference between the initial and computed image orientation angles.

Initial Processing Details

System Information

Hardware	CPU: Intel(R) Core(TM) i7-8700 CPU @ 3.20GHz RAM: 32GB GPU: Intel(R) UHD Graphics 630 (Driver: 23.20.16.4974), NVIDIA Quadro P3200 (Driver: 23.21.13.9174)
Operating System	Windows 10 Pro, 64-bit

Coordinate Systems

Image Coordinate System	WGS 84 (EGM96 Geoid)
Ground Control Point (GCP) Coordinate System	WGS 84 / UTMzone 30N (EGM96 Geoid)
Output Coordinate System	WGS 84 / UTMzone 30N (EGM96 Geoid)

Processing Options

Detected Template	No Template Available
Keypoints Image Scale	Full, Image Scale: 1
Advanced: Matching Image Pairs	Aerial Grid or Corridor
Advanced: Matching Strategy	Use Geometrically Verified Matching: no
Advanced: Keypoint Extraction	Targeted Number of Keypoints: Automatic
Advanced: Calibration	Calibration Method: Standard Internal Parameters Optimization: All External Parameters Optimization: All Rematch: Auto, no

Point Cloud Densification details

Processing Options

Image Scale	multiscale, 1/2 (Half image size, Default)
Point Density	Optimal
Minimum Number of Matches	3
3D Textured Mesh Generation	yes
3D Textured Mesh Settings:	Resolution: Medium Resolution (default) Color Balancing: no
LOD	Generated: no
Advanced: 3D Textured Mesh Settings	Sample Density Divider: 1
Advanced: Image Groups	group1
Advanced: Use Processing Area	yes
Advanced: Use Annotations	yes

Results

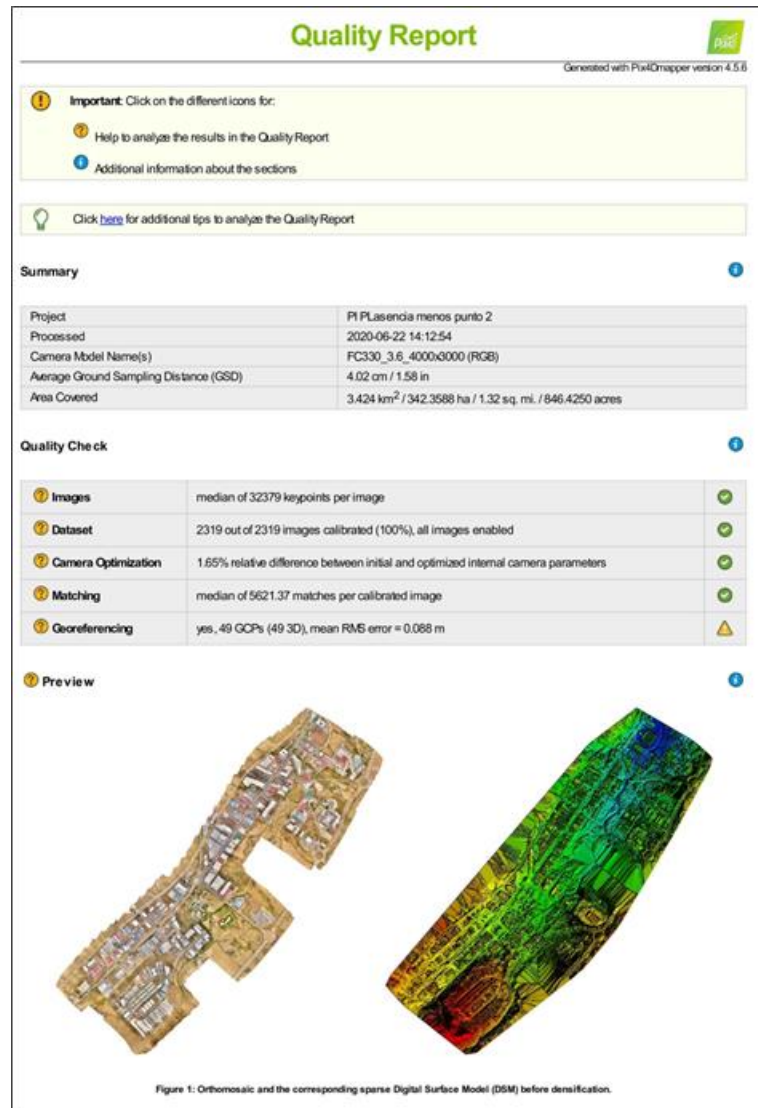
Number of Generated Tiles	7
Number of 3D Densified Points	192955370
Average Density (per m ³)	48.49

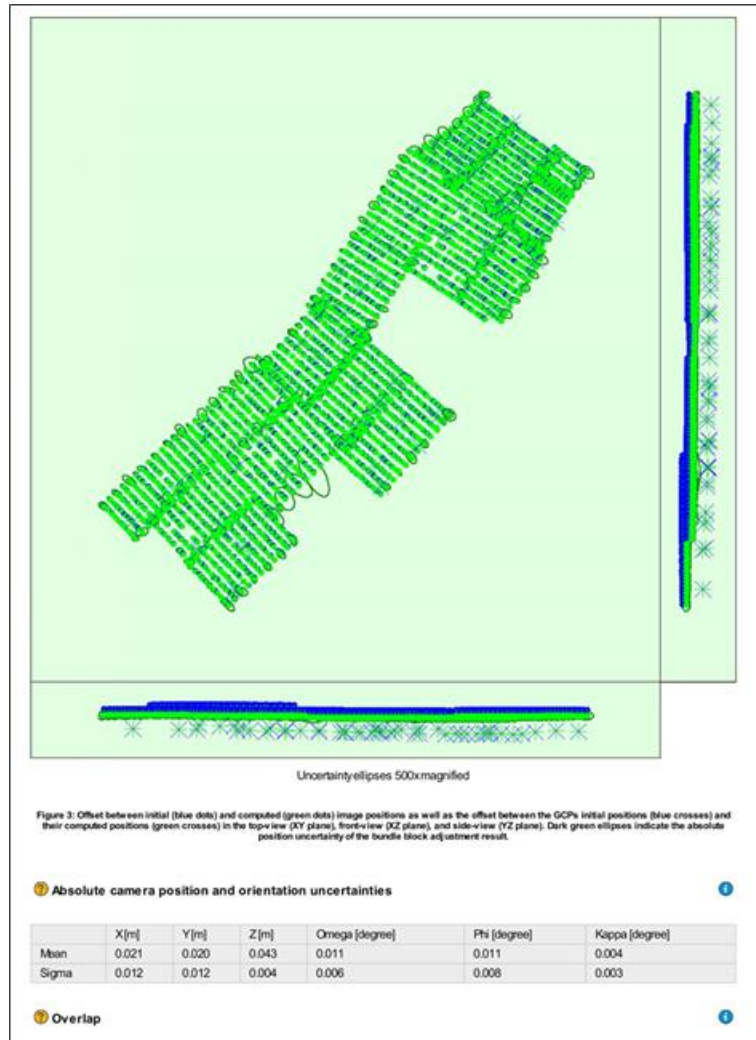
DSM, Orthomosaic and Index Details

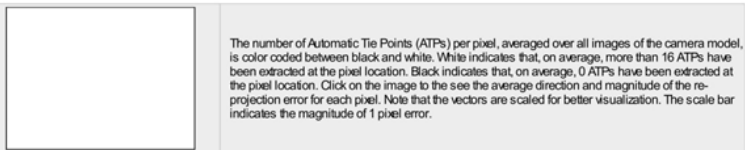
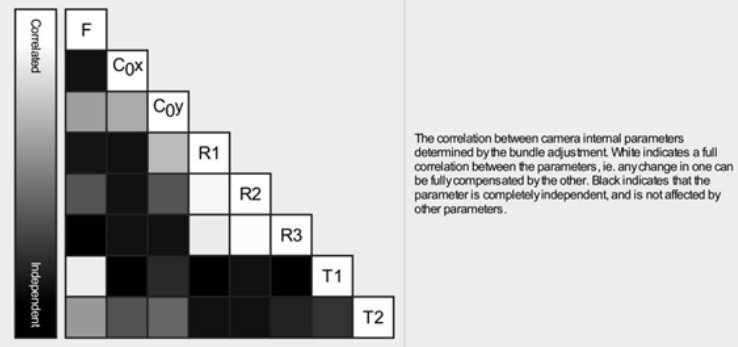
Processing Options

DSM and Orthomosaic Resolution	2 x GSD (4.05 [cm/pixel])
DSM Filters	Noise Filtering: yes Surface Smoothing: yes, Type: Sharp

APPENDIX III. QUALITY REPORT OF PLASENCIA







2D Keypoints Table

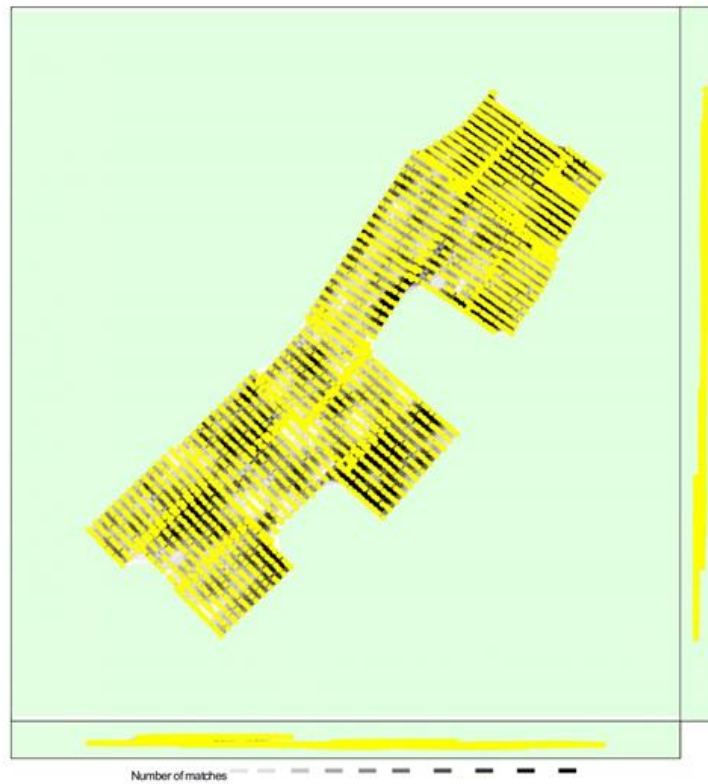
	Number of 2D Keypoints per Image	Number of Matched 2D Keypoints per Image
Median	32379	5621
Mn	14334	216
Max	60078	22638
Mean	32420	6061

3D Points from 2D Keypoint Matches

	Number of 3D Points Observed
In 2 Images	2770008
In 3 Images	772807
In 4 Images	348561
In 5 Images	187129
In 6 Images	117272
In 7 Images	79958
In 8 Images	56714
In 9 Images	40947
In 10 Images	31968
In 11 Images	23830
In 12 Images	17013
In 13 Images	12114
In 14 Images	9516
In 15 Images	7734
In 16 Images	6395
In 17 Images	5162
In 18 Images	4020
In 19 Images	3245
In 20 Images	2704
In 21 Images	2100
In 22 Images	1648

In 23 Images	1166
In 24 Images	876
In 25 Images	681
In 26 Images	532
In 27 Images	440
In 28 Images	338
In 29 Images	253
In 30 Images	235
In 31 Images	160
In 32 Images	118
In 33 Images	91
In 34 Images	52
In 35 Images	45
In 36 Images	15
In 37 Images	3
In 38 Images	2

2D Keypoint Matches



25 222 444 666 888 1111 1333 1555 1777 2000

Figure 5: Computed image positions with links between matched images. The darkness of the links indicates the number of matched 2D keypoints between the images. Bright links indicate weak links and require manual tie points or more images.

Geolocation Details

Ground Control Points

GCP Name	Accuracy XYZ [m]	Error X [m]	Error Y [m]	Error Z [m]	Projection Error [pixel]	Verified/Marked
40 (3D)	0.020/0.020	0.136	0.037	-0.033	0.573	11 / 11
46 (3D)	0.020/0.020	0.032	0.241	-0.021	0.590	15 / 15
35 (3D)	0.020/0.020	0.080	-0.028	0.012	0.672	27 / 27
25 (3D)	0.020/0.020	-0.016	-0.082	0.012	0.609	14 / 14
37 (3D)	0.020/0.020	-0.170	-0.097	0.004	0.508	16 / 16
33 (3D)	0.020/0.020	-0.099	-0.076	0.002	0.380	13 / 13
51 (3D)	0.020/0.020	-0.239	0.078	-0.016	0.696	19 / 19
34 (3D)	0.020/0.020	-0.198	0.187	-0.000	1.222	10 / 10
39 (3D)	0.020/0.020	-0.027	0.214	0.015	0.562	10 / 10
38 (3D)	0.020/0.020	-0.065	0.054	0.027	0.786	38 / 38
45 (3D)	0.020/0.020	0.016	0.276	-0.006	0.572	16 / 16
30 (3D)	0.020/0.020	0.216	-0.099	-0.015	0.365	10 / 10
32 (3D)	0.020/0.020	-0.221	-0.082	0.014	0.654	24 / 24
49 (3D)	0.020/0.020	-0.196	0.033	0.018	0.478	8 / 8
50 (3D)	0.020/0.020	0.176	-0.109	-0.021	0.384	10 / 10
20 (3D)	0.020/0.020	0.143	-0.098	-0.012	0.464	10 / 10
24 (3D)	0.020/0.020	-0.024	0.129	0.018	0.605	13 / 13
23 (3D)	0.020/0.020	-0.020	0.071	0.031	0.445	8 / 8
14 (3D)	0.020/0.020	0.120	0.163	0.033	0.892	18 / 18
13 (3D)	0.020/0.020	0.049	0.018	-0.025	0.743	20 / 20
18 (3D)	0.020/0.020	-0.035	0.082	-0.001	0.407	11 / 11
8 (3D)	0.020/0.020	-0.143	-0.076	0.012	0.858	18 / 18
19 (3D)	0.020/0.020	-0.130	-0.052	0.006	0.390	11 / 11
1 (3D)	0.020/0.020	-0.065	0.200	-0.032	0.615	12 / 12
5 (3D)	0.020/0.020	-0.119	0.107	-0.003	0.490	17 / 17
4 (3D)	0.020/0.020	-0.129	0.004	-0.009	0.442	13 / 13
47 (3D)	0.020/0.020	-0.107	-0.145	-0.012	2.111	16 / 16
3 (3D)	0.020/0.020	-0.019	-0.050	0.003	0.421	10 / 10
17 (3D)	0.020/0.020	-0.209	0.085	-0.031	1.000	7 / 7
16 (3D)	0.020/0.020	-0.039	-0.004	-0.015	0.355	11 / 11
15 (3D)	0.020/0.020	0.023	0.214	-0.012	0.646	12 / 12
22 (3D)	0.020/0.020	0.073	-0.015	0.023	0.845	12 / 12
27 (3D)	0.020/0.020	-0.007	0.058	-0.013	0.556	18 / 18
28 (3D)	0.020/0.020	-0.070	0.024	0.028	0.751	8 / 8
29 (3D)	0.020/0.020	0.025	-0.043	-0.008	0.696	15 / 15
31 (3D)	0.020/0.020	0.233	-0.031	-0.007	0.525	15 / 15
41 (3D)	0.020/0.020	0.244	-0.184	-0.021	0.611	17 / 17
42 (3D)	0.020/0.020	0.204	-0.093	-0.023	0.471	22 / 22
43 (3D)	0.020/0.020	0.071	0.041	0.011	0.753	27 / 27
36 (3D)	0.020/0.020	-0.082	-0.067	-0.012	0.698	12 / 12
21 (3D)	0.020/0.020	0.152	-0.154	-0.036	0.487	8 / 8
9 (3D)	0.020/0.020	0.065	-0.073	0.006	0.366	16 / 16
10 (3D)	0.020/0.020	0.250	-0.173	-0.022	0.946	11 / 11
2 (3D)	0.020/0.020	0.177	-0.164	0.001	0.917	18 / 18
7 (3D)	0.020/0.020	0.069	-0.167	0.020	0.819	19 / 19
48 (3D)	0.020/0.020	-0.023	0.003	0.015	0.652	23 / 23

11 (3D)	0.020/0.020	0.002	-0.004	0.030	0.530	12 / 12
12 (3D)	0.020/0.020	-0.186	0.114	-0.020	0.461	7 / 7
6 (3D)	0.020/0.020	-0.050	-0.030	-0.045	0.659	11 / 11
Mean [m]		-0.002676	0.004844	-0.002637		
Sigma [m]		0.131070	0.116109	0.019400		
RMS Error [m]		0.131098	0.116210	0.019578		

Localisation accuracy per GCP and mean errors in the three coordinate directions. The last column counts the number of calibrated images where the GCP has been automatically verified vs. manually marked.

Absolute Geolocation Variance

Mn Error [m]	Mx Error [m]	Geolocation Error X [%]	Geolocation Error Y [%]	Geolocation Error Z [%]
-	-15.00	0.00	0.00	0.00
-15.00	-12.00	0.00	0.00	1.34
-12.00	-9.00	0.00	0.00	14.96
-9.00	-6.00	2.41	0.82	12.68
-6.00	-3.00	12.25	10.65	2.54
-3.00	0.00	33.94	39.84	4.44
0.00	3.00	36.96	36.57	12.68
3.00	6.00	12.46	11.56	36.48
6.00	9.00	1.98	0.52	14.88
9.00	12.00	0.00	0.04	0.00
12.00	15.00	0.00	0.00	0.00
15.00	-	0.00	0.00	0.00
Mean [m]		0.114815	1.767127	34.451203
Sigma [m]		2.853023	2.495562	6.508554
RMS Error [m]		2.855332	3.057870	35.060615

Min Error and Max Error represent geolocation error intervals between -1.5 and 1.5 times the maximum accuracy of all the images. Columns X, Y, Z show the percentage of images with geolocation errors within the predefined error intervals. The geolocation error is the difference between the initial and computed image positions. Note that the image geolocation errors do not correspond to the accuracy of the observed 3D points.

Geolocation Bias	X	Y	Z
Translation [m]	0.114815	1.767127	34.451203

Bias between image initial and computed geolocation given in output coordinate system.

Relative Geolocation Variance

Relative Geolocation Error	Images X [%]	Images Y [%]	Images Z [%]
[-1.00, 1.00]	89.95	94.74	89.13
[-2.00, 2.00]	100.00	99.96	100.00
[-3.00, 3.00]	100.00	100.00	100.00
Mean of Geolocation Accuracy [m]	5.000000	5.000000	10.000000
Sigma of Geolocation Accuracy [m]	0.000000	0.000000	0.000000

Images X, Y, Z represent the percentage of images with a relative geolocation error in X, Y, Z.

Geolocation Orientation Variance	RMS [degree]
Omega	0.844
Phi	1.071
Kappa	5.129

Geolocation RMS error of the orientation angles given by the difference between the initial and computed image orientation angles.

Initial Processing Details

System Information

Hardware	CPU: Intel(R) Core(TM) i7-8700 CPU @ 3.20GHz RAM: 32GB GPU: NVIDIA Quadro P3200 (Driver: 23.21.13.9174)
Operating System	Windows 10 Pro, 64-bit

Coordinate Systems

Image Coordinate System	WGS 84 (EGM96 Geoid)
Ground Control Point (GCP) Coordinate System	WGS 84 / UTMzone 29N (EGM96 Geoid)
Output Coordinate System	WGS 84 / UTMzone 29N (EGM96 Geoid)

Processing Options

Detected Template	3D Maps
Keypoints Image Scale	Full, Image Scale: 1
Advanced: Matching Image Pairs	Aerial Grid or Corridor
Advanced: Matching Strategy	Use Geometrically Verified Matching: no
Advanced: Keypoint Extraction	Targeted Number of Keypoints: Automatic
Advanced: Calibration	Calibration Method: Standard Internal Parameters Optimization: All External Parameters Optimization: All Rematch: Auto, no

Point Cloud Densification details

Processing Options

Image Scale	multiscale, 1/2 (Half image size, Default)
Point Density	Optimal
Minimum Number of Matches	3
3D Textured Mesh Generation	yes
3D Textured Mesh Settings:	Resolution: Medium Resolution (default) Color Balancing: no
LOD	Generated: no
Advanced: 3D Textured Mesh Settings	Sample Density Divider: 1
Advanced: Image Groups	group1
Advanced: Use Processing Area	yes
Advanced: Use Annotations	yes
Time for Point Cloud Densification	03h:06m:36s
Time for Point Cloud Classification	NA
Time for 3D Textured Mesh Generation	30m:14s

Results

Number of Processed Clusters	7
Number of Generated Tiles	7
Number of 3D Densified Points	183679880
Average Density (per m ³)	54.83

DSM, Orthomosaic and Index Details

Processing Options

DSM and Orthomosaic Resolution	2 x GSD (4.02 [cm/pixel])
DSM Filters	Noise Filtering: yes Surface Smoothing: yes, Type: Sharp
Raster DSM	Generated: yes Method: Inverse Distance Weighting Merge Tiles: yes
Orthomosaic	Generated: yes Merge Tiles: yes GeoTIFF Without Transparency: no Google Maps Tiles and KML: no
Grid DSM	Generated: yes, Spacing [cm]: 50
Time for DSM Generation	22m:18s
Time for Orthomosaic Generation	46m:36s
Time for DTM Generation	00s
Time for Contour Lines Generation	00s
Time for Reflectance Map Generation	00s
Time for Index Map Generation	00s

APPENDIX IV. GEOWEB GSOLARROOF USER MANUAL

This guide describes the working of the geoweb of the project that provides users access to information about solar energy through search, visualization and navigation tools on a map.

In the geoweb, users can consult data related to each building of the industrial estates of the municipalities of Plasencia and Don Benito, considering the cadastre plot as the basic unit of representation. In its design, an attempt has been made to present a simple and easy to understand interface that includes the following functionalities:

- Pop-ups.
- Control widget.
- Utilities widget.
- Depolyable widget.

POP-UPS

Pop-ups are generated by selecting any building on the map and show its basic data with a brief description of its characteristics in an attachment pdf file that can be downloaded.



Figure A 3 Pop-ups of buildings.

CONTROL WIDGET

ADDRESS SEARCH

Allows users to search for locations by addresses on the map. Being an international search system, you must specify the municipality corresponding to the address.

When the name of a location is entered in the search box, suggestions for different locations appear as in any address search system.

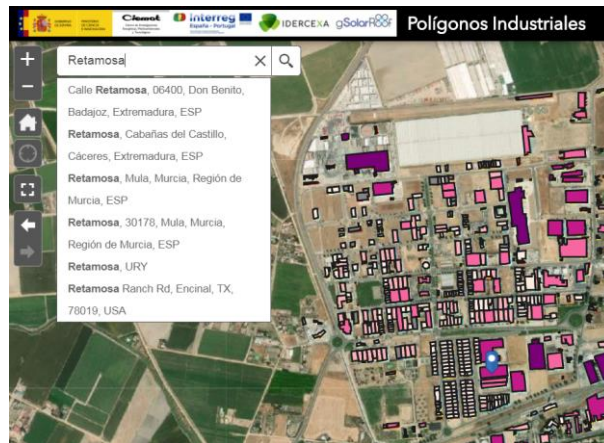


Figure A 4 Widget 'Address search'.

A pop-up appears at the location in that position with the available information.

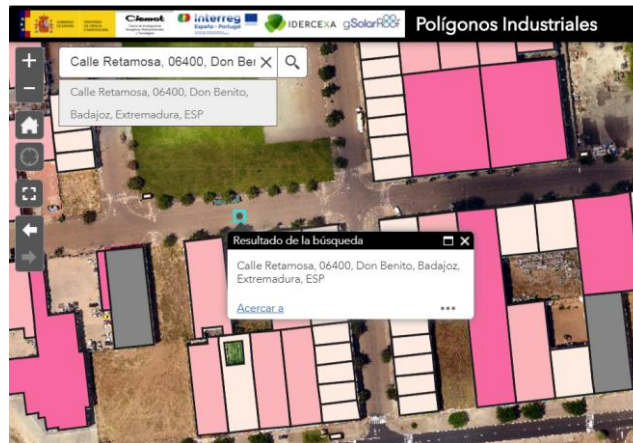


Figure A 5. Result widget 'Address search'.

ZOOM SLIDER

Buttons to zoom in (+) or zoom out (-) the map view.



Figure A 6. Widget 'Zoom slider'.

To control the zoom in the map display it is also possible to use the mouse wheel. Additionally, you can press and hold the 'Shift' key and drag a box on the map.

You use the arrow keys to pan around the map. Another way to scroll is to hold down the mouse and drag.

HOME BUTTON

Sets the view to the extent of the initial map.

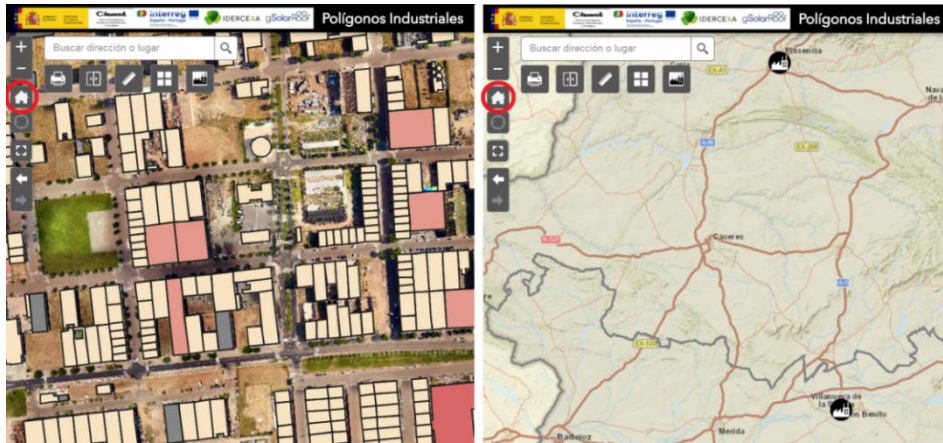


Figure A 7 Widget 'Home button'.

MY LOCATION

If the computer has GPS, the system detects its location and zooms by centring the map view on that position.



Figure A 8. Widget 'My location'.

FULL SCREEN

Using full screen mode to view the map. To exit this view and recover the previous situation, use the button or press the 'Esc' key.



Figure A 9 Widget 'Full screen'.

EXTENT NAVIGATE

Browse the map recovering the extent of the previous views, moving forward and backward through all those that have been previously viewed.



Figure A 10 Widget 'Extent navigate'.

OVERVIEW MAP

Drop-down button that shows the position and extent of the visible window, at any time as a rectangle within the general view of the map. It allows its movement to modify the position of the current view.

To expand the image, use the maximize icon  and to hide the map overview, select the icon .

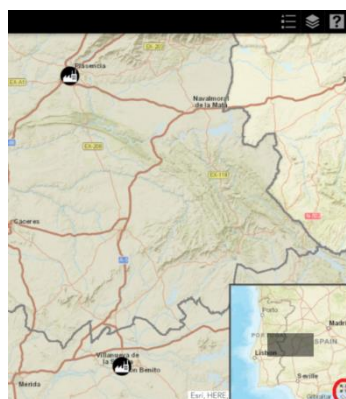


Figure A 11 Widget 'Overview map'.

UTILITIES WIDGET

BOOKMARK INDUSTRIAL ESTATES

Displays a list with the industrial estates defined on the map. Where one of them is selected the view centres the map on its location.

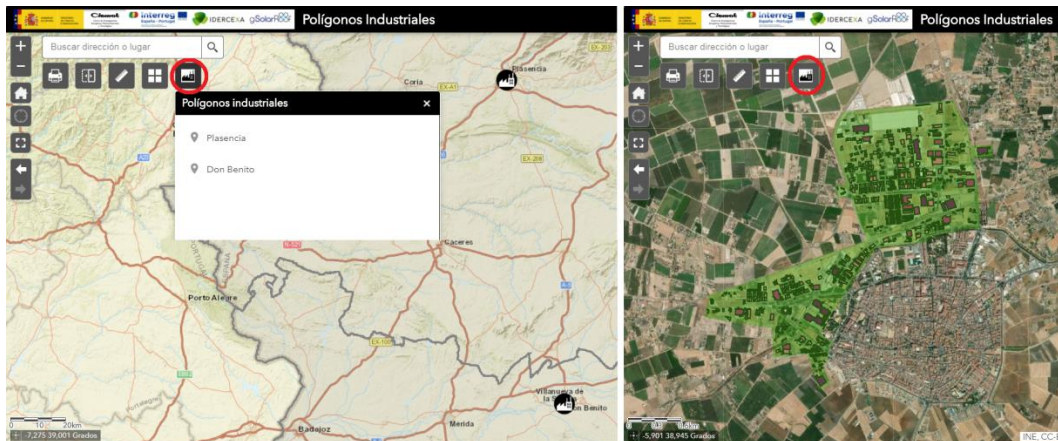


Figure A 12 Widget 'Bookmark industrial estate'.

BASEMAP GALLERY


It presents a set of basemaps and allows the user to change it for one that suits them best. The map represents physical maps or satellite images to road maps.



Figure A 13 Widget 'Basemap gallery'.

MEASUREMENT

Measure the area of a polygon, the length of a line, or find the coordinates of a point:

1. Area measurement : Select the area measurement icon, and then draw a polygon on the map. To finish drawing the polygon, double click. You can change the area units in the drop-down menu.



2. Distance measurement : Select the distance measurement icon, then draw a line on the map with two or more points. To finish drawing the line, double click. Distance units can be changed in the drop-down menu.
3. Point measurement : Select the location measurement icon, and then mark a point on the map. The coordinates of the point are displayed in degrees. You can change the coordinate display format to degrees / minutes / seconds from the drop-down menu.



Figure A 14 Widget 'Measurement'.

'Delete' is to remove from the map the measurements.

SWIPE

This is a slider that allows you to compare two layers displayed simultaneously on the map.



Figure A 15 Widget 'Swipe'.

Always compare the visible marked layer with the one immediately below it. In order for the layers to be displayed correctly, in the drop-down window that is generated when the application is run, the top layer currently visible must be selected.

Once activated, slide the tool to show the contents of the visible layers of the map.

Select the 'Swipe' icon to disable it.

PRINT

Allows the users to print the current map view with different image formats:

1. Select the 'Map title', 'Design' and 'Format' for the map you want to export. The MAP_ONLY format shows the map on print but not additional information such as the title or legend.
2. In the 'Advanced' tab there is a menu with the printing options to set the scale, author and quality of the printing.
3. After setting the map options, when the printing process is complete, the map can be downloaded.
4. Once the printing is finished, it is possible to remove the printing history in the "Delete printing" tab.

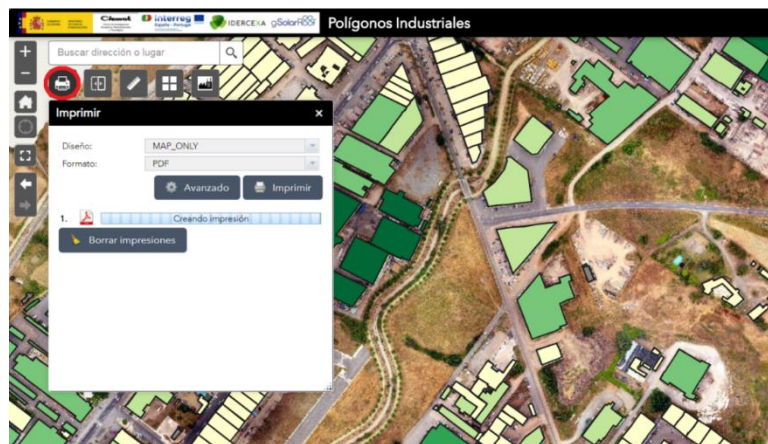


Figure A 16 Widget 'Print'.

DROP-DOWN BUTTONS

LEGEND

Shows the legend corresponding to the layers visible at all times.



Figure A 17. Widget 'Legend'.

LAYER LIST

Shows the information layers. Checking or unchecking the box of each layer can make them visible or not.

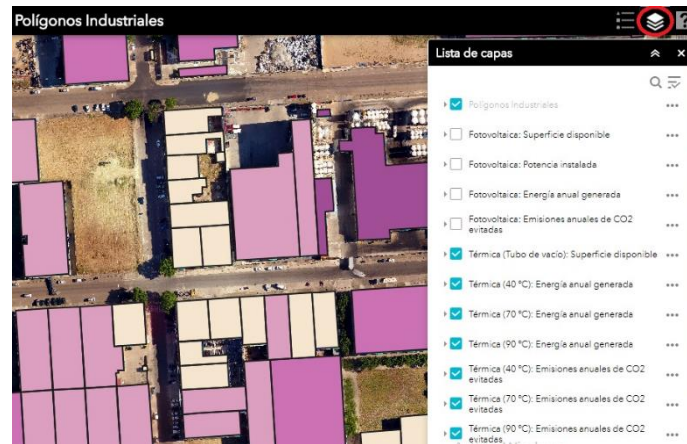


Figure A 18. Widget 'Layer list'.

By marking each of the layers its symbology is shown and using the drop-down menu they are activated and expanded.

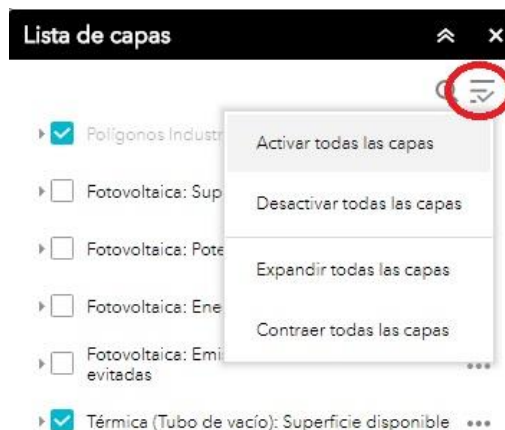


Figure A 19. Drop-down of widget 'Layer list'.

Using the drop-down menu of each layer with the icon (...), options appear to zoom in on the layer in the map view, modify the transparency of the colour and move them up or down in the list.



Figure A 20. Drop-down options of a layer.

HELP

User manual with a brief description of the operation of the tools, buttons and pop-up.



Figure A 21. Widget 'Help'.

APPENDIX V. THEMATIC MAPS OF DON BENITO INDUSTRIAL ESTATE

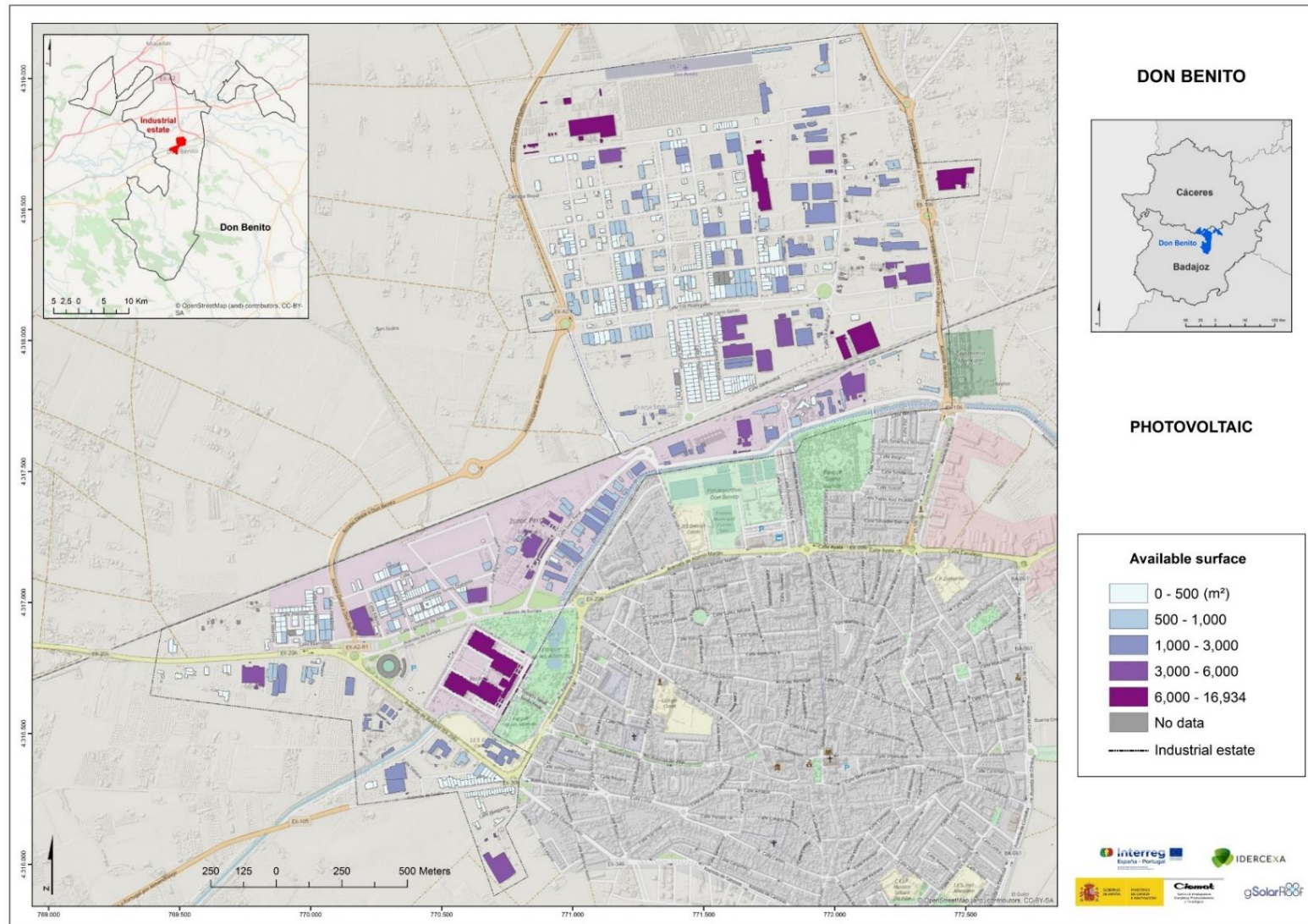


Figure A 22. Photovoltaic: Available surface of rooftop. Don Benito.

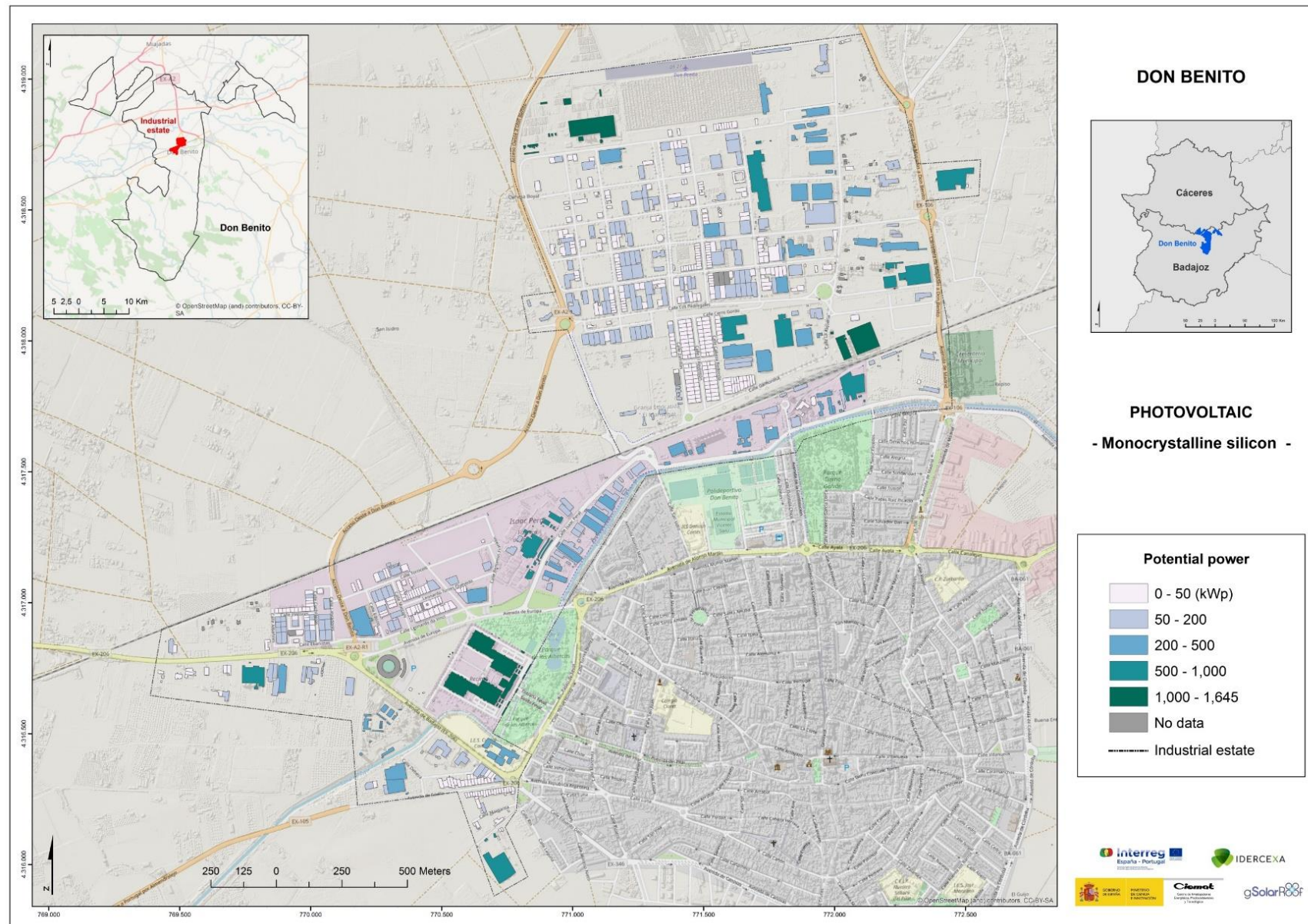


Figure A 23. Photovoltaic: Potential power (Monocrystalline silicon module). Don Benito.

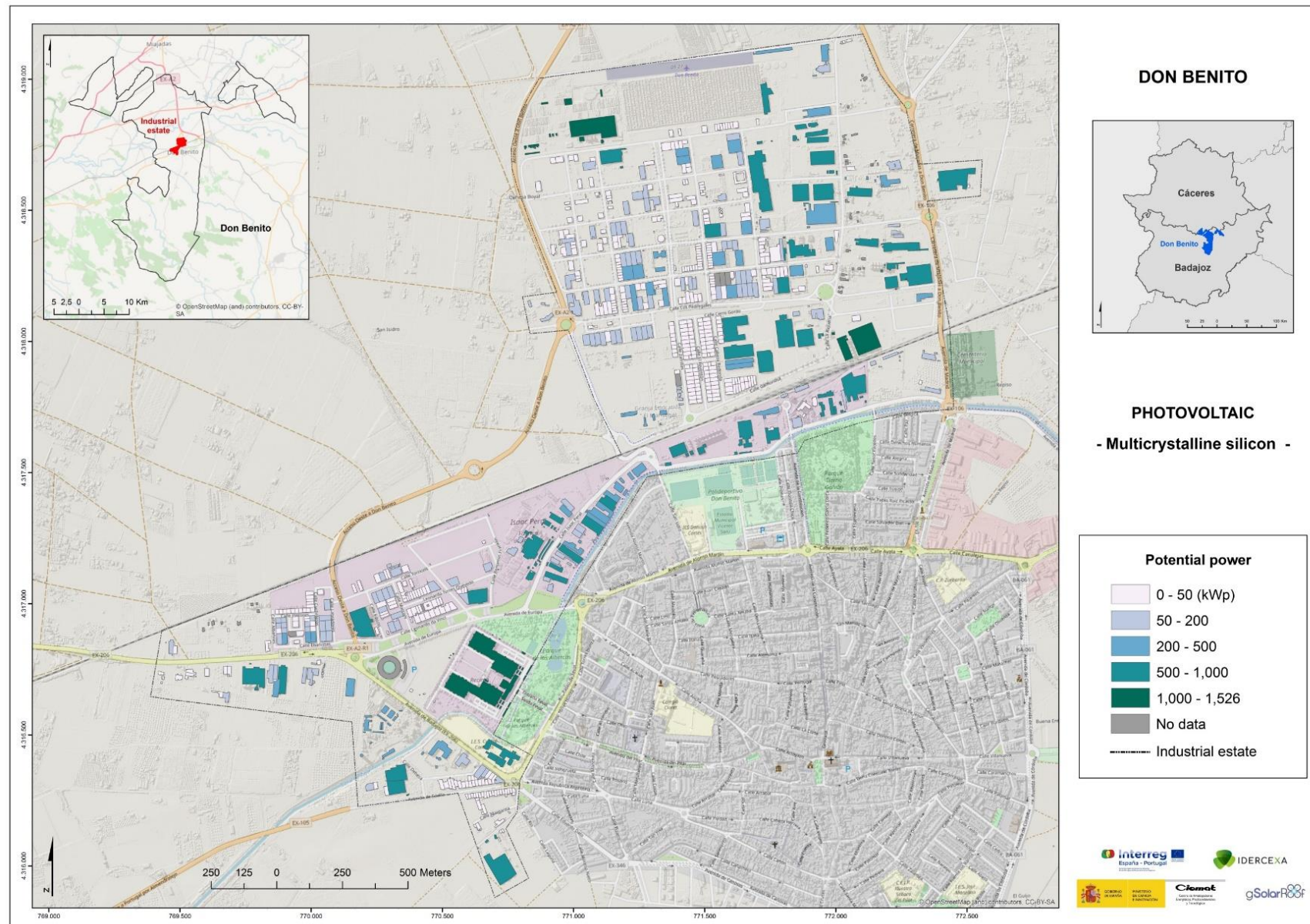


Figure A 24. Photovoltaic: Potential power (Multicrystalline silicon module). Don Benito.

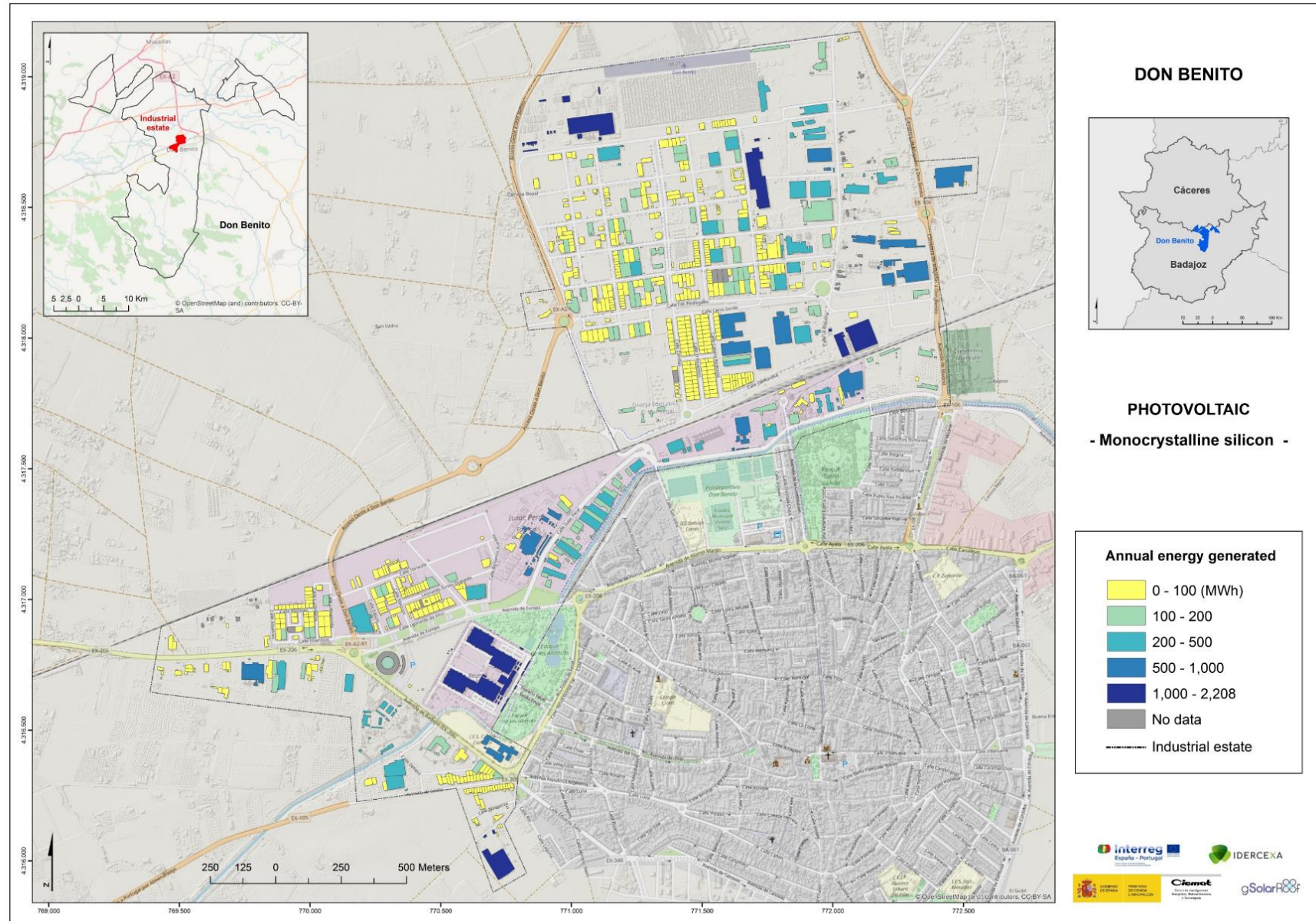


Figure A 25. Photovoltaic: Annual energy generated (Monocrystalline silicon module). Don Benito.

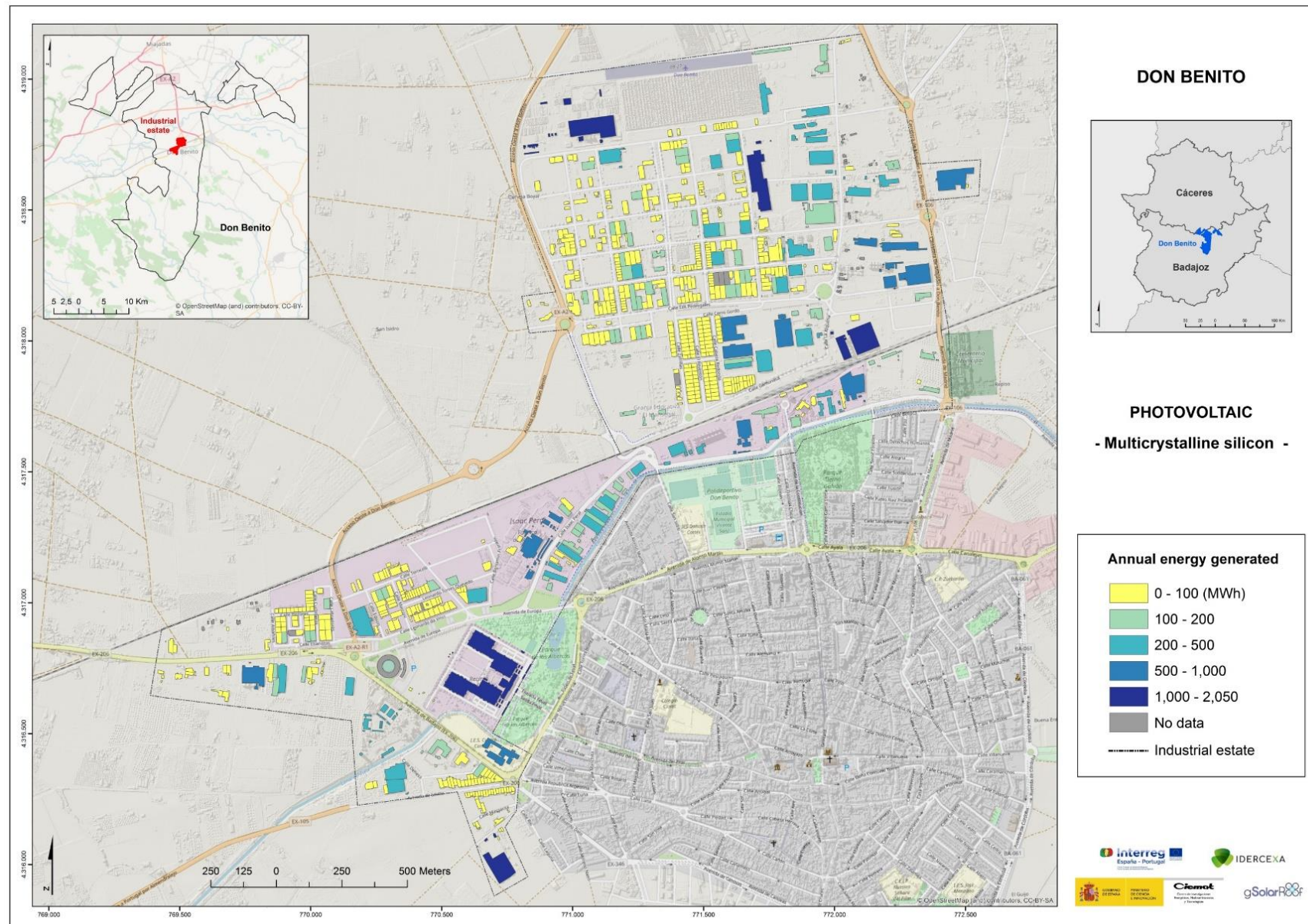


Figure A 26. Photovoltaic: Annual energy generated (Multicrystalline silicon module). Don Benito.

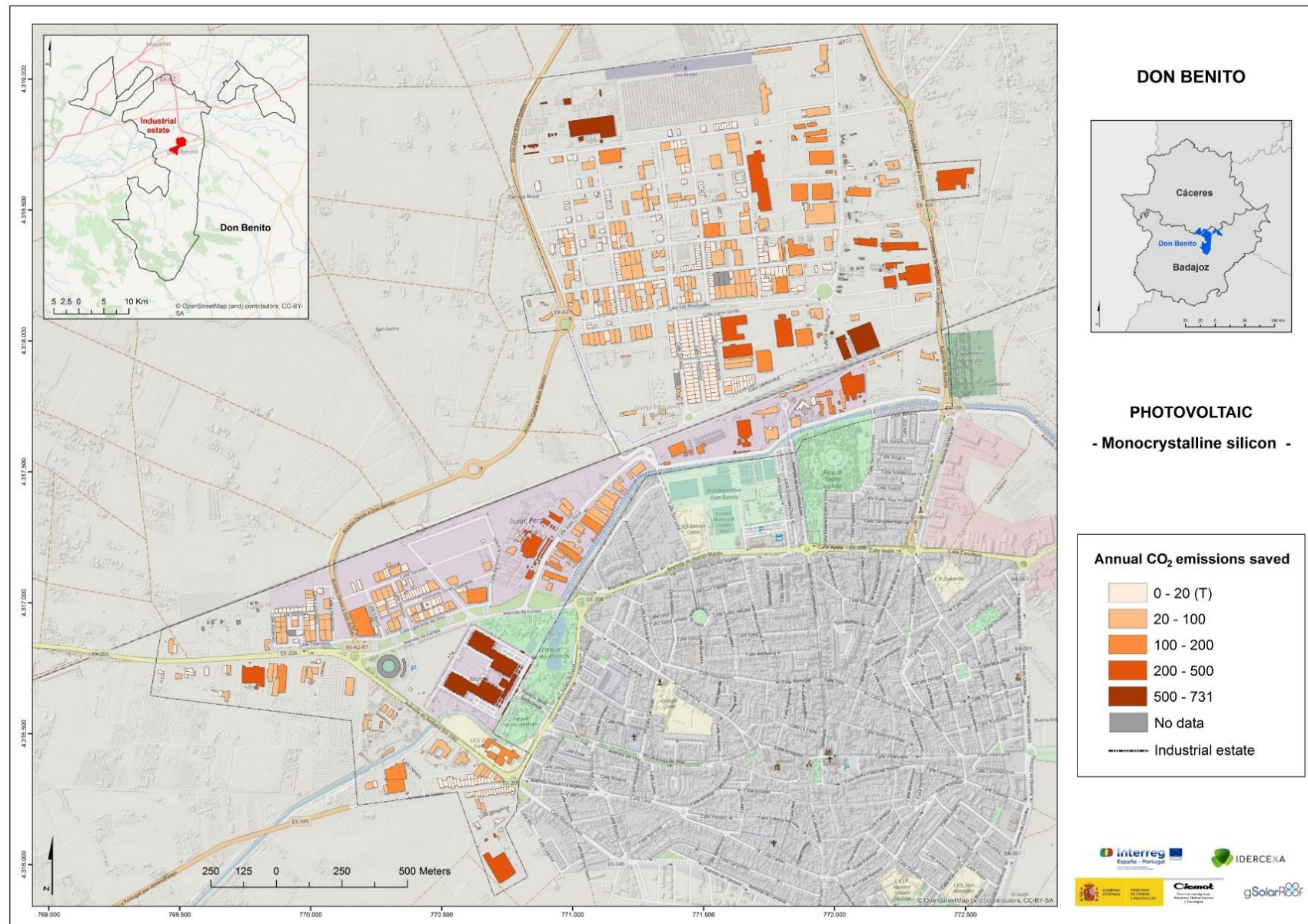


Figure A 27. Photovoltaic: Annual CO₂ emissions saved (Monocrystalline silicon module). Don Benito.

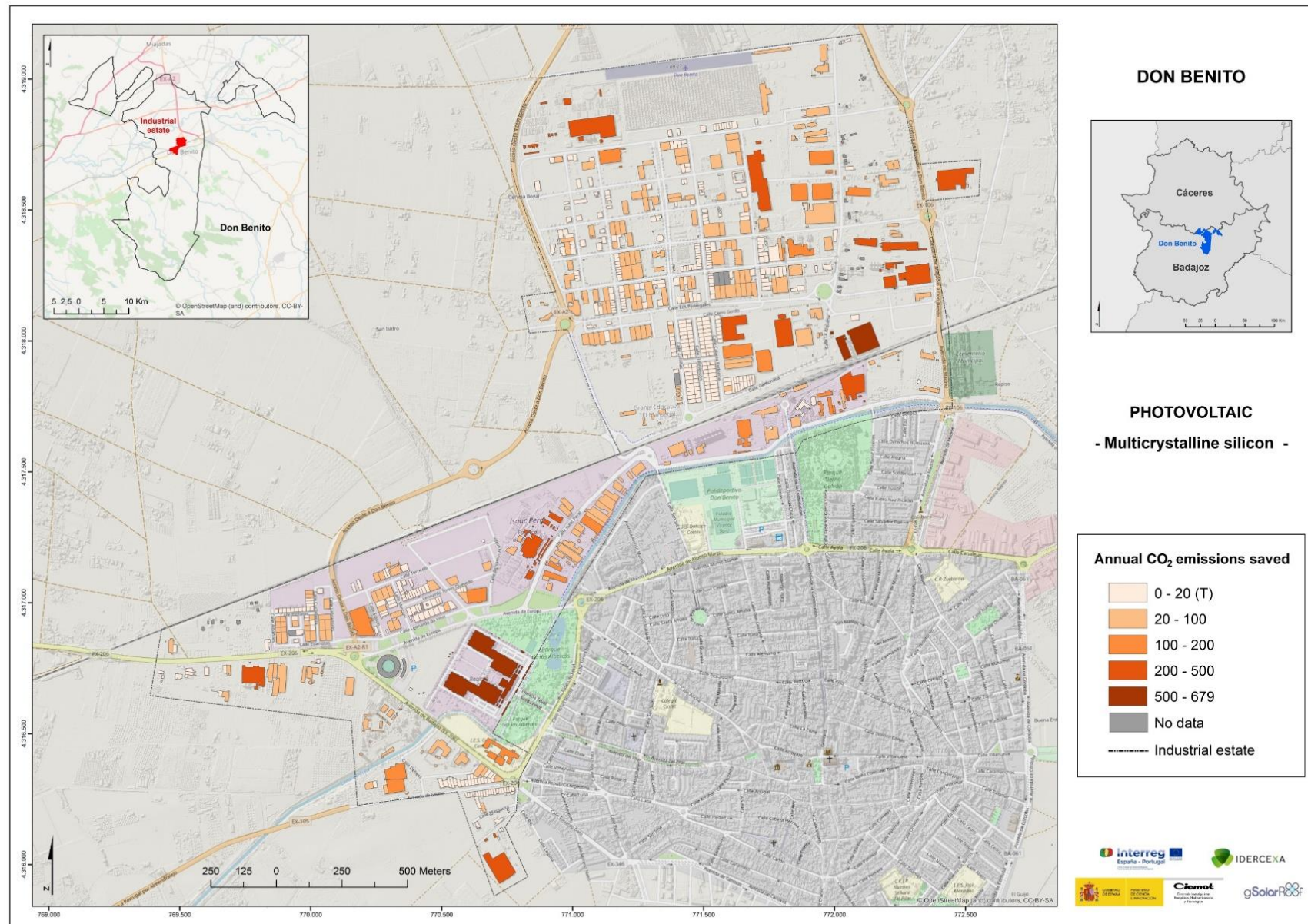


Figure A 28. Photovoltaic: Annual CO₂ emissions saved (Multicrystalline silicon module). Don Benito.

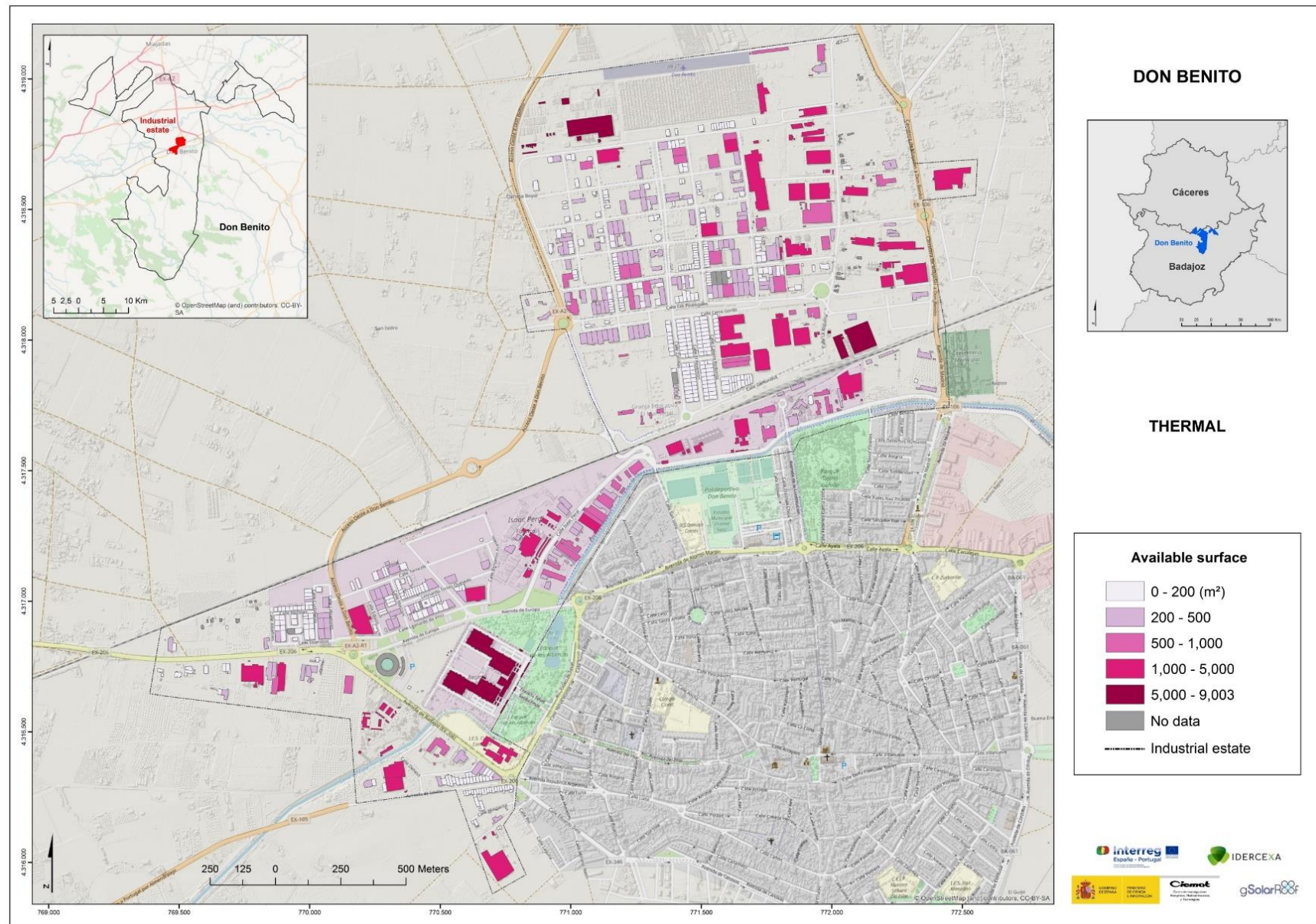


Figure A 29. Thermal: Available surface of rooftop. Don Benito.

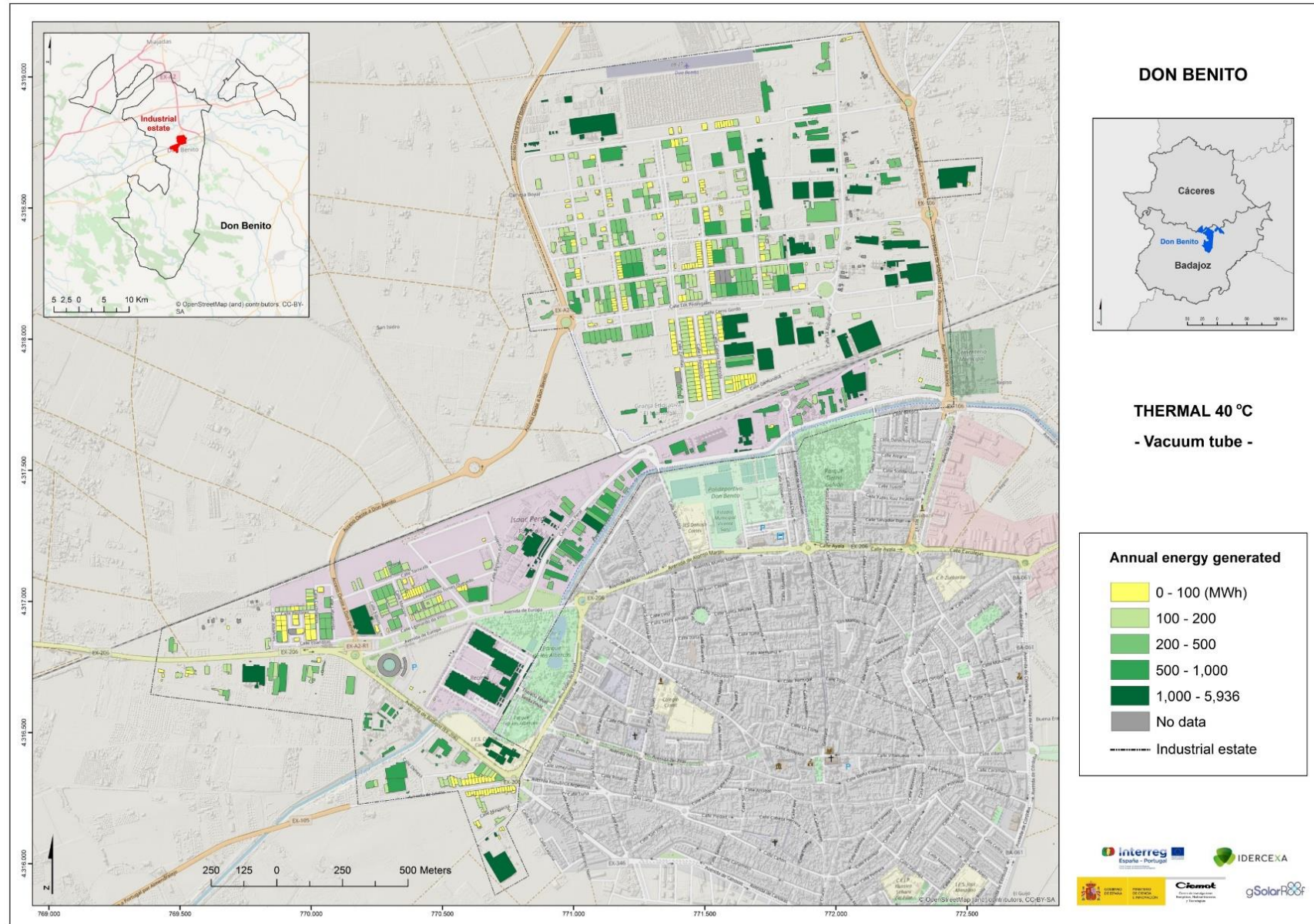


Figure A 30. Thermal: Annual energy generated (Vacuum tube collector) at the temperature of 40 °C. Don Benito.

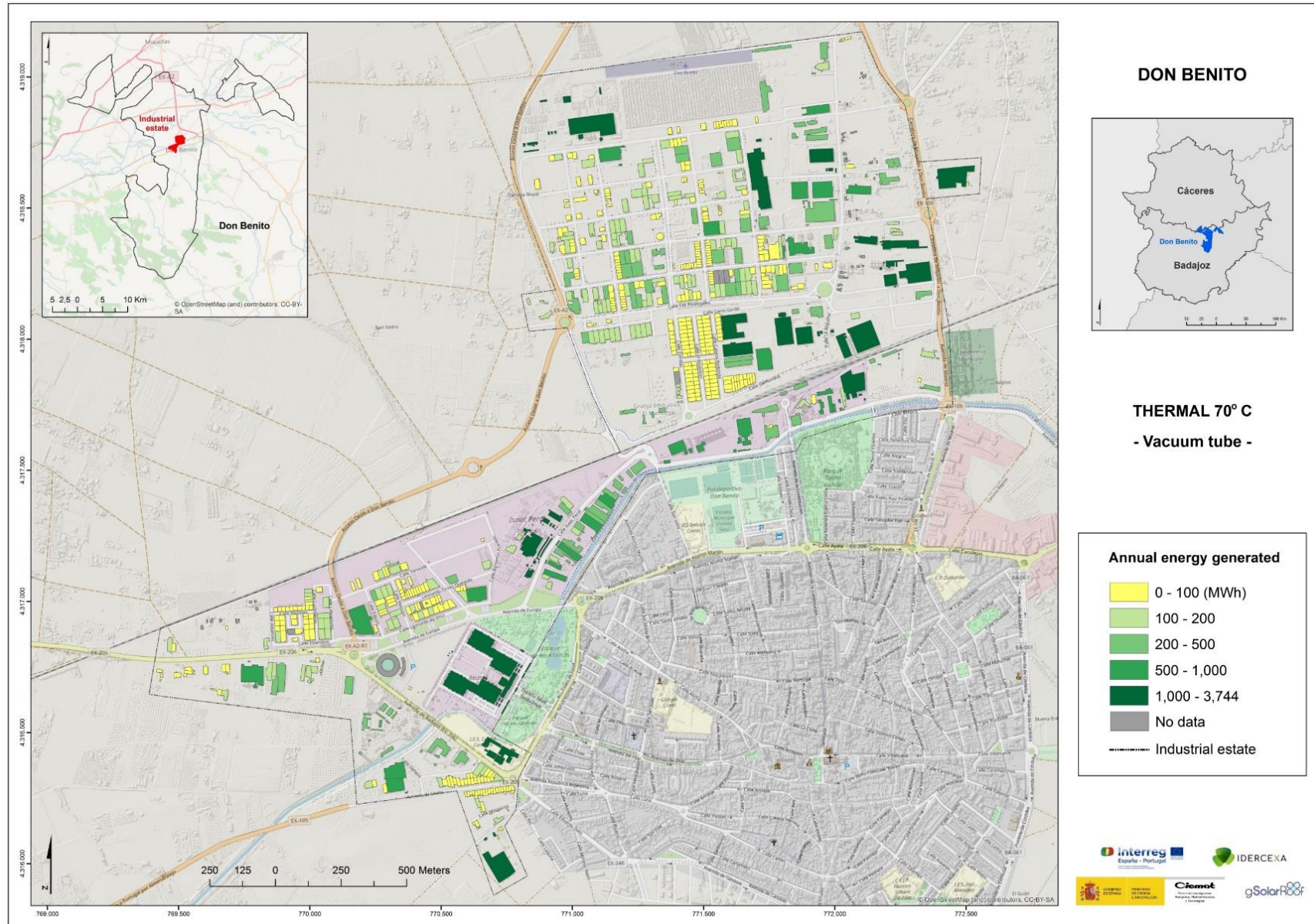


Figure A 31. Thermal: Annual energy generated (Vacuum tube collector) at the temperature of 70 °C. Don Benito.

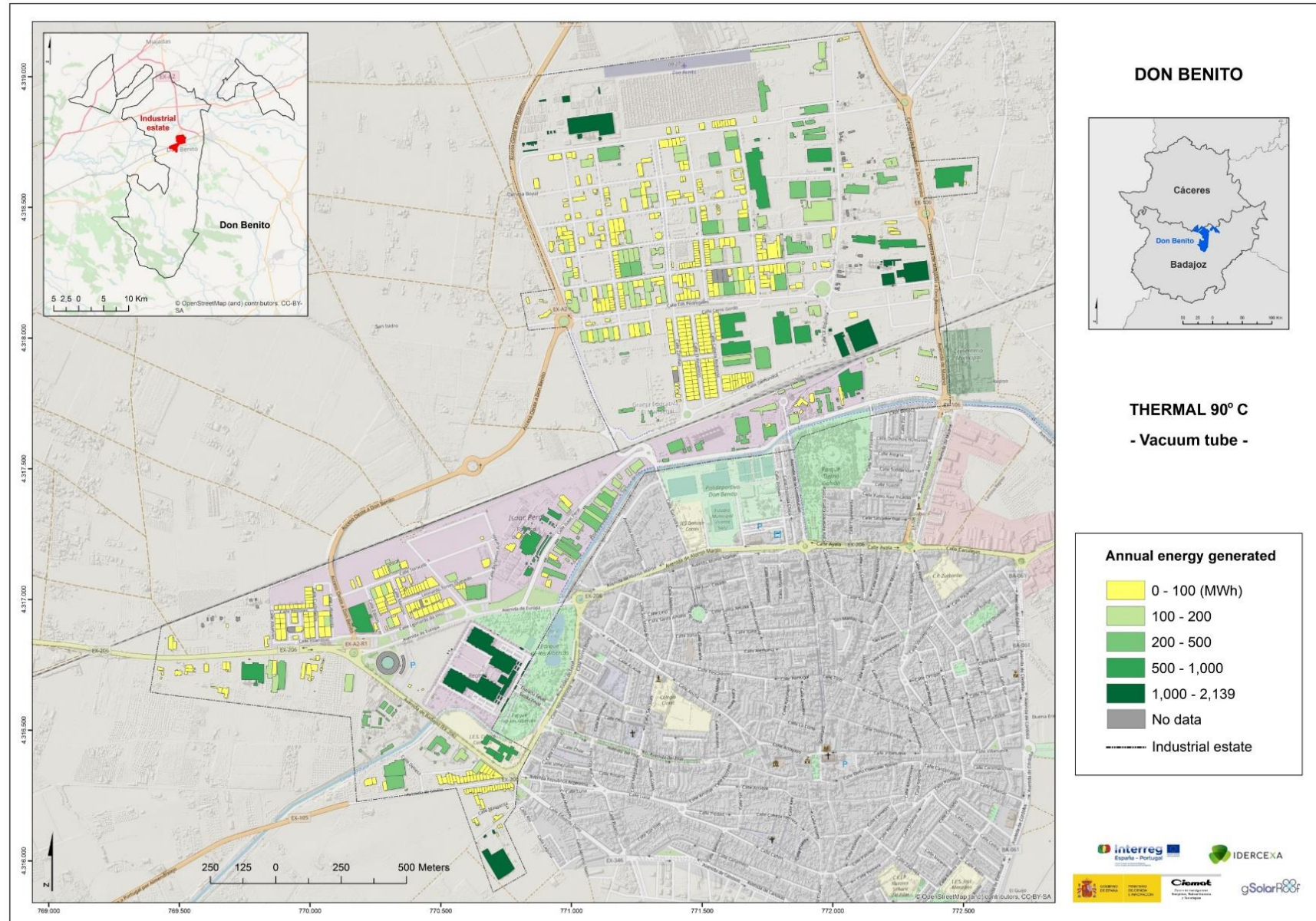


Figure A 32. Thermal: Annual energy generated (Vacuum tube collector) at the temperature of 90 °C. Don Benito.

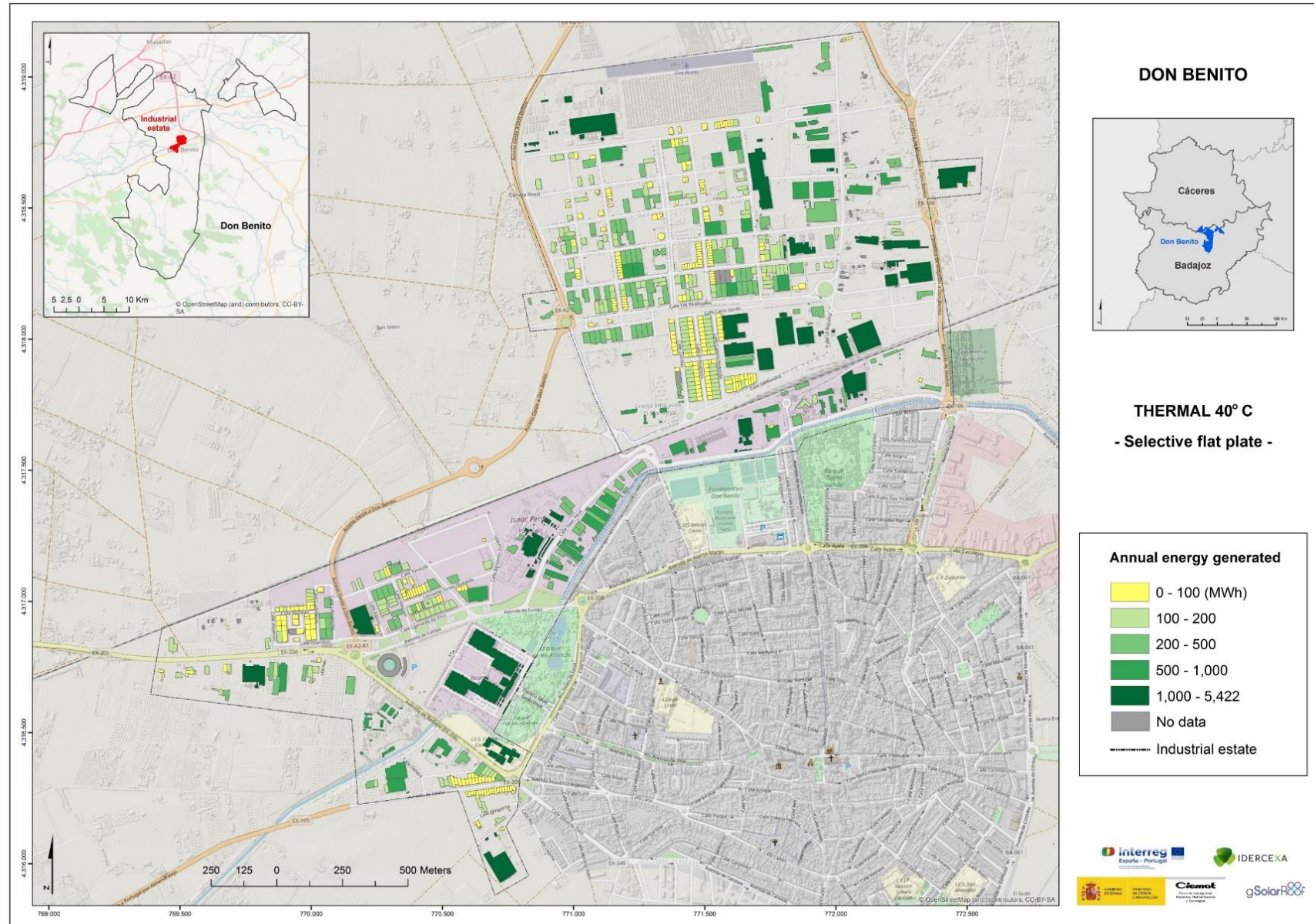


Figure A 33. Thermal: Annual energy generated (Selective flat plate collector) at the temperature of 40 °C. Don Benito.

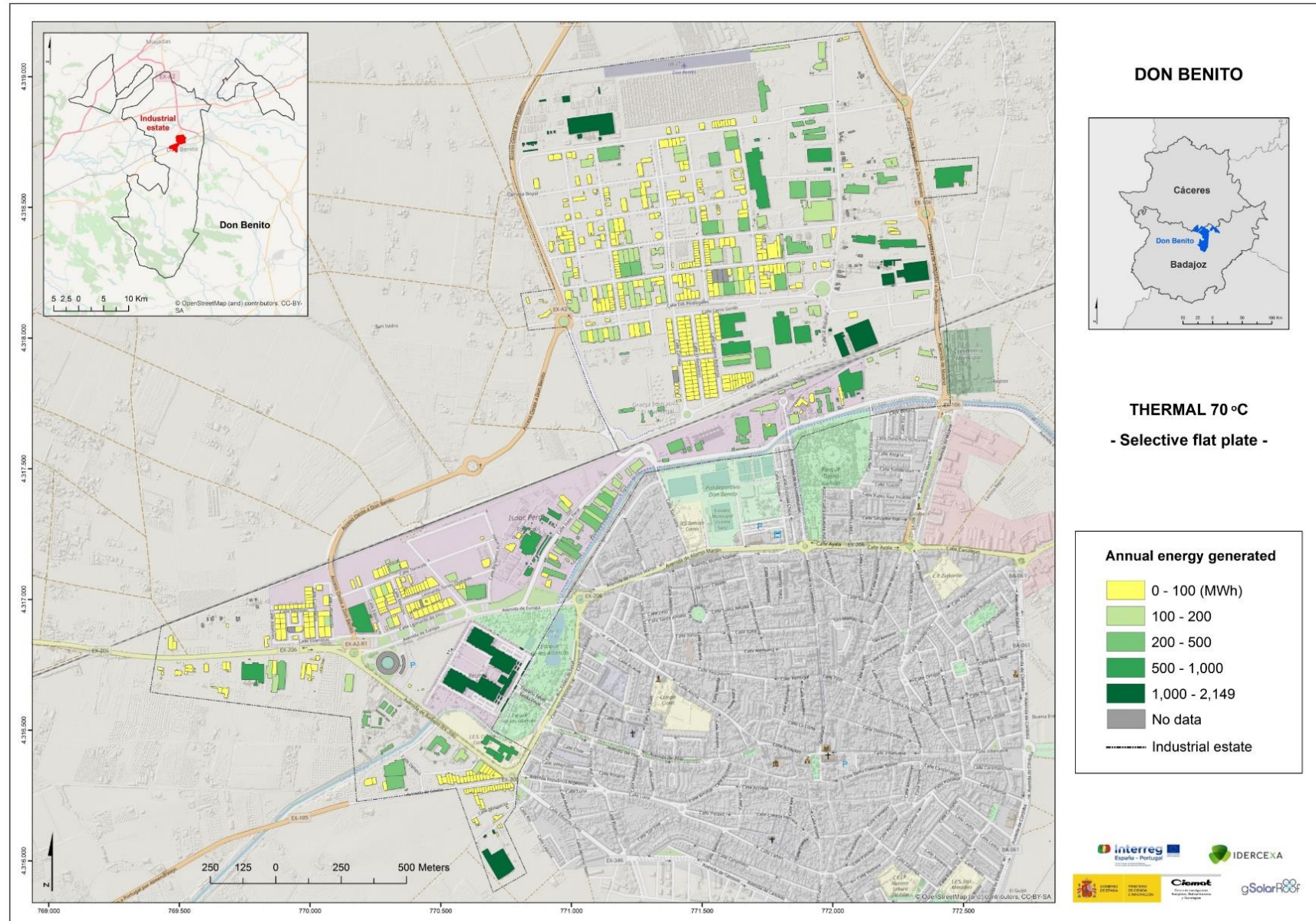


Figure A 34. Thermal: Annual energy generated (Selective flat plate collector) at the temperature of 70 °C. Don Benito.

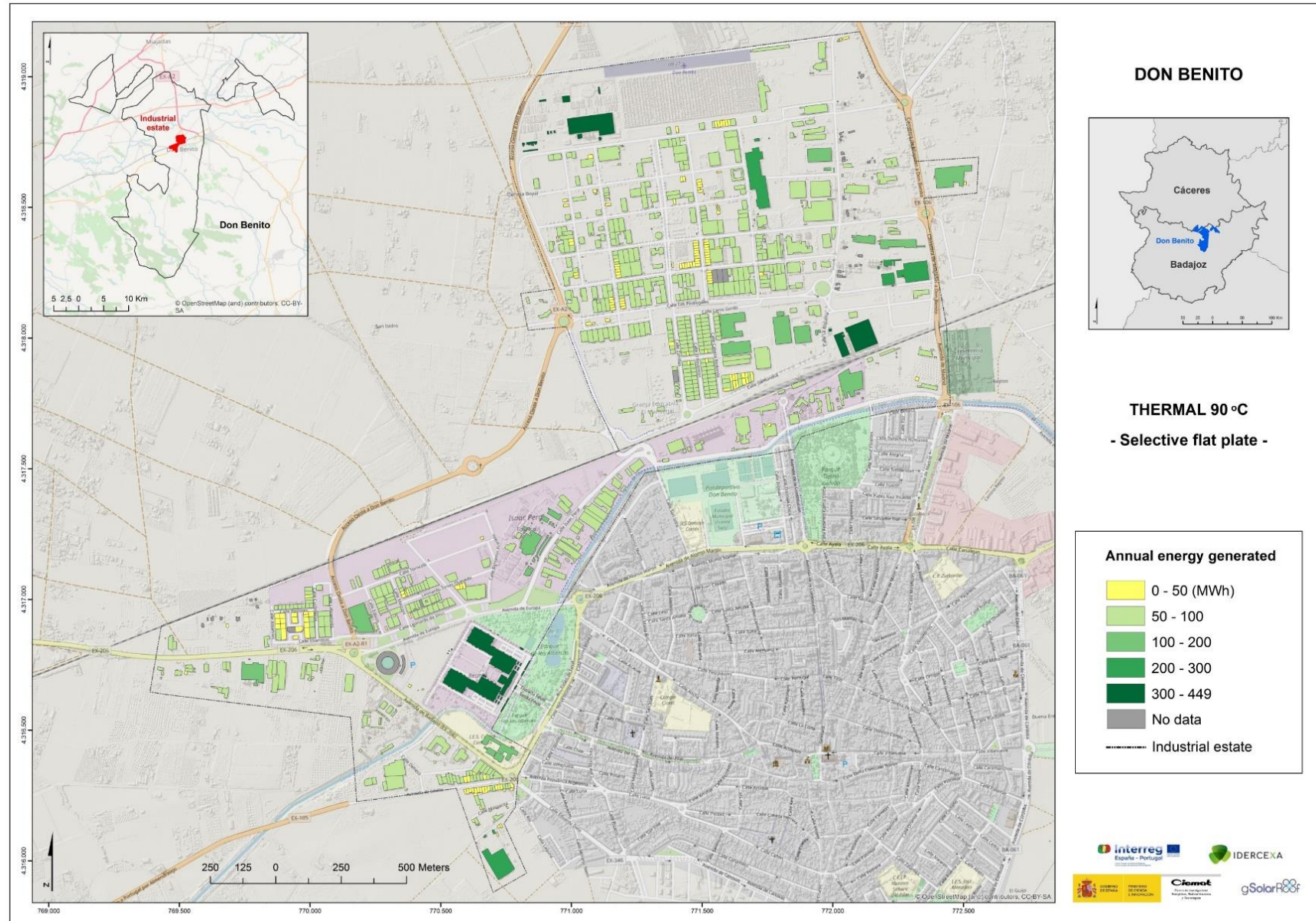


Figure A 35. Thermal: Annual energy generated (Selective flat plate collector) at the temperature of 90 °C. Don Benito.

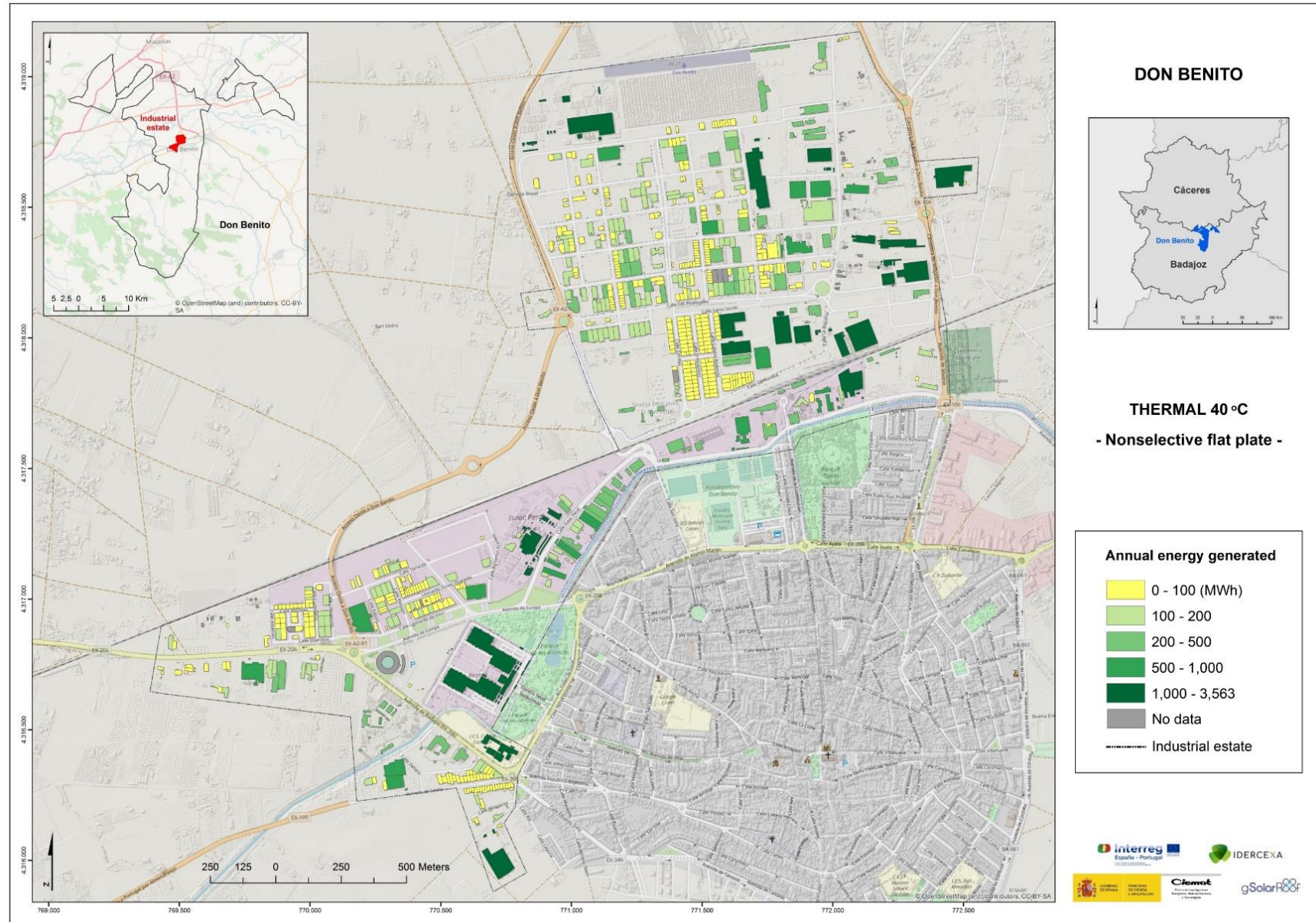


Figure A 36. Thermal: Annual energy generated (Nonselective flat plate collector) at the temperature of 40 °C. Don Benito.

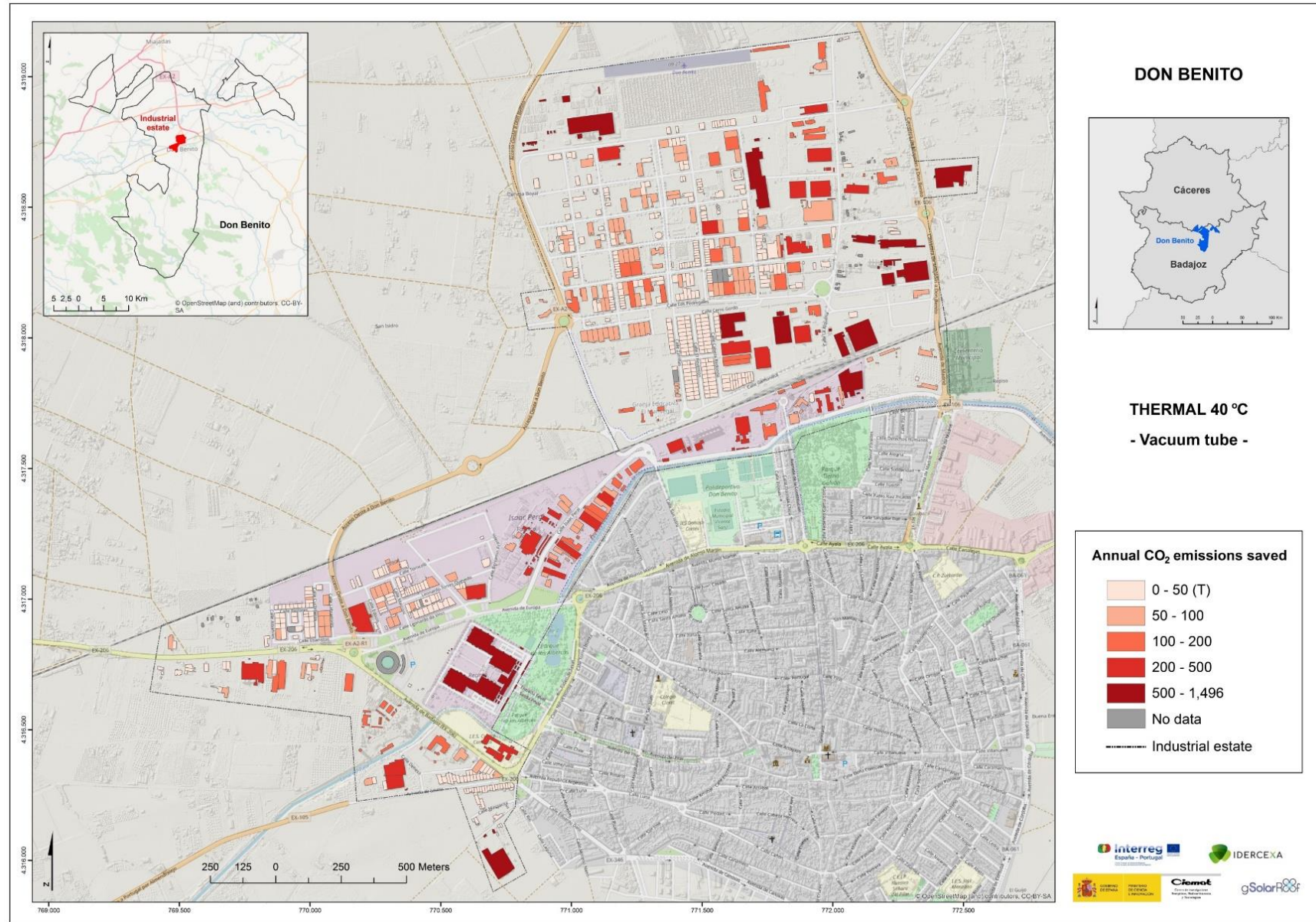


Figure A 37. Thermal: Annual CO₂ emissions saved (Vacuum tube collector) at the temperature of 40 °C. Don Benito.

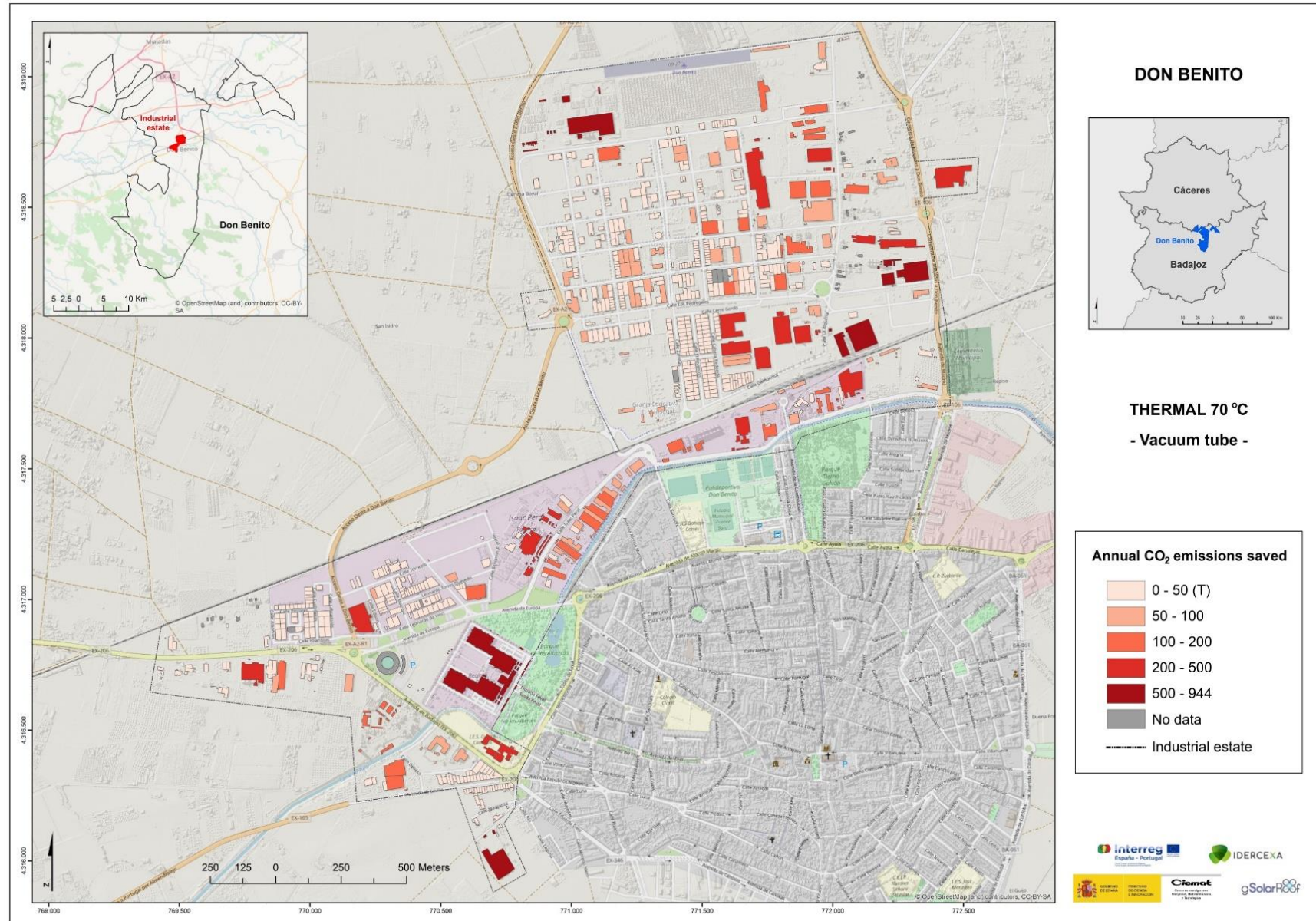


Figure A 38. Thermal: Annual CO₂ emissions saved (Vacuum tube collector) at the temperature of 70 °C. Don Benito.

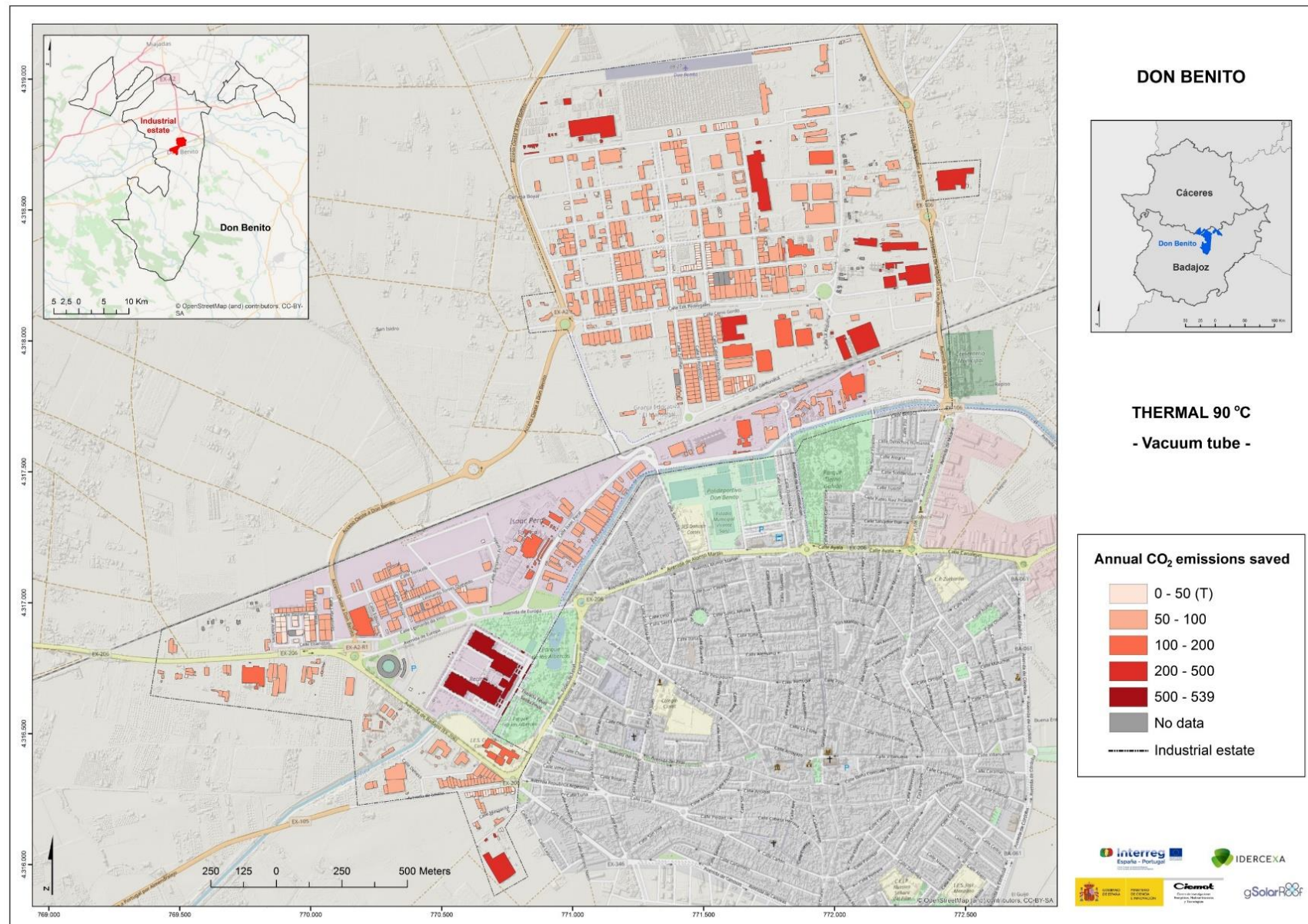


Figure A 39. Thermal: Annual CO₂ emissions saved (Vacuum tube collector) at the temperature of 90 °C. Don Benito.

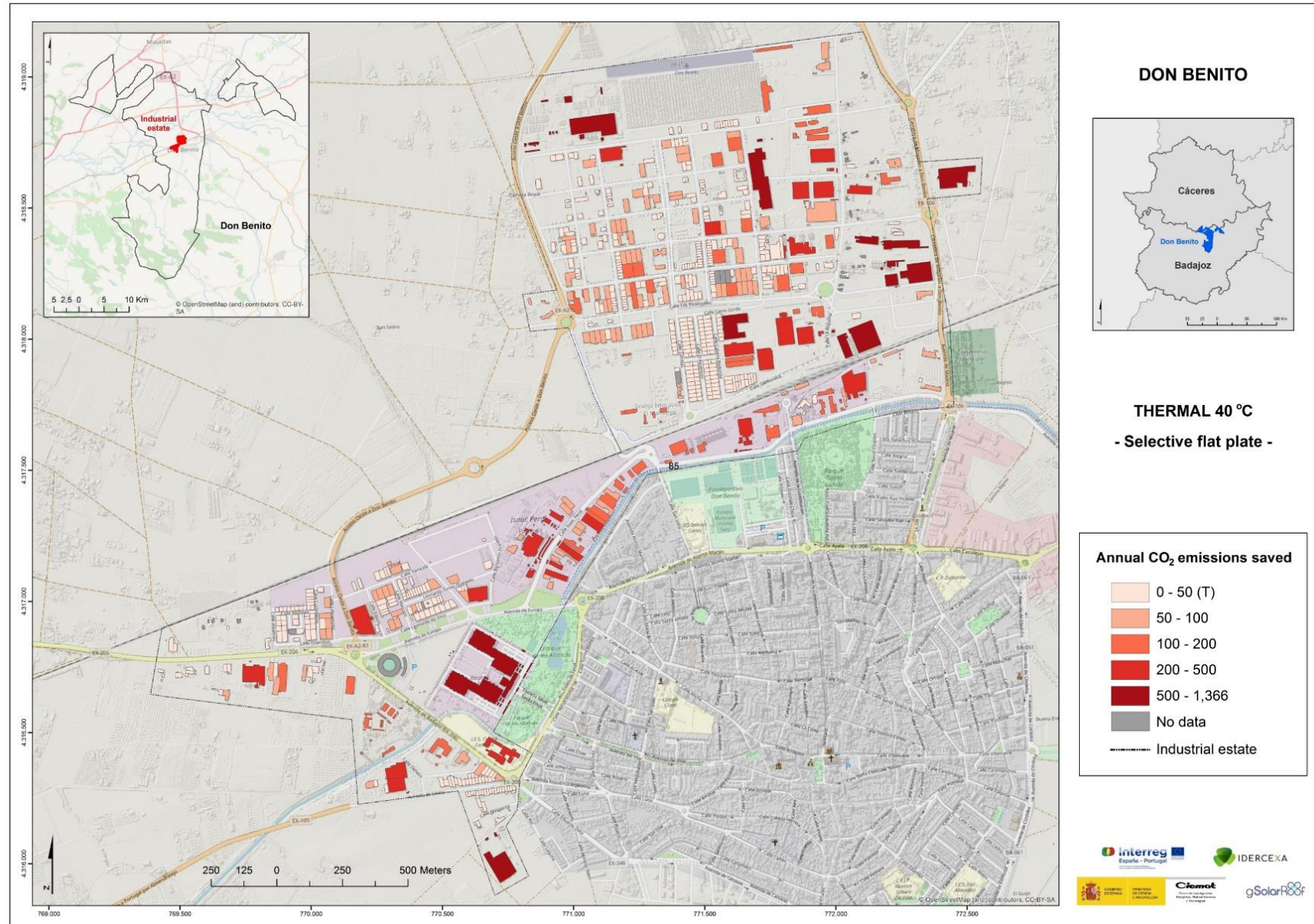


Figure A 40. Thermal: Annual CO₂ emissions saved (Selective flat plate collector) at the temperature of 40 °C. Don Benito.

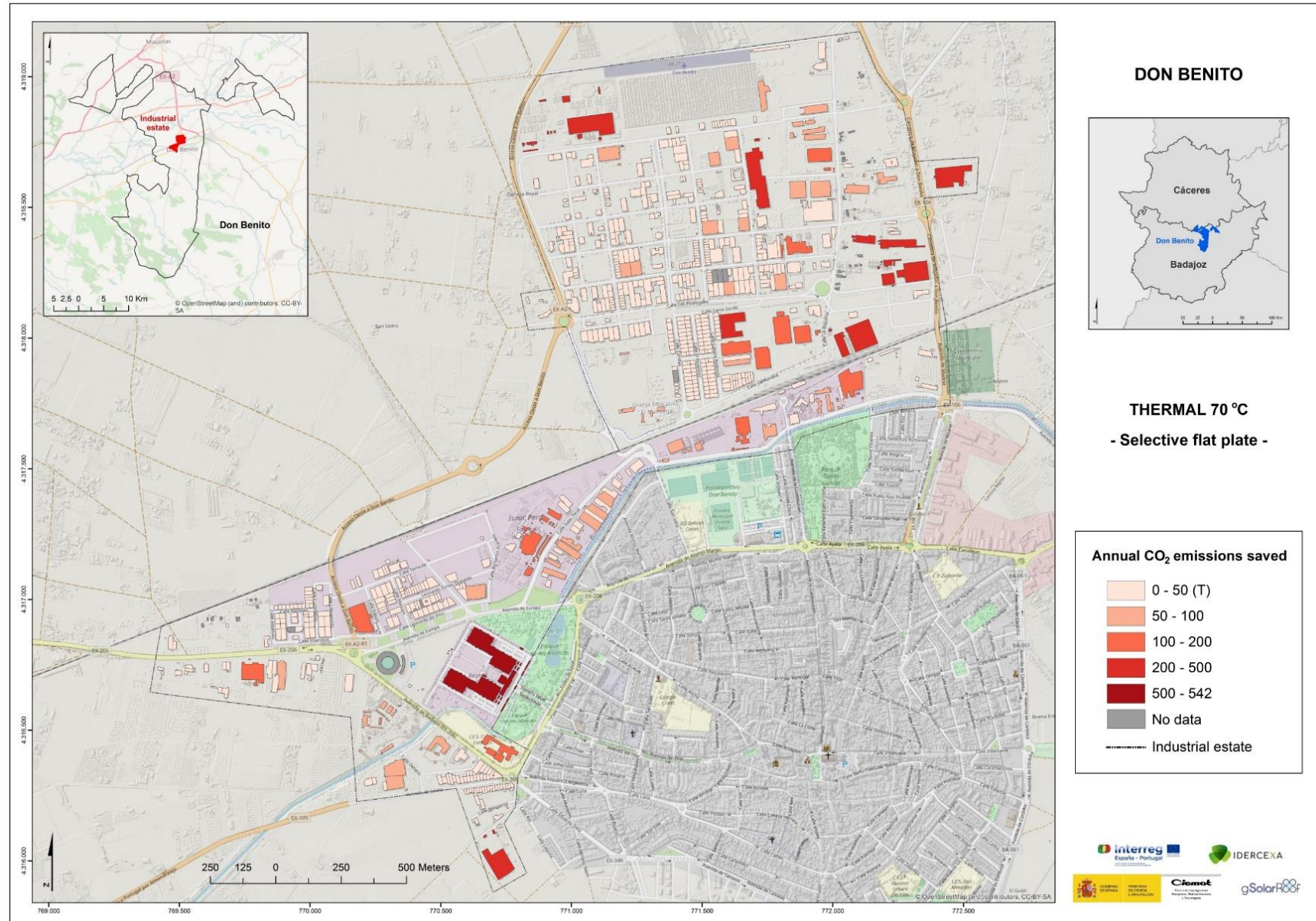


Figure A 41. Thermal: Annual CO₂ emissions saved (Selective flat plate collector) at the temperature of 70 °C. Don Benito.

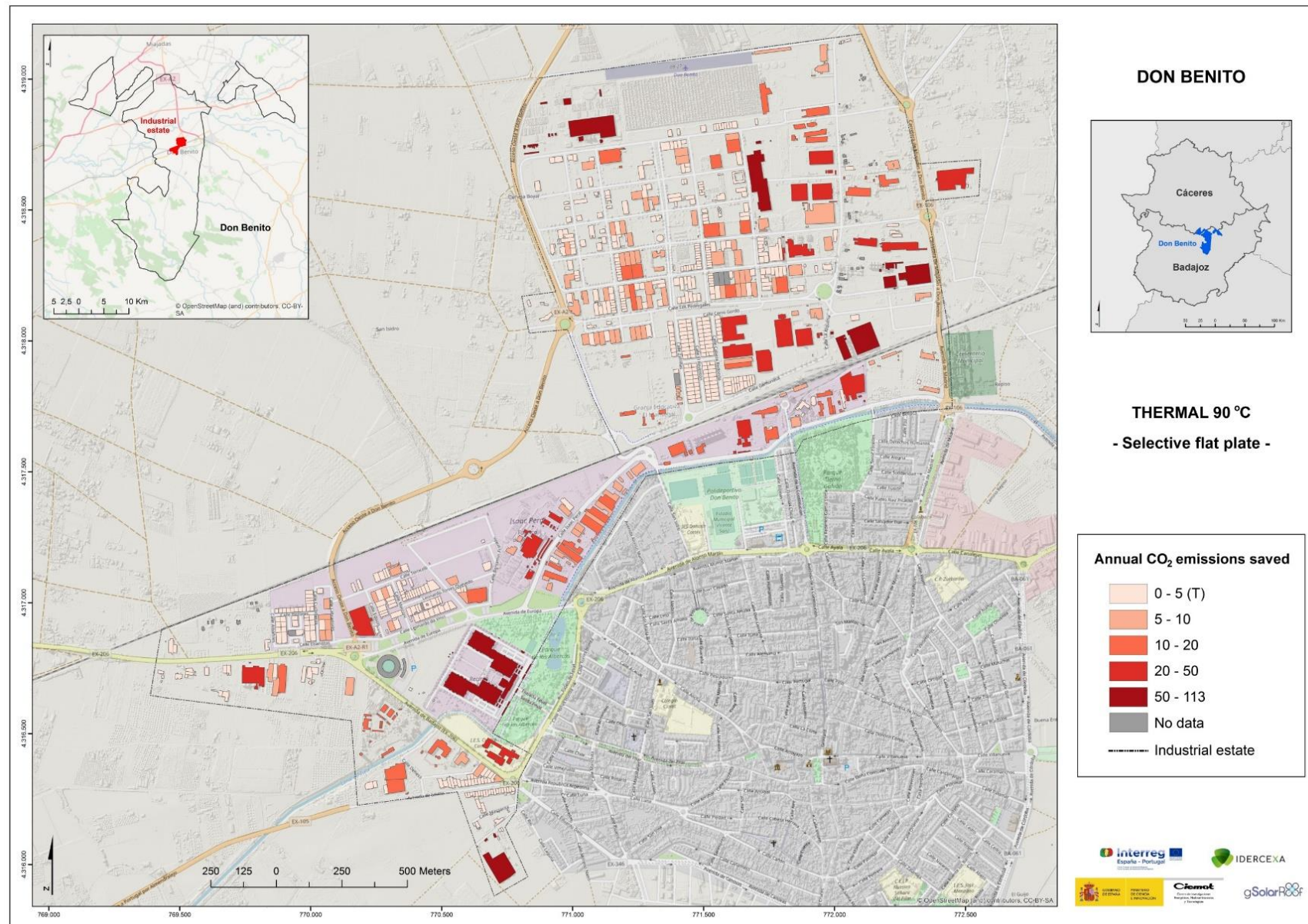


Figure A 42. Thermal: Annual CO₂ emissions saved (Selective flat plate collector) at the temperature of 90 °C. Don Benito.

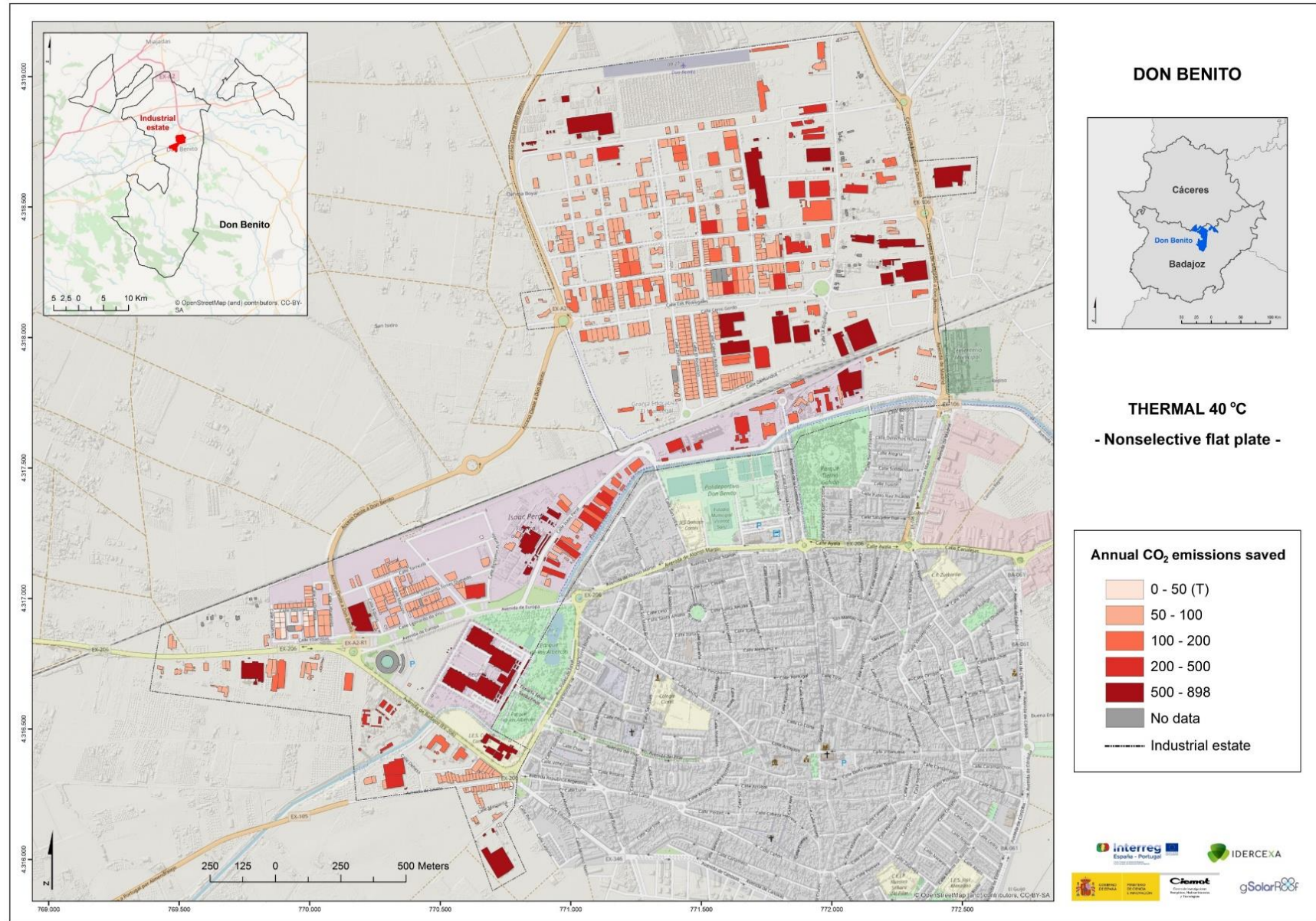


Figure A 43. Thermal: Annual CO₂ emissions saved (Nonselective flat plate collector) at the temperature of 40 °C. Don Benito.

APPENDIX VI. THEMATIC MAPS OF PLASENCIA INDUSTRIAL ESTATE

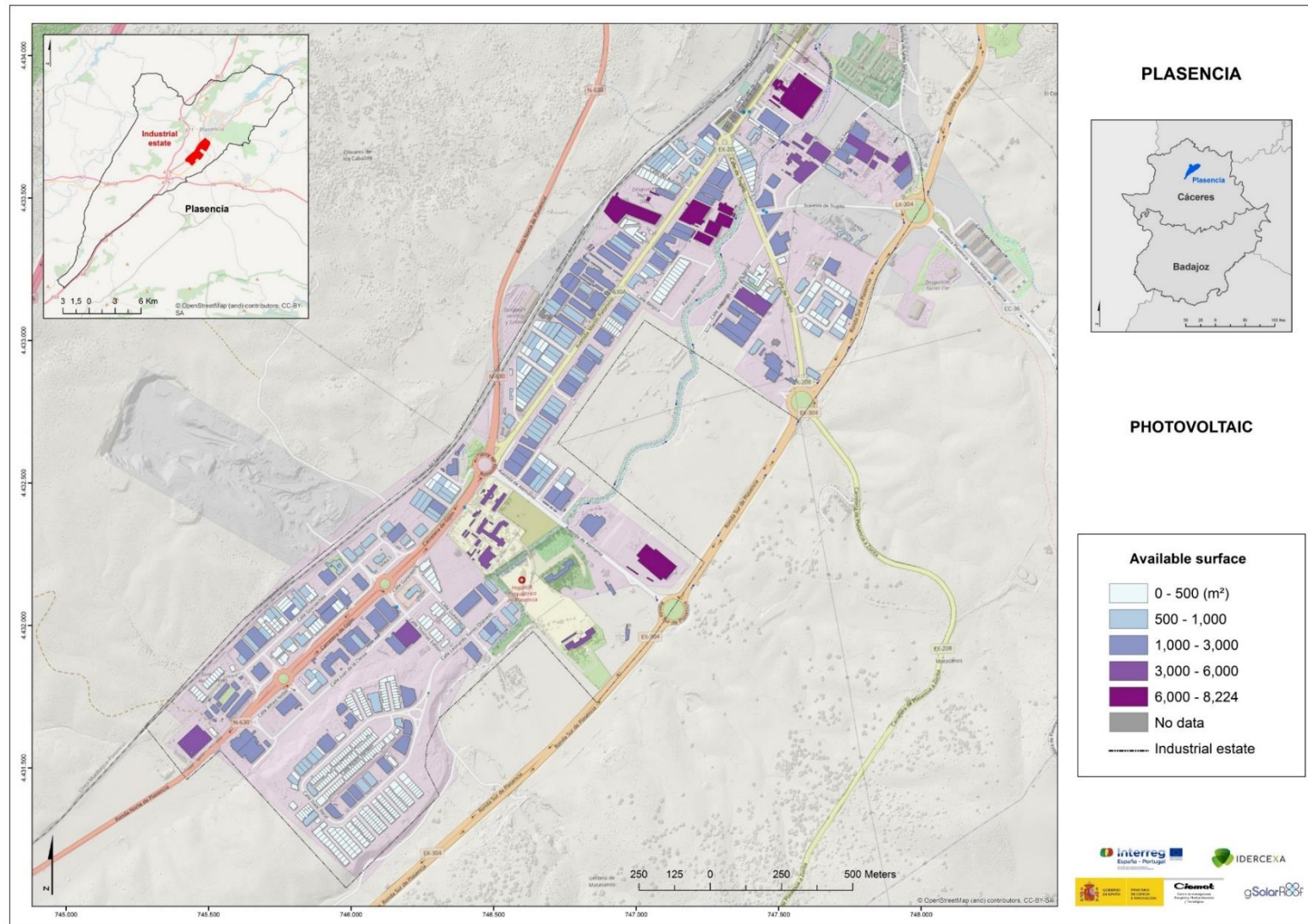
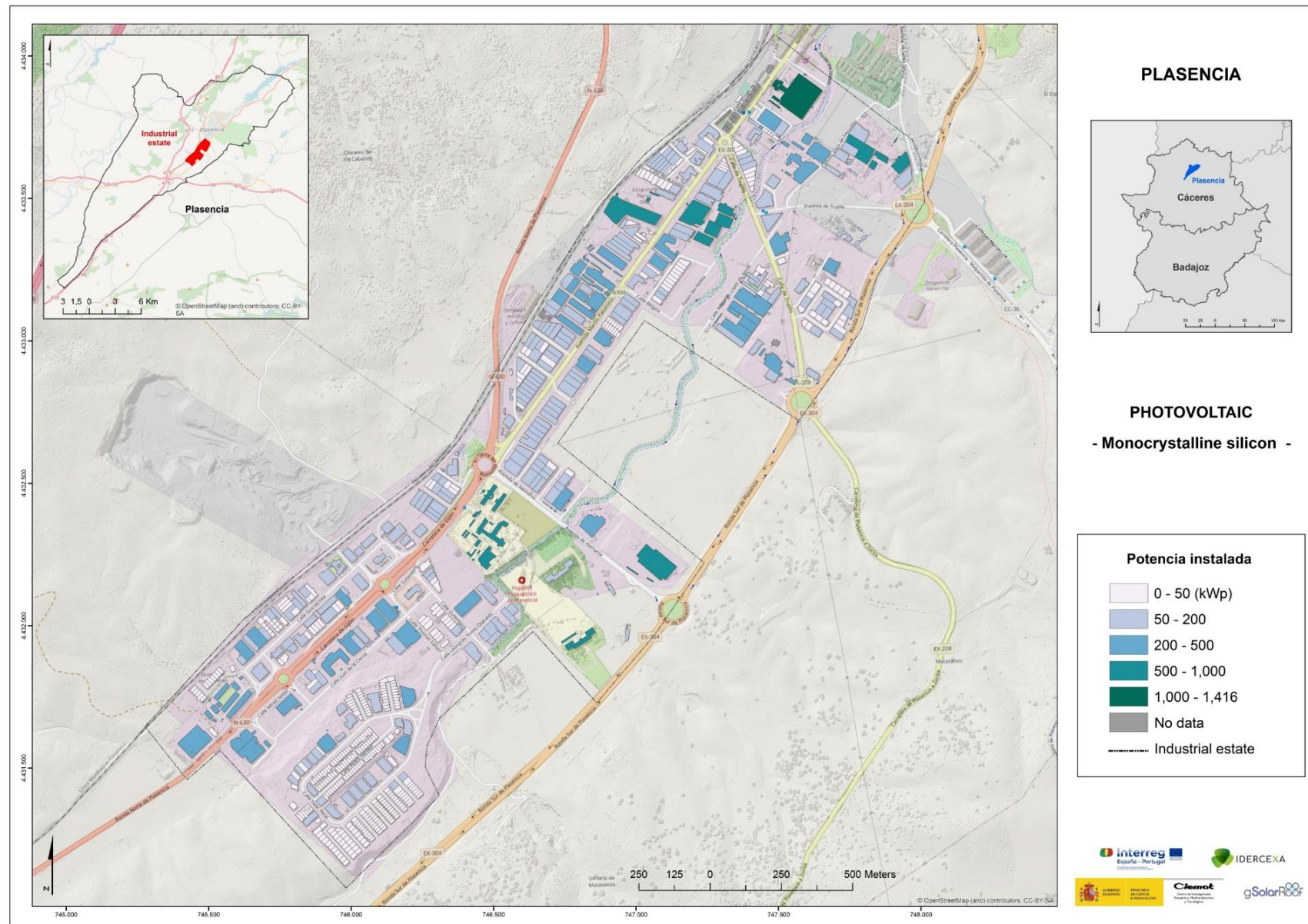


Figure A 44. Photovoltaic: Available surface of rooftop. Plasencia.



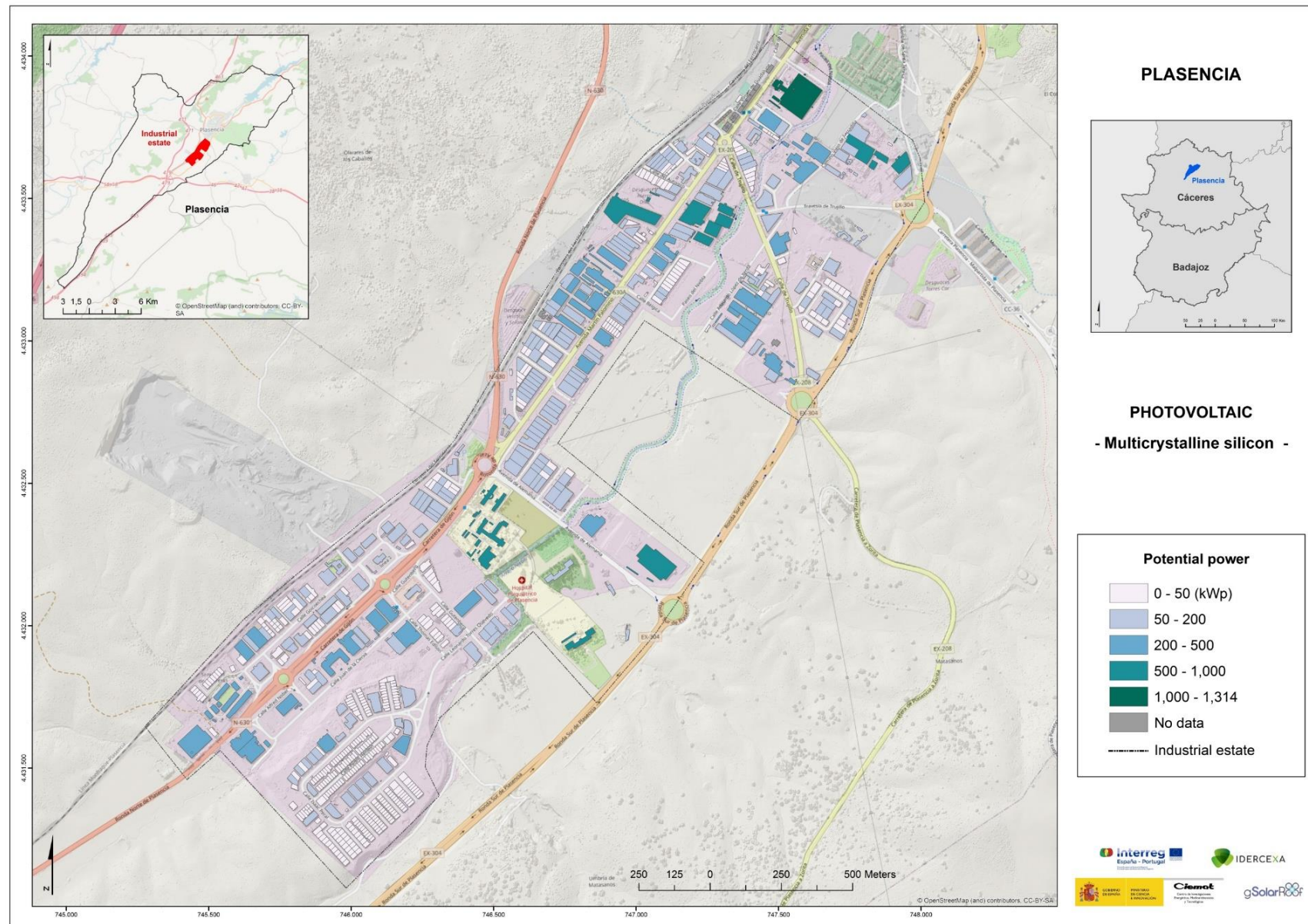


Figure A 46. Photovoltaic: Potential power (Multicrystalline silicon module). Plasencia.

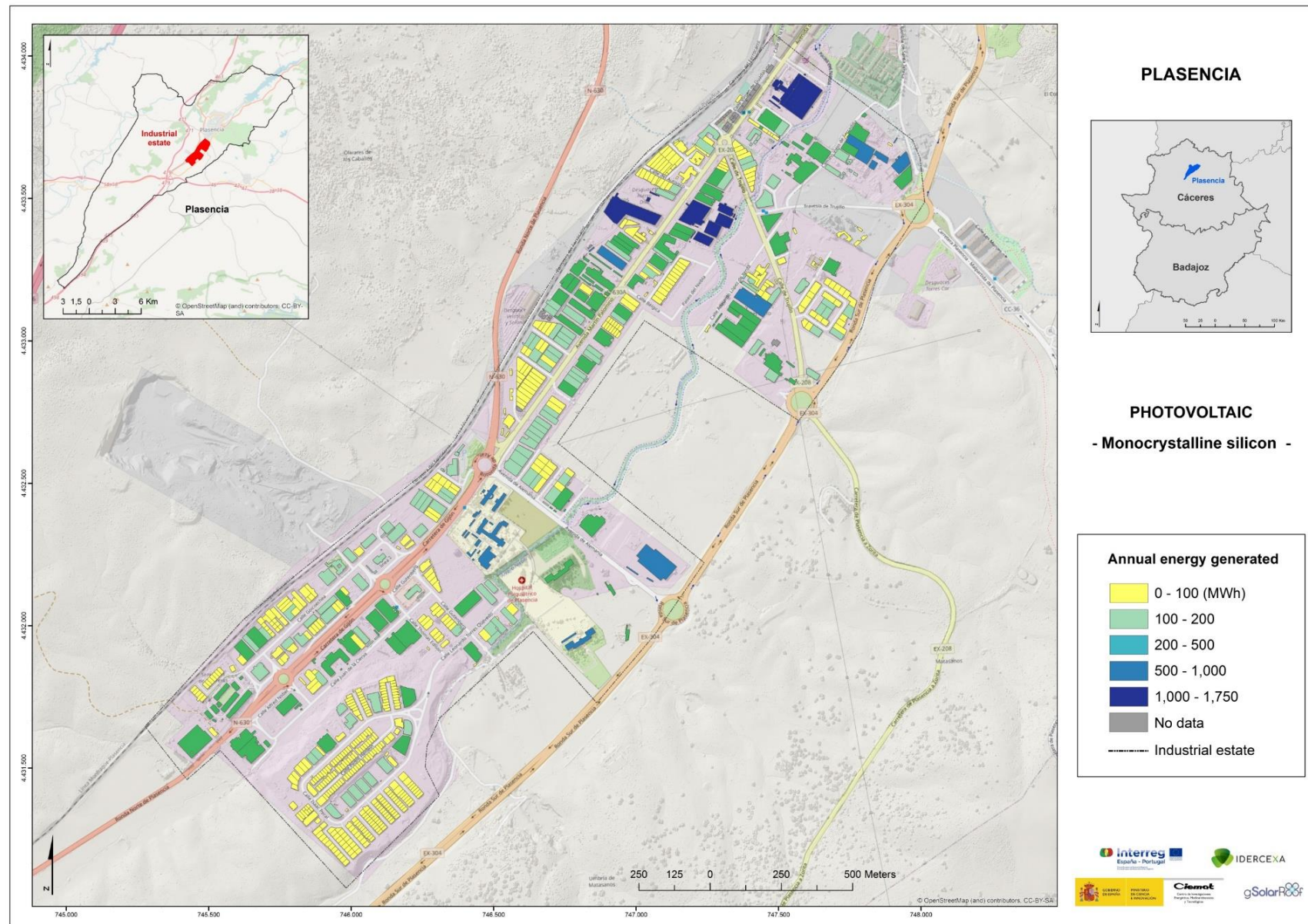


Figure A 47. Photovoltaic: Annual energy generated (Monocrystalline silicon module). Plasencia.

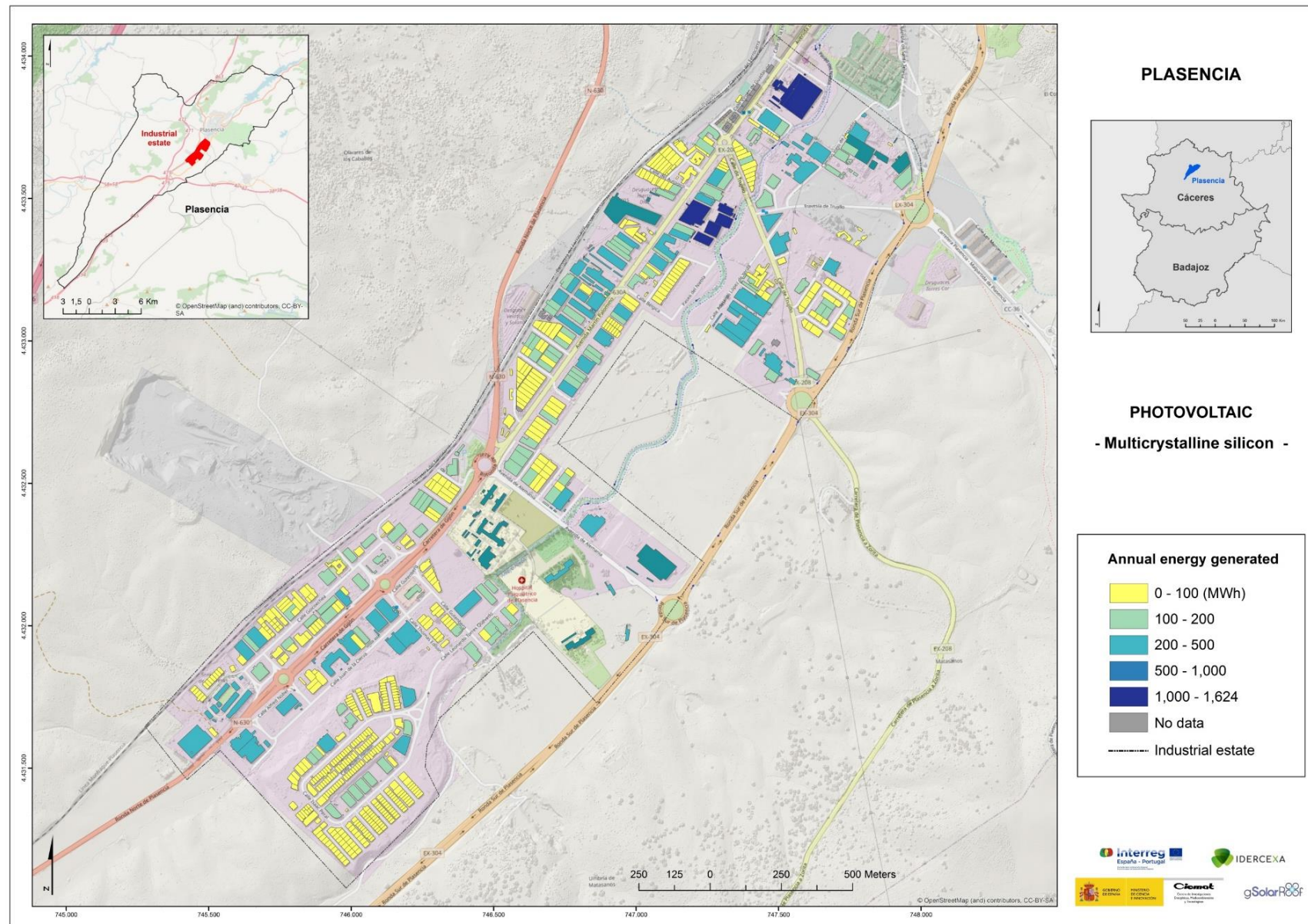


Figure A 48. Photovoltaic: Annual energy generated (Multicrystalline silicon module). Plasencia.

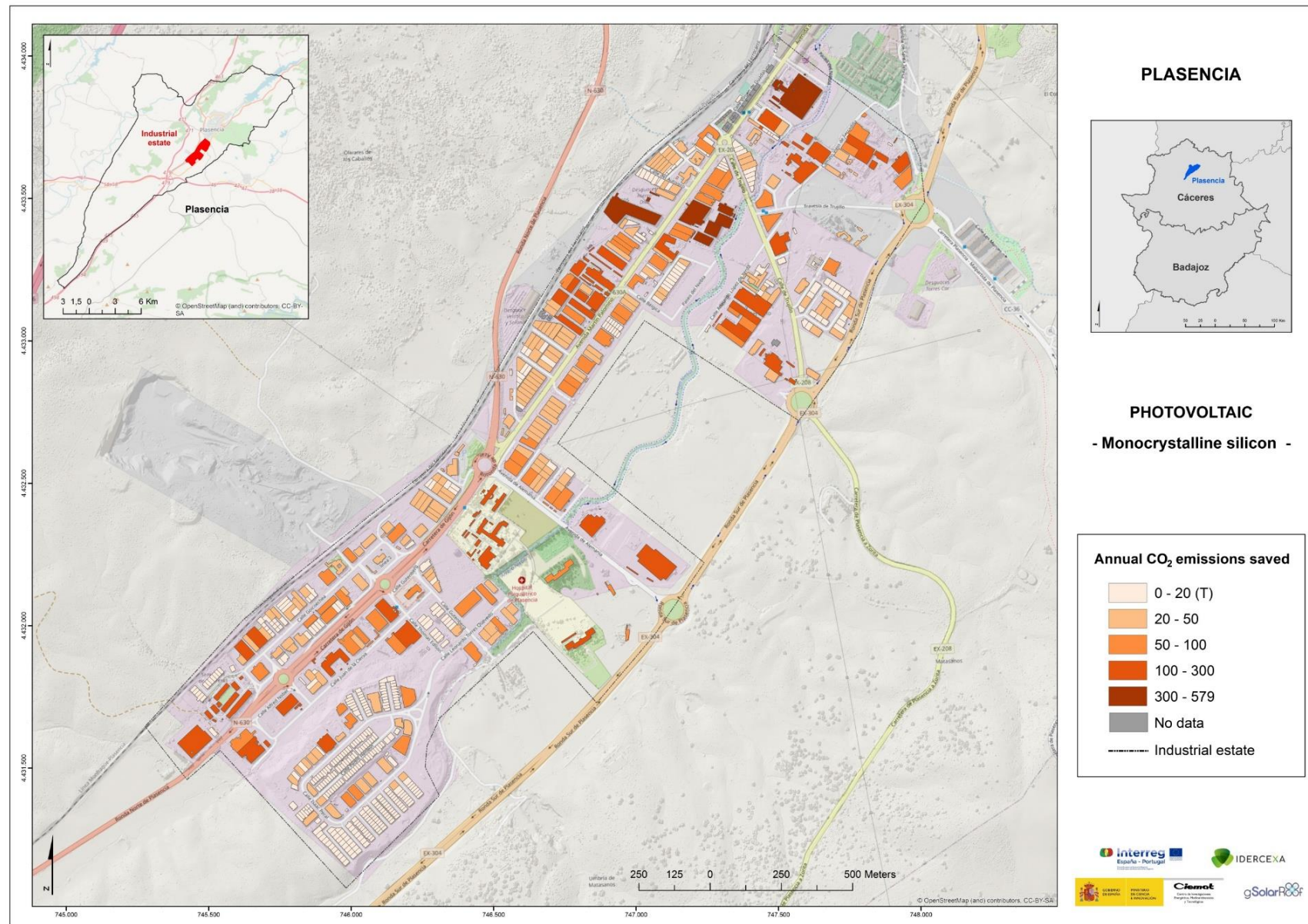


Figure A 49. Photovoltaic: Annual CO₂ emissions saved (Monocrystalline silicon module). Plasencia.

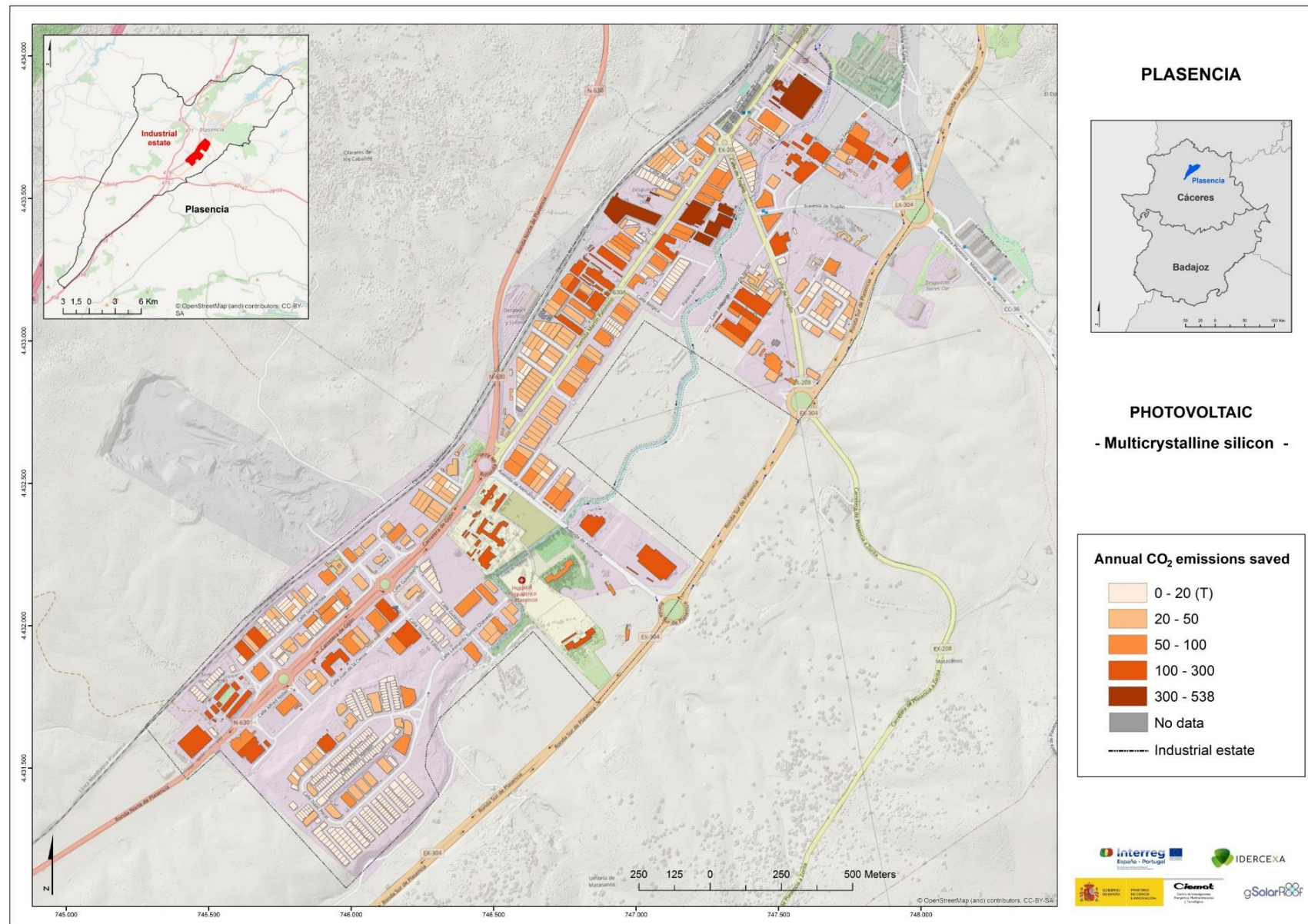


Figure A 50. Photovoltaic: Annual CO₂ emissions saved (Multicrystalline silicon module). Plasencia.

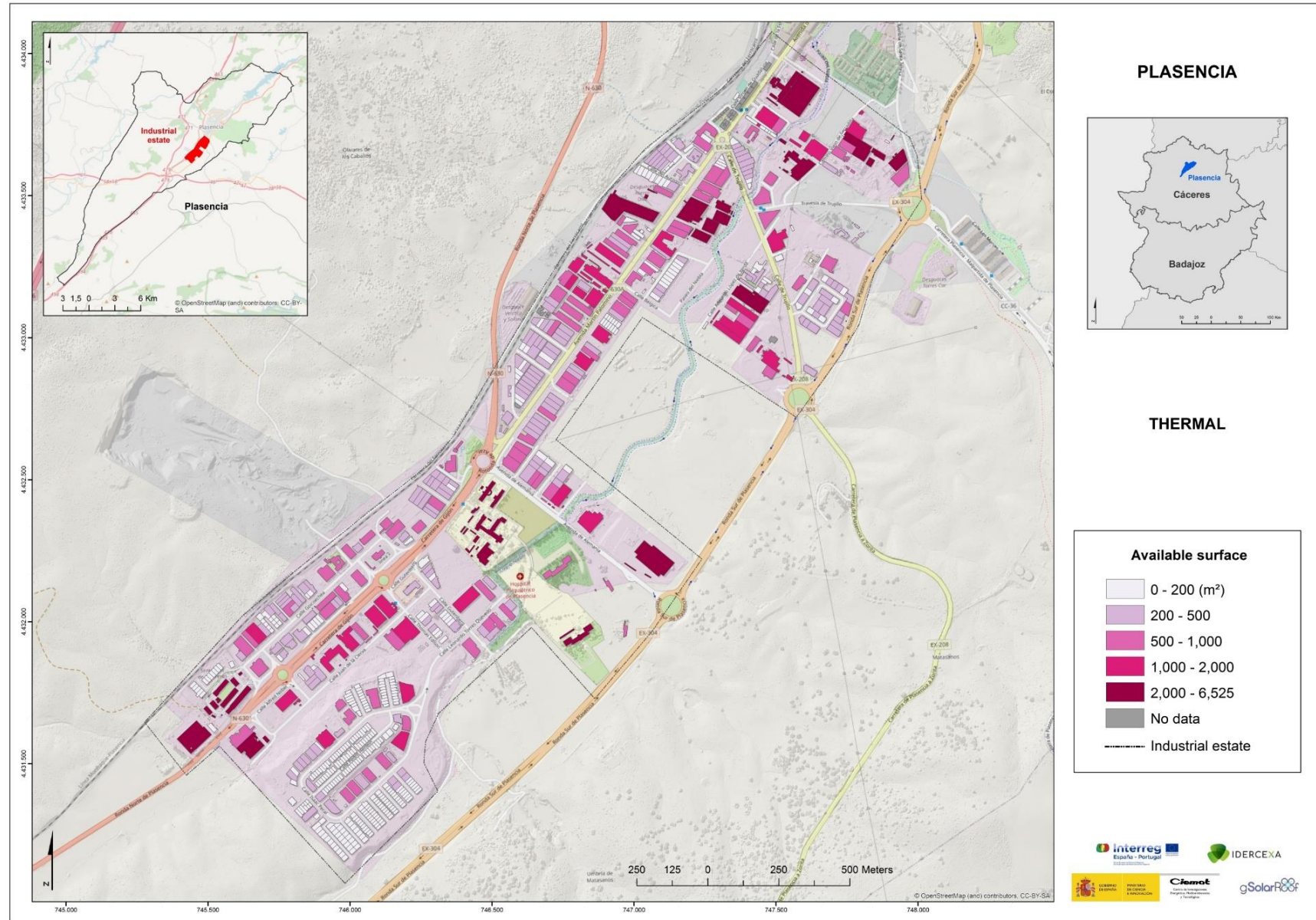


Figure A 51. Thermal: Available surface of rooftop. Plasencia.

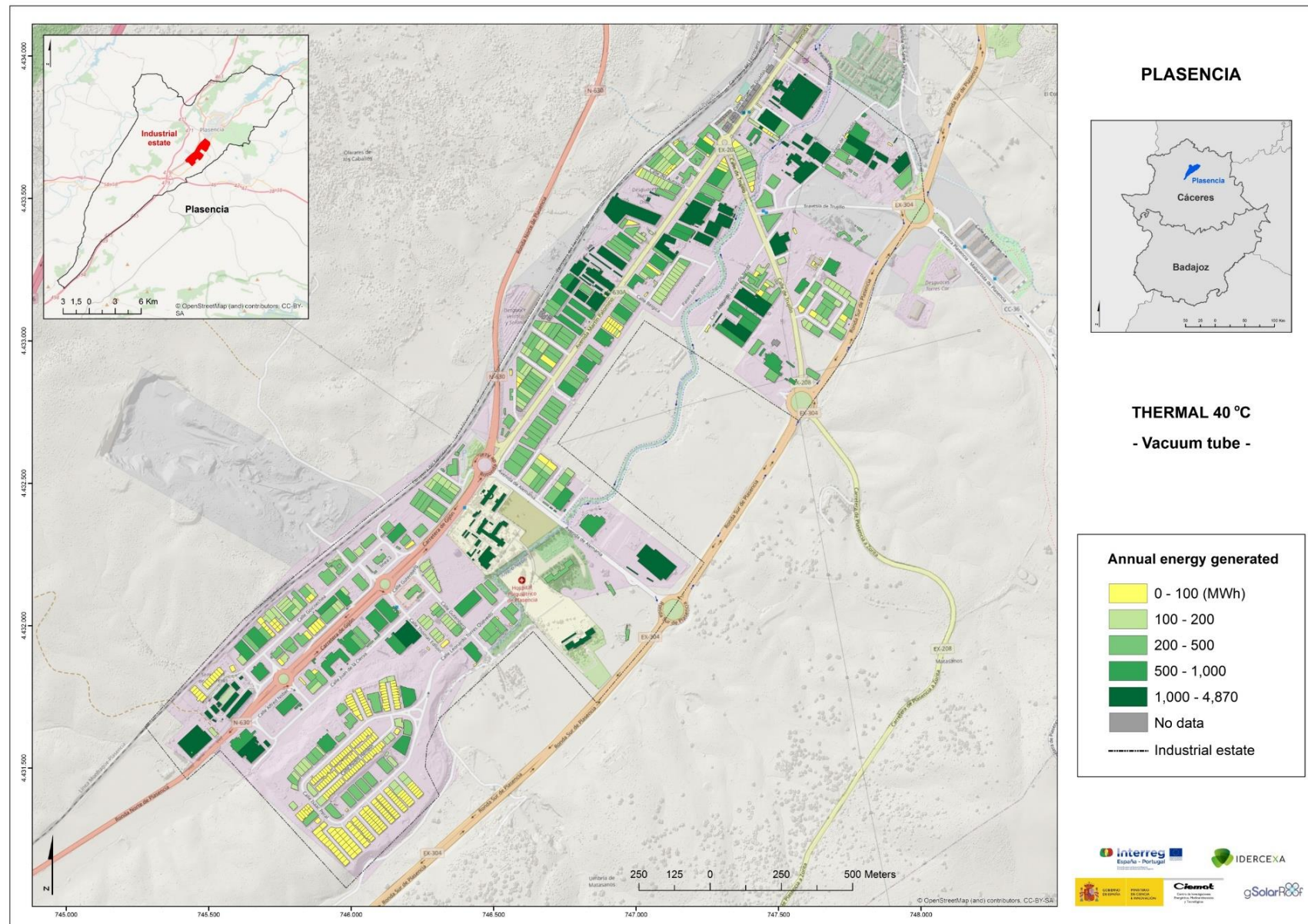


Figure A 52. Thermal: Annual energy generated (Vacuum tube collector) at the temperature of 40 °C. Plasencia.

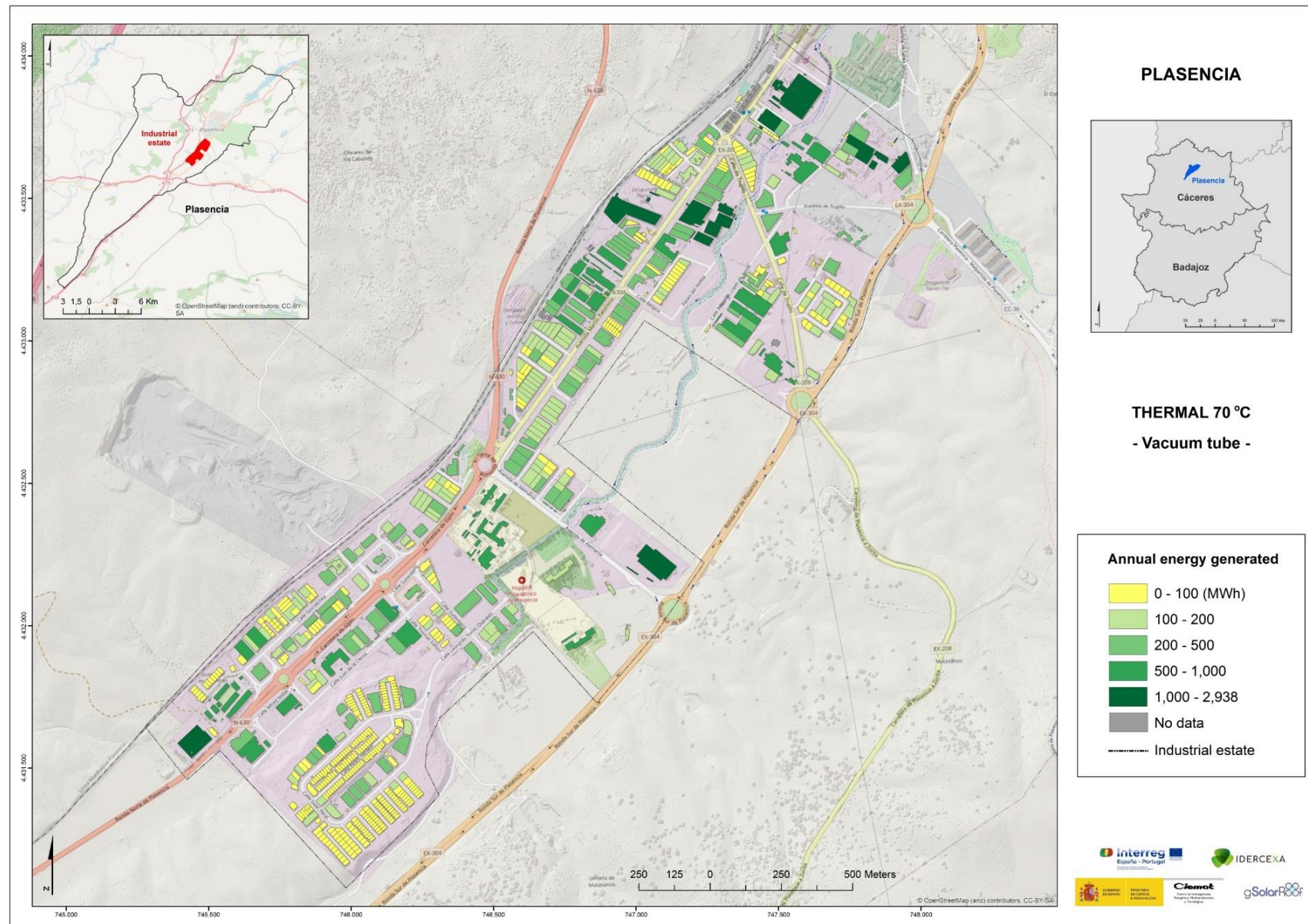


Figure A 53. Thermal: Annual energy generated (Vacuum tube collector) at the temperature of 70 °C. Plasencia.

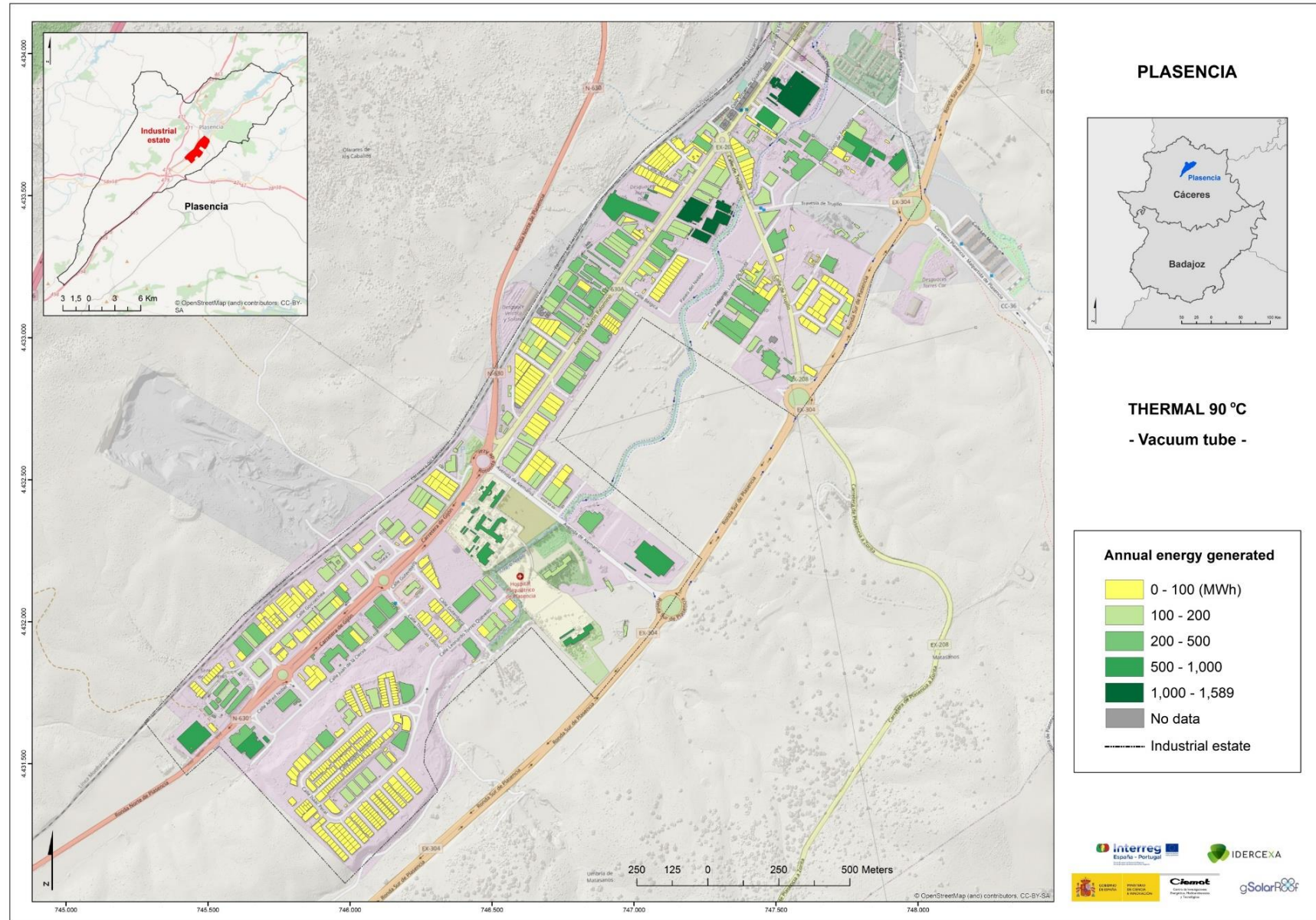


Figure A 54. Thermal: Annual energy generated (Vacuum tube collector) at the temperature of 90 °C. Plasencia.

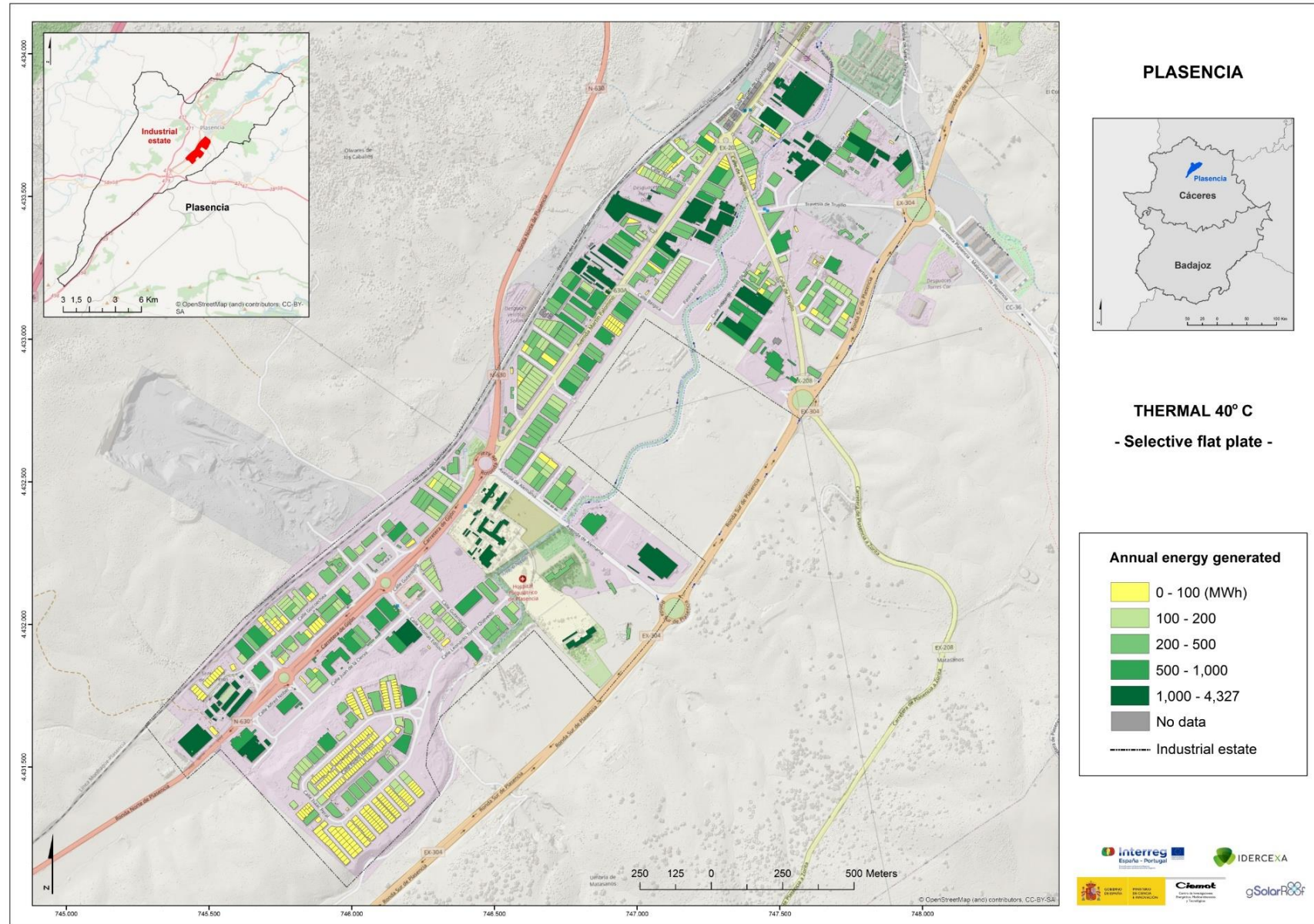


Figure A 55. Thermal: Annual energy generated (Selective flat plate collector) at the temperature of 40 °C. Plasencia.

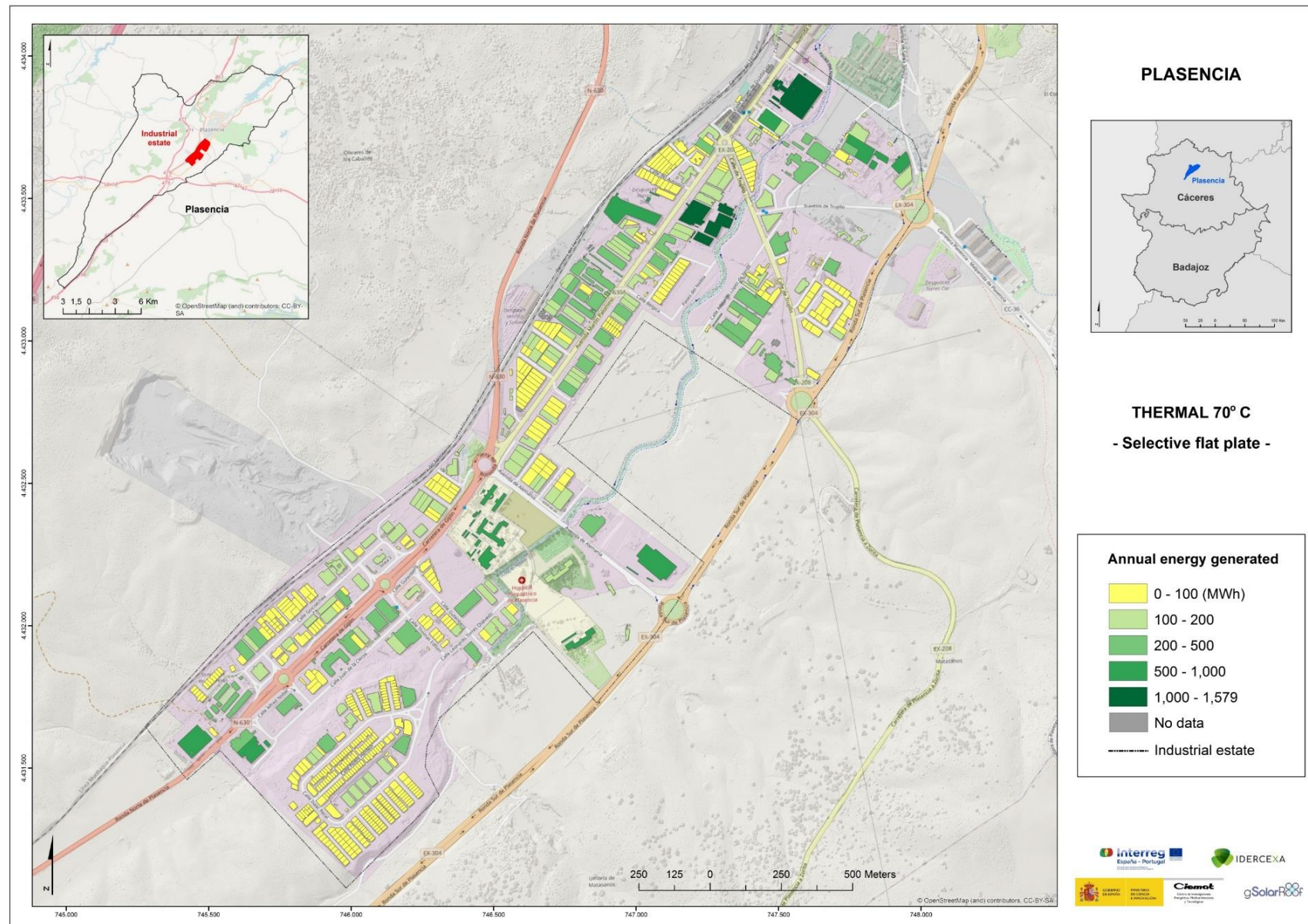


Figure A 56. Thermal: Annual energy generated (Selective flat plate collector) at the temperature of 70 °C. Plasencia.

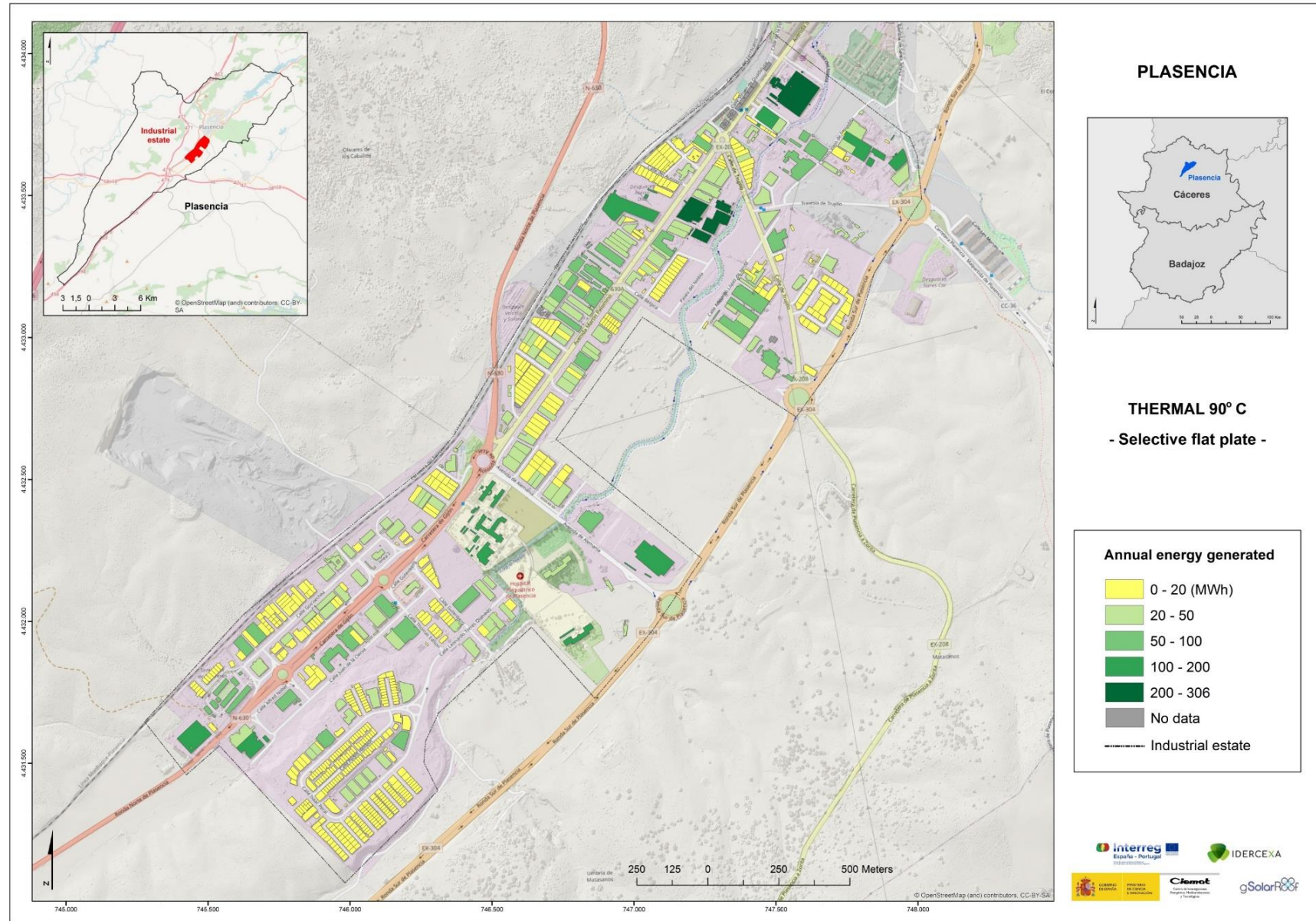


Figure A 57. Thermal: Annual energy generated (Selective flat plate collector) at the temperature of 90 °C. Plasencia.

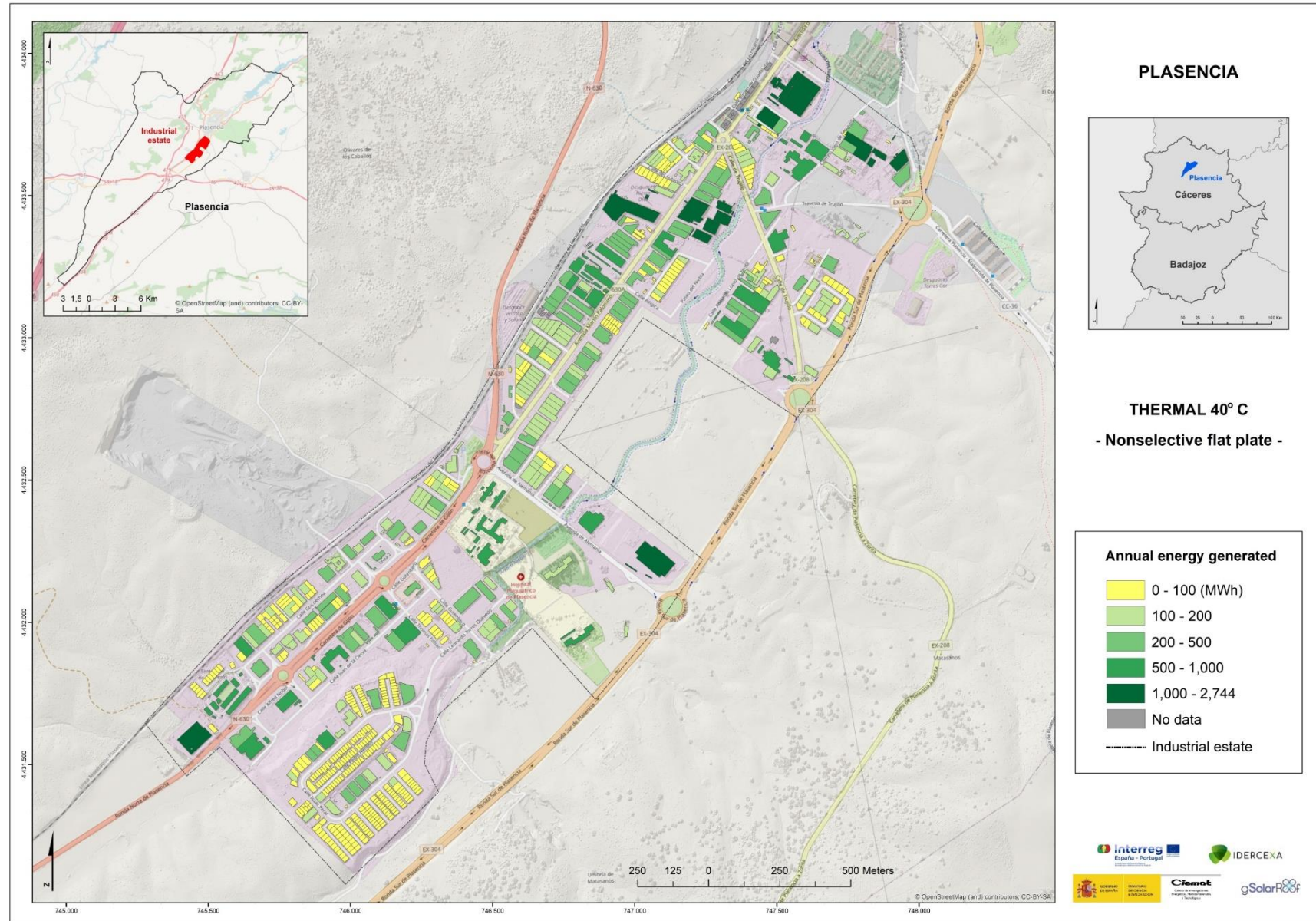


Figure A 58. Thermal: Annual energy generated (Nonselective flat plate collector) at the temperature of 40 °C. Plasencia.

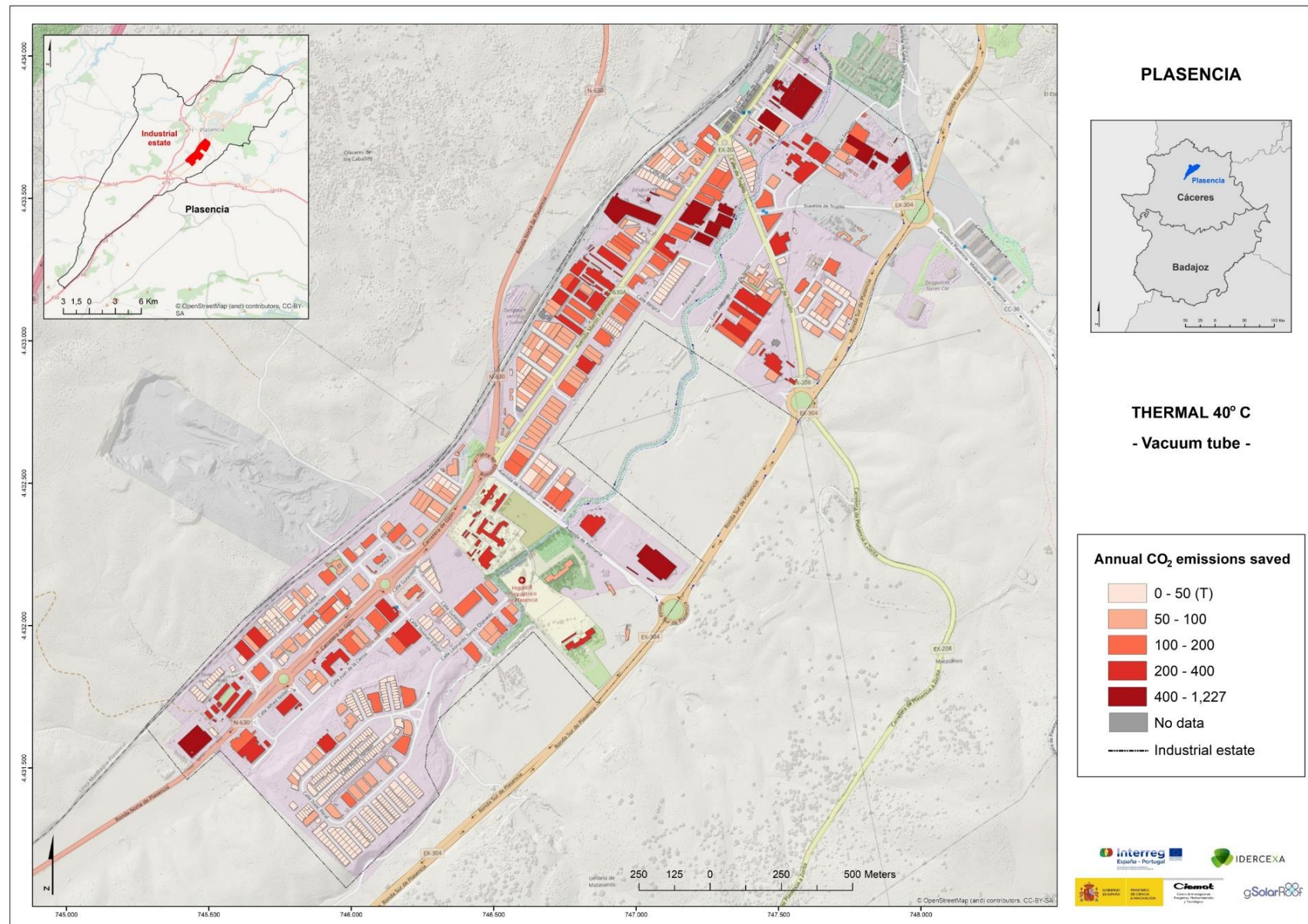


Figure A 59. Thermal: Annual CO₂ emissions saved (Vacuum tube collector) at the temperature of 40 °C. Plasencia.

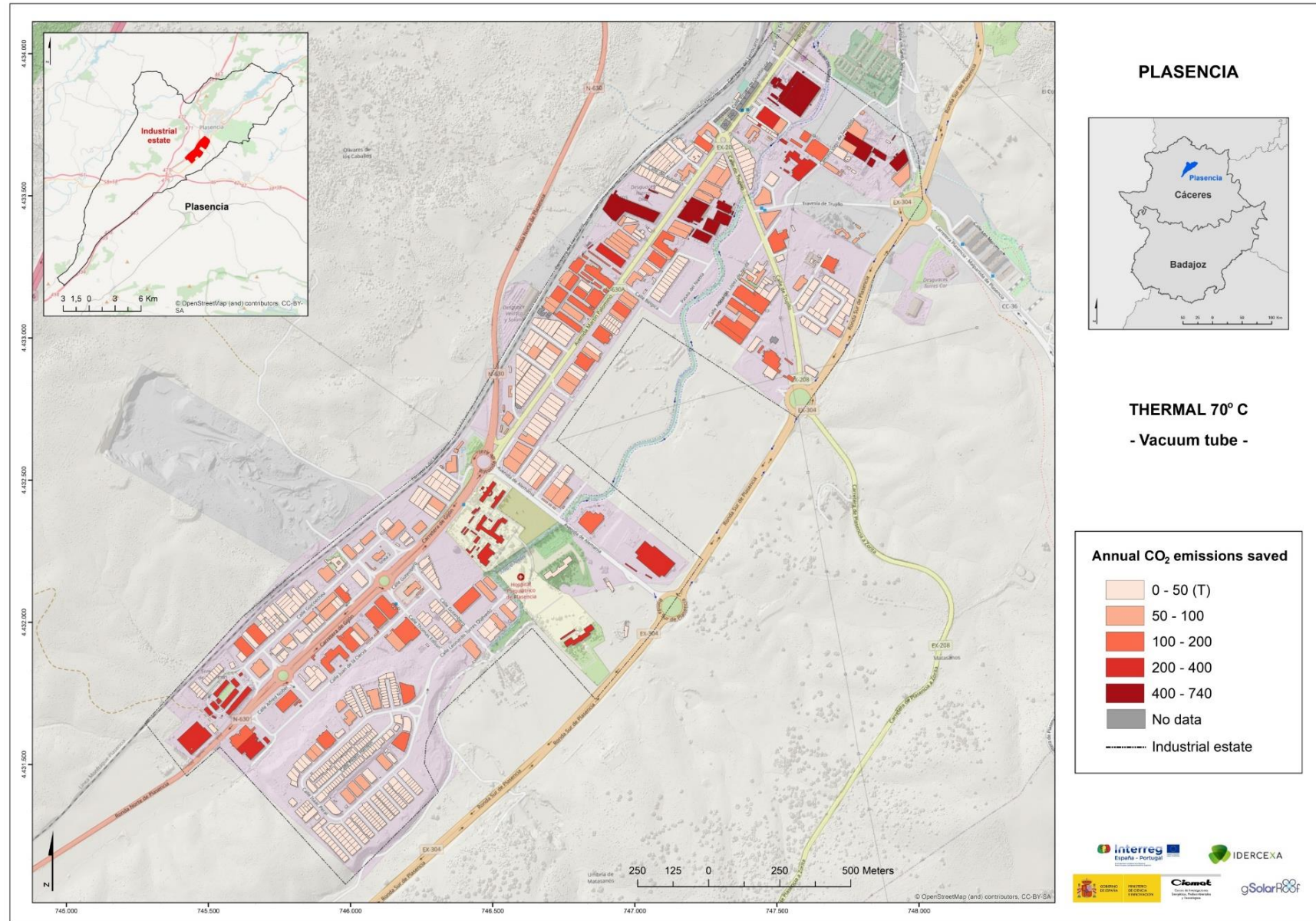


Figure A 60. Thermal: Annual CO₂ emissions saved (Vacuum tube collector) at the temperature of 70 °C. Plasencia.

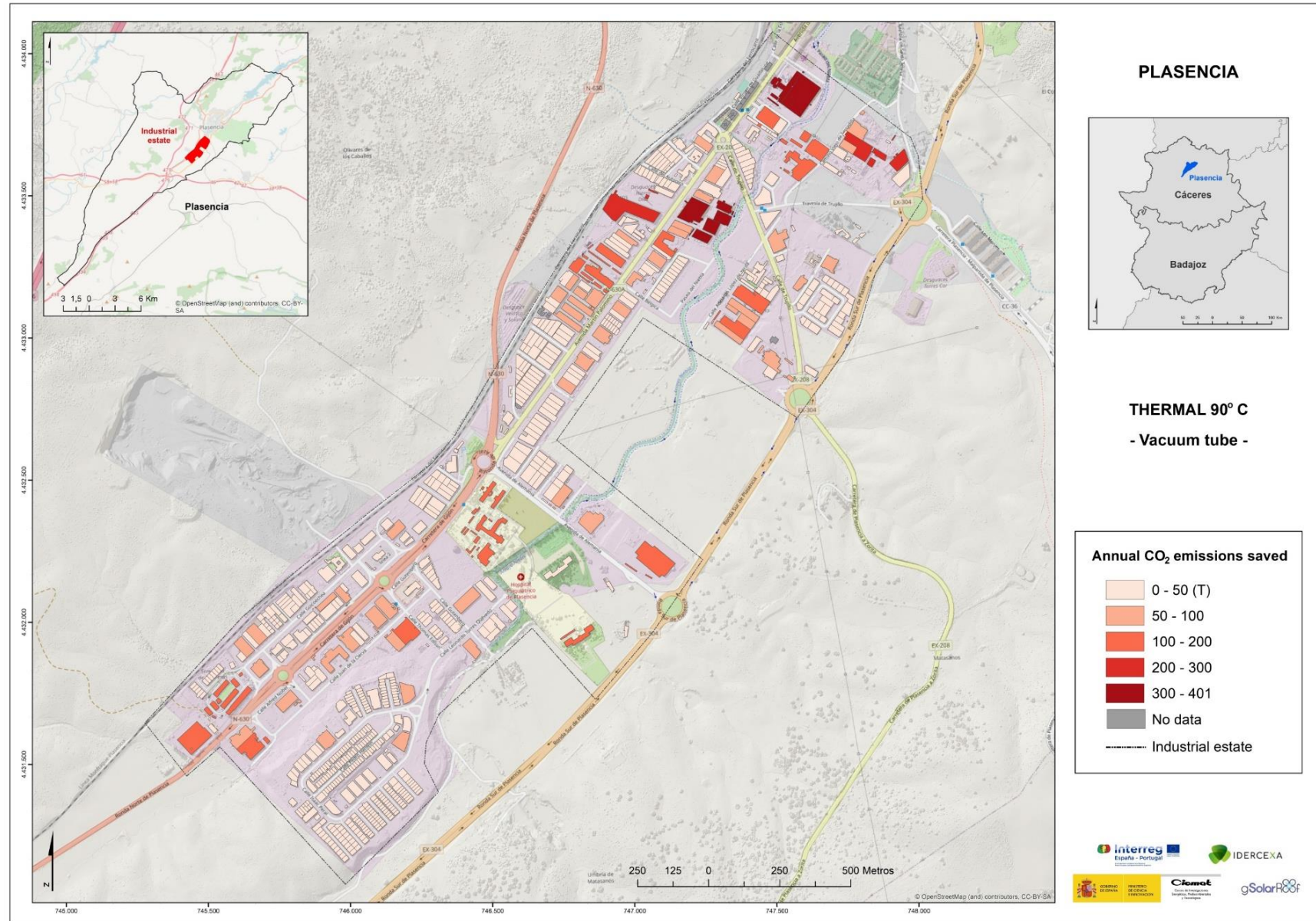


Figure A 61. Thermal: Annual CO₂ emissions saved (Vacuum tube collector) at the temperature of 90 °C. Plasencia.

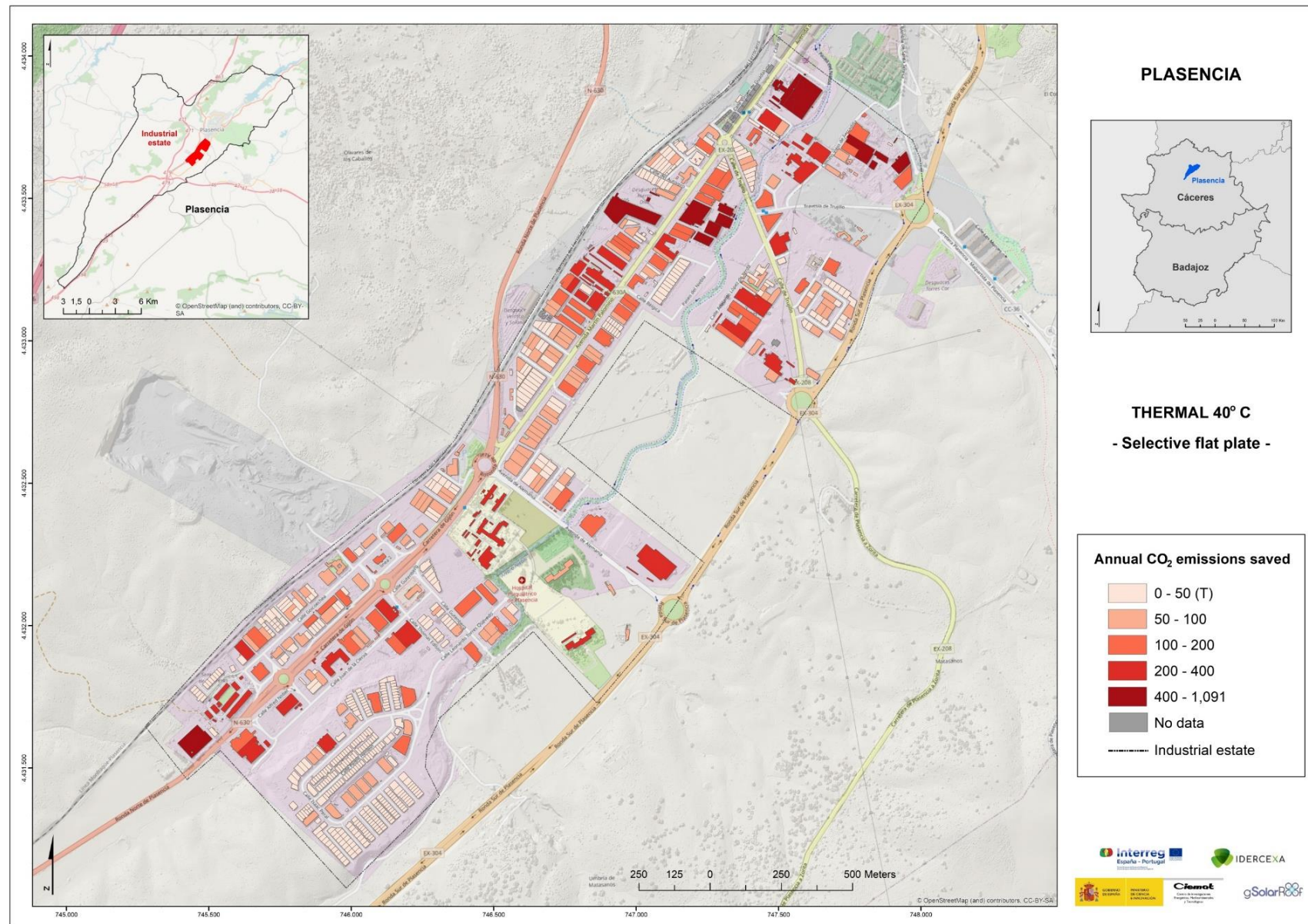


Figure A 62. Thermal: Annual CO₂ emissions saved (Selective flat plate collector) at the temperature of 40 °C. Plasencia.

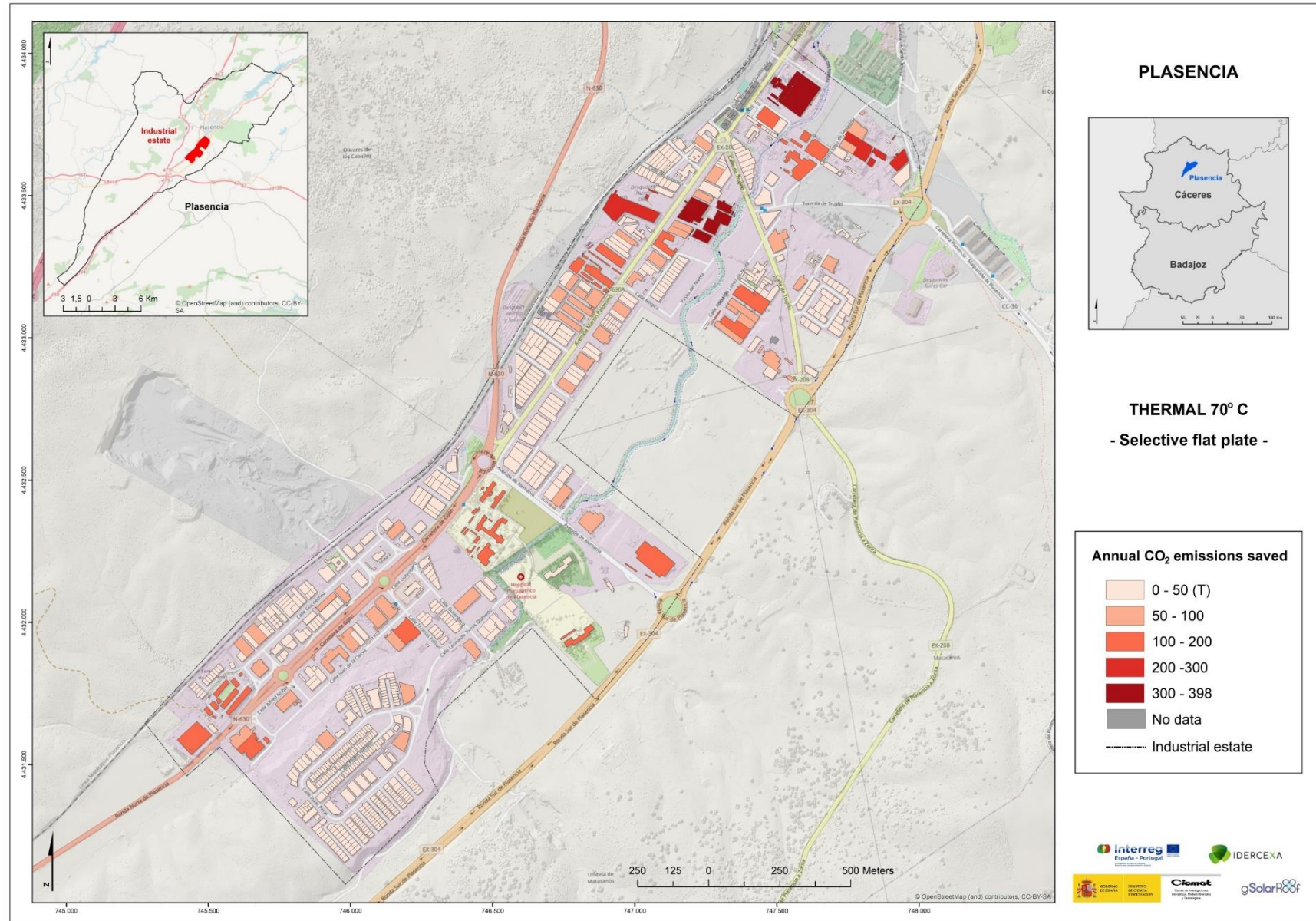


Figure A 63. Thermal: Annual CO₂ emissions saved (Selective flat plate collector) at the temperature of 70 °C. Plasencia.

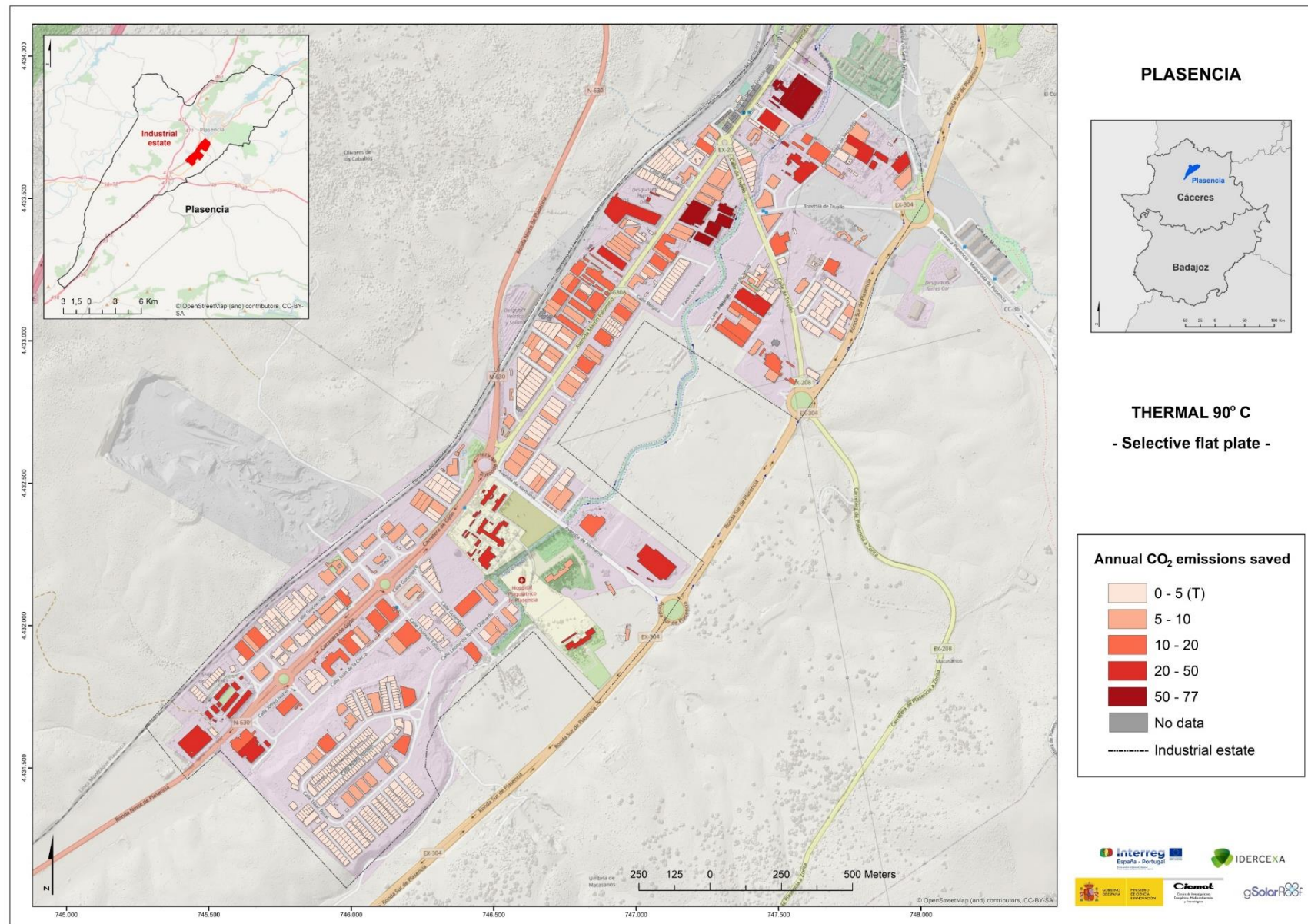


Figure A 64. Thermal: Annual CO₂ emissions saved (Selective flat plate collector) at the temperature of 90 °C. Plasencia.

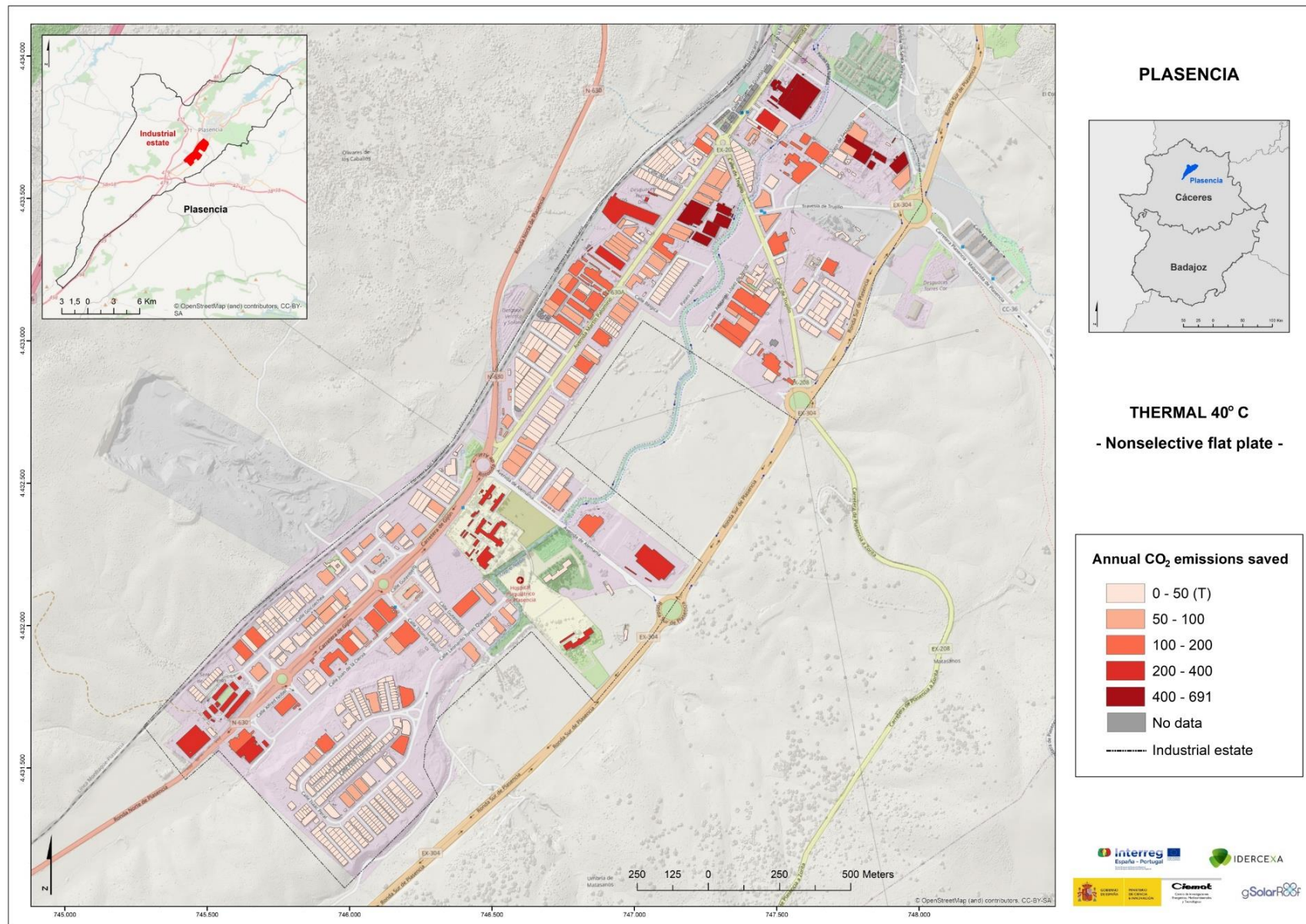


Figure A 65. Thermal: Annual CO₂ emissions saved (Nonselective flat plate collector) at the temperature of 40 °C. Plasencia.

